RFP-3339

MASTER

WIND-SYSTEMS TECHNICAL NOTES: 1979-1980

February 1982

Compiled by Sally A. Shuler
Edited by Joel V. Stafford

Rocky Flats
Wind Systems Program

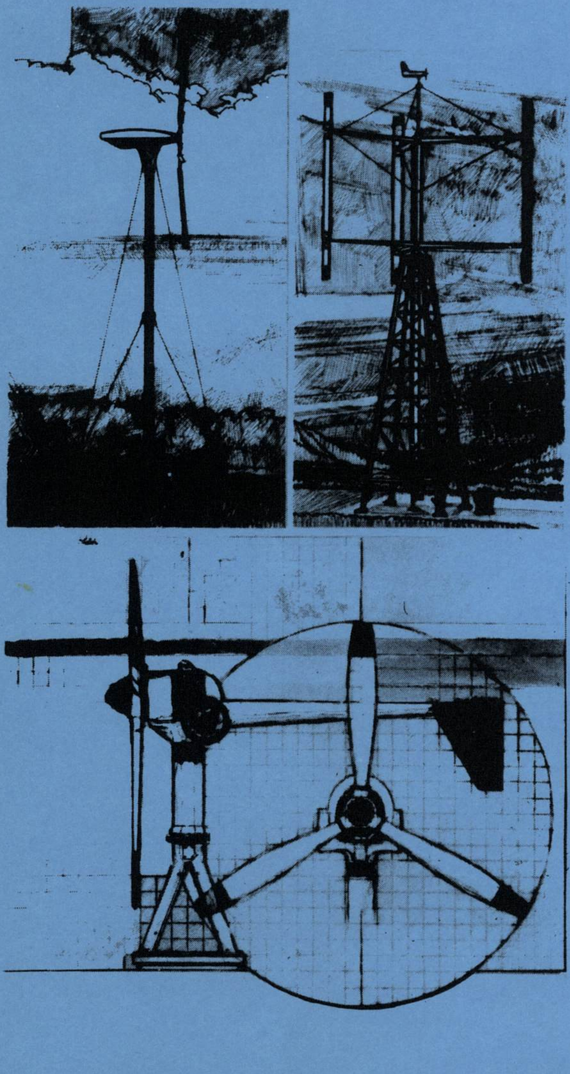

Prepared by:
Rockwell International Corporation
Energy Systems Group
Golden, Colorado 80402-0464

As a Part of:
UNITED STATES DEPARTMENT OF ENERGY
WIND ENERGY TECHNOLOGY DIVISION
FEDERAL WIND ENERGY PROGRAM

DOE Contract No. DE-AC04-76DP03533

DISCLAIMER

This report was prepared as an account of work sponsored by the United States Government. Neither the United States nor the United States Department of Energy, nor any of their employees, makes any warranty, express or implied, or assumes any legal liability or responsibility for the accuracy, completeness, or usefulness of any information, apparatus, product, or process disclosed, or represents that its use would not infringe privately owned rights. Reference herein to any specific commercial product, process, or service by trade name, mark, manufacturer, or otherwise, does not necessarily constitute or imply its endorsement, recommendation, or favoring by the United States Government or any agency thereof. The views and opinions of authors expressed herein do not necessarily state or reflect those of the United States Government or any agency thereof.

Printed in the United States of America

Available from

National Technical Information Service
U.S. Department of Commerce
5285 Port Royal Road
Springfield, VA 22161

Printed Copy: $12.00 Microfiche: $3.50

RFP- 3339

RFP--3339

DE82 016358

WIND-SYSTEMS TECHNICAL NOTES: 1979-1980

February 1982

Compiled by Sally A. Shuler
Edited by Joel V. Stafford

Rocky Flats
Wind Systems Program

Prepared by:

Rockwell International Corporation
Energy Systems Group
Golden, Colorado 80402-0464

As a part of:

UNITED STATES DEPARTMENT OF ENERGY
WIND ENERGY TECHNOLOGY DIVISION
FEDERAL WIND ENERGY PROGRAM

DOE Contract No. DE-AC04-76DP03533

Blank Page

ABSTRACT

This report contains 13 Technical Notes produced by the Rocky Flats Wind Systems Program in 1979-1980 to document specialized tests of small wind systems and other investigations. Subjects include: vibration, dynamometer, and controlled velocity tests of 1-2 kW and 8 kW prototype wind systems; the use of induction generators; data collection and reporting procedures; analog-to-digital data conversion; optical rpm sensors; alternator frequency monitoring; and air density adjustments.

TABLE OF CONTENTS

TABLE OF CONTENTS (CONTINUED)

TABLE OF CONTENTS (CONTINUED)

WIND SYSTEMS TECHNICAL NOTES

INTRODUCTION

The Rocky Flats Wind Systems Program, operated by Rockwell International for the U.S. Department of Energy, was established in 1976 to stimulate the development and use of reliable and cost effective small wind systems (under 100 kW). An integral part of the program is the Rocky Flats Wind Systems Test Center (WSTC) which tests wind systems under natural conditions for performance and reliability data, and conducts specialized component tests as part of the program's research effort. Major specialized capabilities of the WSTC include a dynamometer test facility that is capable of defining the performance characteristics of rotating machines (up to 100 kW) requiring any nominal voltage/frequency used in the world; modal analysis (vibration testing) for defining structural and dynamic problems, such as excessive vibration and fatigue; and controlled velocity testing, which allows the rapid generation of performance data under controlled conditions.

Contained herein are thirteen Technical Notes (TN's) produced in 1979-1980 relative to these types of testing as well as other areas of technical investigation. The TN's are presented in chronological order and have been reproduced using the best available masters. Seven TN's pertain to specialized tests of specific wind machine models. These include dynamometer tests, controlled velocity tests, and modifications to machines developed by the United Technologies Research Center, North Wind Power Company, and Pinson Energy Corporation; and vibration tests of Enertech and United Technologies Research Center prototypes. Of the remaining six TN's, one pertains to utilization of the induction generator, while the other five are concerned with data collection and reporting, analog-to-digital data conversion, optical rpm sensors, alternator frequency monitoring, and air density adjustments.

Technical Notes are produced by the Wind Systems Program primarily as a method of expediting internal communications. Please be aware that all data contained in TN's are preliminary and unchecked and may not reflect the results of additional testing and/or investigations. The TN's in this volume have not been updated or re-edited. Their applicability and value, therefore, has not been substantiated.

LONG TERM DATA ACQUISITION ANALOG CONVERSION

D. A. Chamberlain

December 7, 1979

LONG TERM DATA ACQUISITION ANALOG CONVERSION

The Wind Systems Test Center (WSTC) is using micro computers for long term data collection (LTDC) of data from small wind energy conversion systems (SWECS). The micro computers are running under WEDAS Ver. G software. The analog data is acquired via a 16 channel, 12 bit analog to digital converter. The system, as configured at the WSTC, has an absolute accuracy (0^o to + 70^oc) of $\pm$ 0.5% FSR max. ($\pm$ 50 mv), a linearity of $\pm$ 1 LSB max. (2.44 mv) and a resolution of 2.44 mv. The maximum throughput is 35,000 channels/sec. Under WEDAS Ver. G software the micro computer is digitizing each channel and the count for each channel is summed into a 4 byte memory field. During the time of the A/D conversions, the program checks for communications from the satellite computer. After all 16 channels have been converted and summed, the program checks the load control status. If there is no satellite communications and load control required, it takes 5,850 microsec to convert all 16 channels. Also, the offset in time between the conversion of consecutive channels is 333 microsec.

When data is requested from the micro computer the program stops digitizing the analog data and transmits the last calculated averages. When the data has been transmitted,new averages are calculated from the summed data in memeory and the new averages are stored in a buffer while the old sums are set to zero. With the existing LTDC program this communications takes 100 to 200 msec. Load control can add up to 433 microsec to the 5,850 micro sec A/D conversion time. A problem can exist when the time between the conversions of the same channel and the period of a repetitive waveform are equal. When this happens the same point on the waveform are sampled each time and the resultant average can be grossly in error. With this system this will happen when the period of the waveform is 5,850 microsec (171 Hz) and there is no load control running. This not considered a serious problem because of the following:

1) A variation in the analog frequency of ± 1.2 Hz or more will destroy the synchronization.

2) The 171 Hz frequency is not normally encountered when producing power from SWECS.

3) The asynchronous nature of the communications will introduce a shift in the sampling point after each poll (once per second when producing power). If the frequency is 171 Hz the shift in the sampling point will tend toward the average when processed by the "method of bins" program used for data reduction.

4) The use of load control will introduce an additional asynchronous element in the sampling period which greatly reduces the chance of synchronization.

In an effort to check the performance of the system a 0.0v to 7.974 V square wave was connected to one channel of the A/D converter. The frequency was varied between 10 Hz and 10,000 Hz and a total of 240 measurements were made, 10 at each of 24 frequencies. The micro computer was polled at a 1 sec rate and the values were read off the CRT screen at the central computer. The measured average was 3.960 V and the standard dev. was 0.093 V. The results of the above test indicate that the system does calculate accurately the average of non D. C. inputs.

ENERTECH PROTOTYPE VIBRATION ANALYSIS

J. H. Sexton

January 1980

Additional available reports on the Enertech wind system are listed below and are available from National Technical Information Service.

Development of a 2 Kilowatt High Reliability Wind Machine, Phase I - Design and Analysis, January 1980, W. Drake, et al., Enertech Corporation, Volume I - Executive Summary, 18 pp., $5.00 (RFP-3025-1): Volume II - Technical Report, 78 pp., $8.00 (RFP-3025-2).

TABLES

FIGURES

ENERTECH PROTOTYPE VIBRATION ANALYSIS

SUMMARY

Results of vibration tests indicate the Enertech High-Reliability Wind Turbine Generator (WTG) and the support structure are mismatched dynamically. The system's (WTG/support structure) second mode bending was determined to be 13.2 Hz, while the blade's first mode bending frequencies were found to be 12.4 Hz for Blade 2 and 14.6 Hz for Blade 1.

INTRODUCTION

Dynamic analysis of structures and their components is becoming an increasingly more important part of the design process. Dynamic testing is an effective way to insure that wind turbine generators, support structures, and their components meet their design performance expectation and behave in a predictable manner when used in a dynamic operating environment.

One area of structural dynamics testing is referred to as "modal analysis." Modal analysis is the process of characterizing the dynamic properties of an elastic structure by identifying its modes of vibration. In other words, each mode has a specific natural frequency and damping factor. In addition, each mode of vibration has a characteristic "mode shape" which is defined spatially over the entire structure.

Actual measurements of the dynamic properties and behavior of a WTG is an essential part of any dynamic analysis. The dynamic properties of a component or structure may be determined by using finite element computer modeling techniques, however, most structures still require further experimental vertifications of analytical results.

TEST DESCRIPTION/THEORY

A technique currently being used at the Wind Systems Test Center (WSTC) for dynamic testing is commonly known as impact testing. The structure can be excited with a hammer. With a load cell attached to

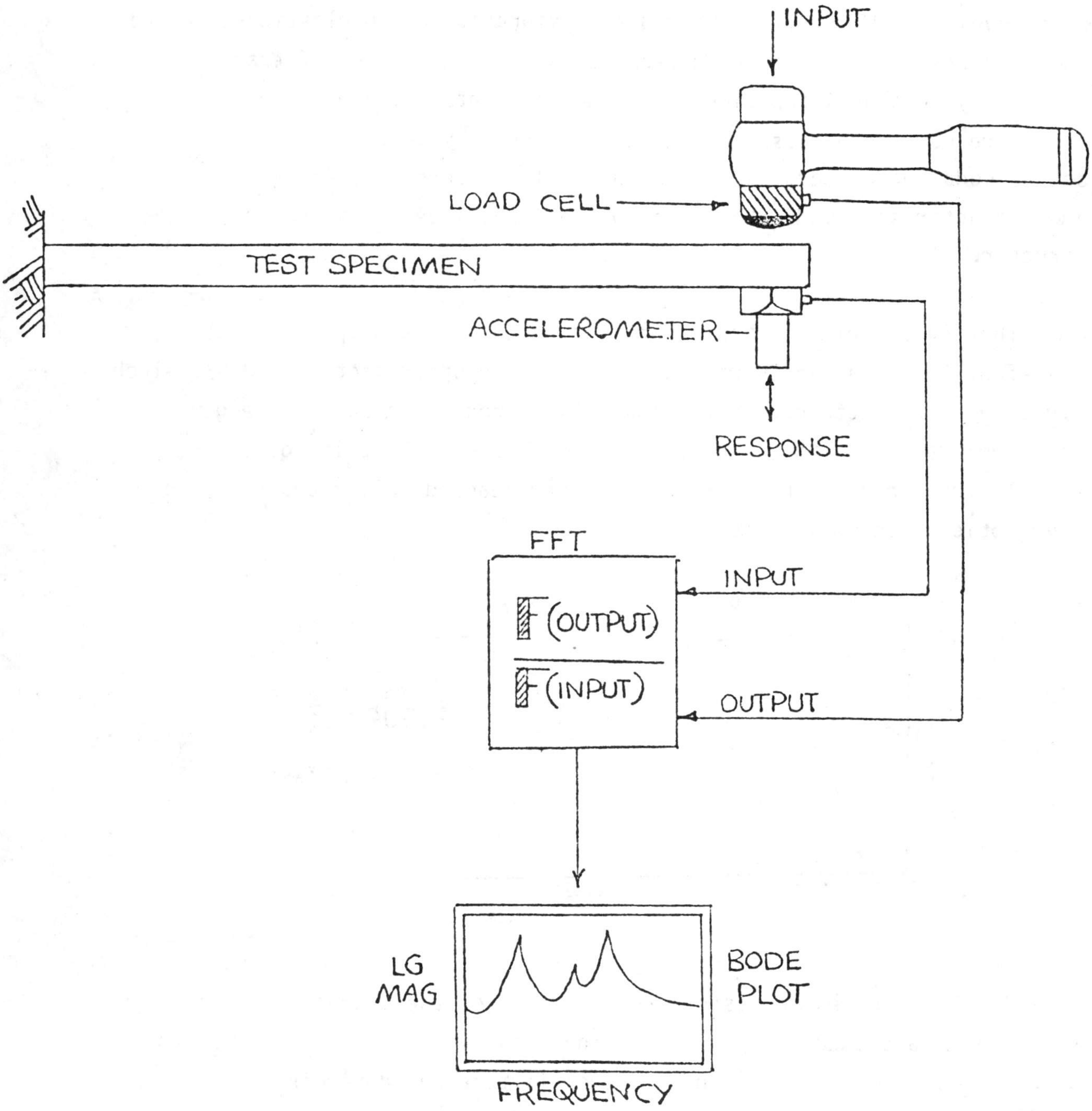

Figure 1
Driving Point Measurement

the hammer, the input force can be accurately recorded. The response (output) of the structure is measured with the use of an accelerometer. A generalized test setup is depicted in Figure 1. Techniques have been developed which allow the modes of vibration of an elastic structure to be identified from measured transfer data. Once a set of transfer (frequency response) functions relating to points of interest on the structure have been measured and stored, they may be operated on to obtain modal parameters, i.e., the natural frequencies, damping factors, and characteristic mode shapes for predominant modes of vibration of the structure.

The first series of tests were conducted on the support structure, a 40-foot (ft) Rohn 45GSR with a double-braced upper section and 9/16-inch (in.) guy wires attached to the tower 31 ft above its base. The guy wires were adjusted to a frequency of 6.8 ±.1 Hz. At this point, the overall frequency of the support structure reached 6.2 Hz and then became asymptotic as shown in Figure 2.

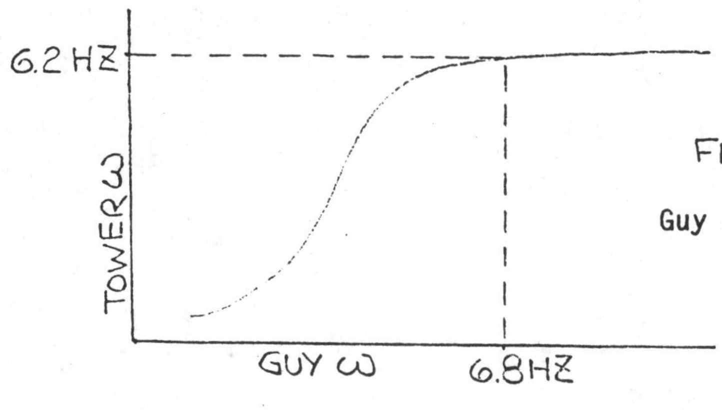

FIGURE 2

Guy ω vs ω Tower

The next series of tests were conducted on the blades. Each blade was rigidly attached to a fixture. The setup is similar to that shown in Figure 1. The frequency of the test fixture was determined to be over 500 Hz, well above the frequencies of interest of the Enertech blades. Using the impulse techniques described earlier, the first three modes of vibration were determined. It is important to note that the blades were tested as cantilevered beams, not attached to the hub.

The third series of tests were conducted on the entire system and with the WTG atop the support structure.

The fourth series of tests were conducted on the blades, which were excited in bending and in torsion. The blades were attached to the hub during this test and different frequencies would be expected from those in Series 2. While the blades were excited, these tests were also a measure of the control system, i.e., Enertech's torsion arm used for pitch control.

Series five tests were conducted on the system with the blades removed.

TABLE I

SUMMARY OF VIBRATION TESTS

Series	Component	Method of Excitation	Location of Excitation
1	Support Structure	*Hand Shake	Tower Top
2	Blades	Impulse	**Modal Study
3	System	Hand Shake/ Impulse	Tower Top
4	Blades	Impulse	Blade Tip and Blade Root Trailing Edge
5	System Blade Removed	Hand Shake/ Impulse	Tower Top

*The tower was excited by hand from the bucket truck at the tower, thus exciting the first mode bending.

**For the modal study, the blade was excited in 26 locations, thus transfer functions could be obtained at each location for identification of mode shapes for predominant modes of vibration of the blade.

RESULTS

Support Structure (S1):

The first bending mode of the support structure was found to be 6.2 Hz as shown in Figure 3.

Enertech Blades (S2):

The results of Series 2 tests are shown in Figures 4-7. Figure 4 shows the transfer function of Blade 2. As can be seen, the predominant modes of vibration are 15.3 Hz, 54 Hz, and 105.5 Hz. Figures 5-7 show the mode shapes for the predominant modes of vibration. It is very important to note Enertech's prediction of the blade's first mode bending was over 18 Hz.

System (S3):

Figure 8 shows the auto spectrum of the system. This is a result of a "hand" shake. The data are collected during the system's ring down. As can be seen, the first mode bending of the system is 3.1 Hz. In order to obtain other predominant modes of vibration of the system, an impulse test was initiated. During the ring down of the system all resonant frequencies are excited. Figure 9 shows the first 3 modes of vibration to be 3.1 Hz, 7.5 Hz, and 14.6 Hz. The first bending mode is clearly 3.1 Hz, and one would expect the second mode of the system to be approximately 14 Hz. This, coupled with the fact that the 14.6 Hz was dangerously close to the first bending of the blades, dictated further investigation of the system and its components.

Blades (S4):

Figure 10 shows the 3 predominant modes of vibration. The 7.5 Hz is the first torsional of the blade attached to the pitch torsion arm, as predicted by Enertech. Due to the fact that the two blades are coupled, the two upper modes, 12.3 Hz and 14.6 Hz, were excited. When

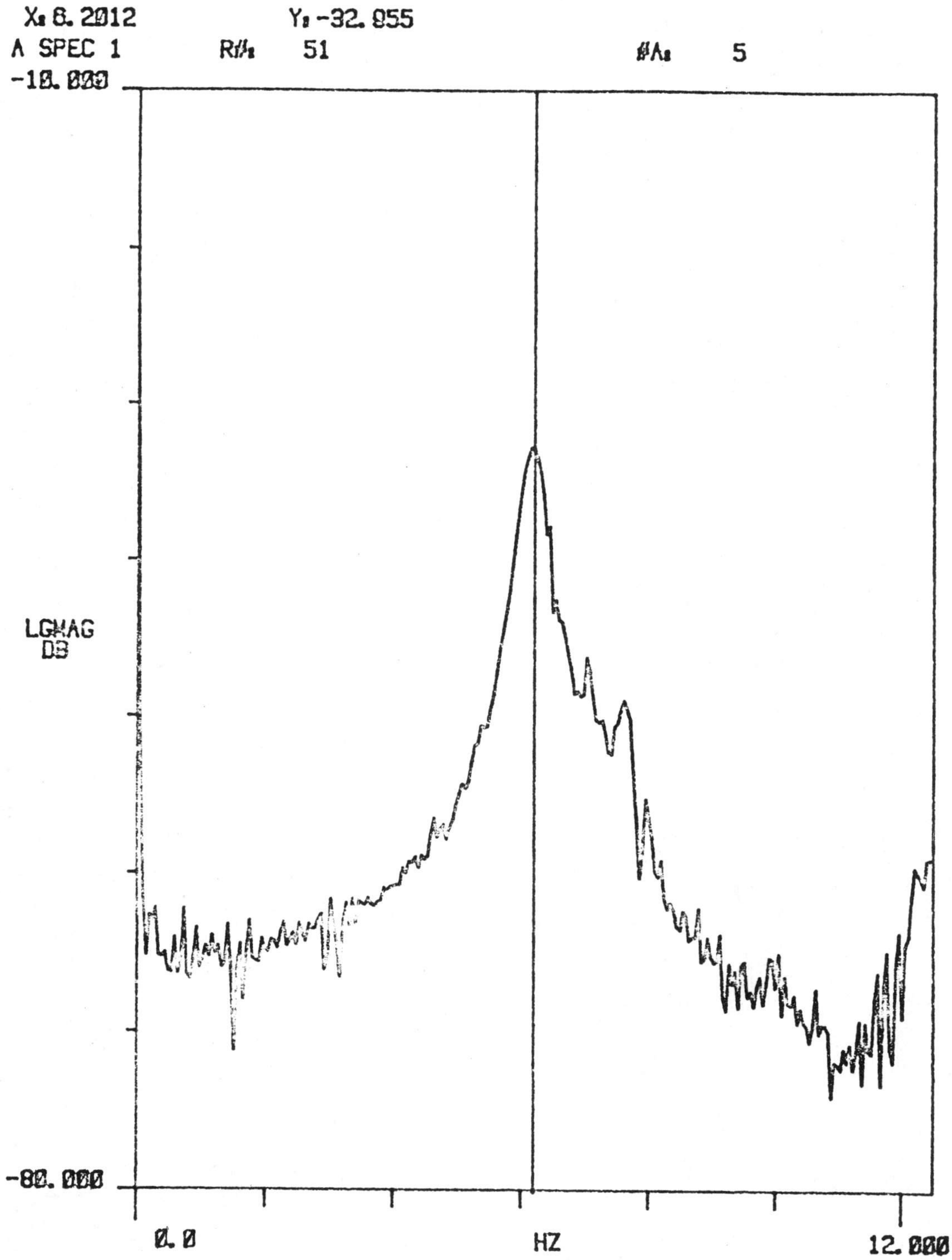

WIND SYSTEMS TEST CENTER
VIBRATION TEST FACILITY

FIGURE 3

Auto Spectrum (Support Structure)

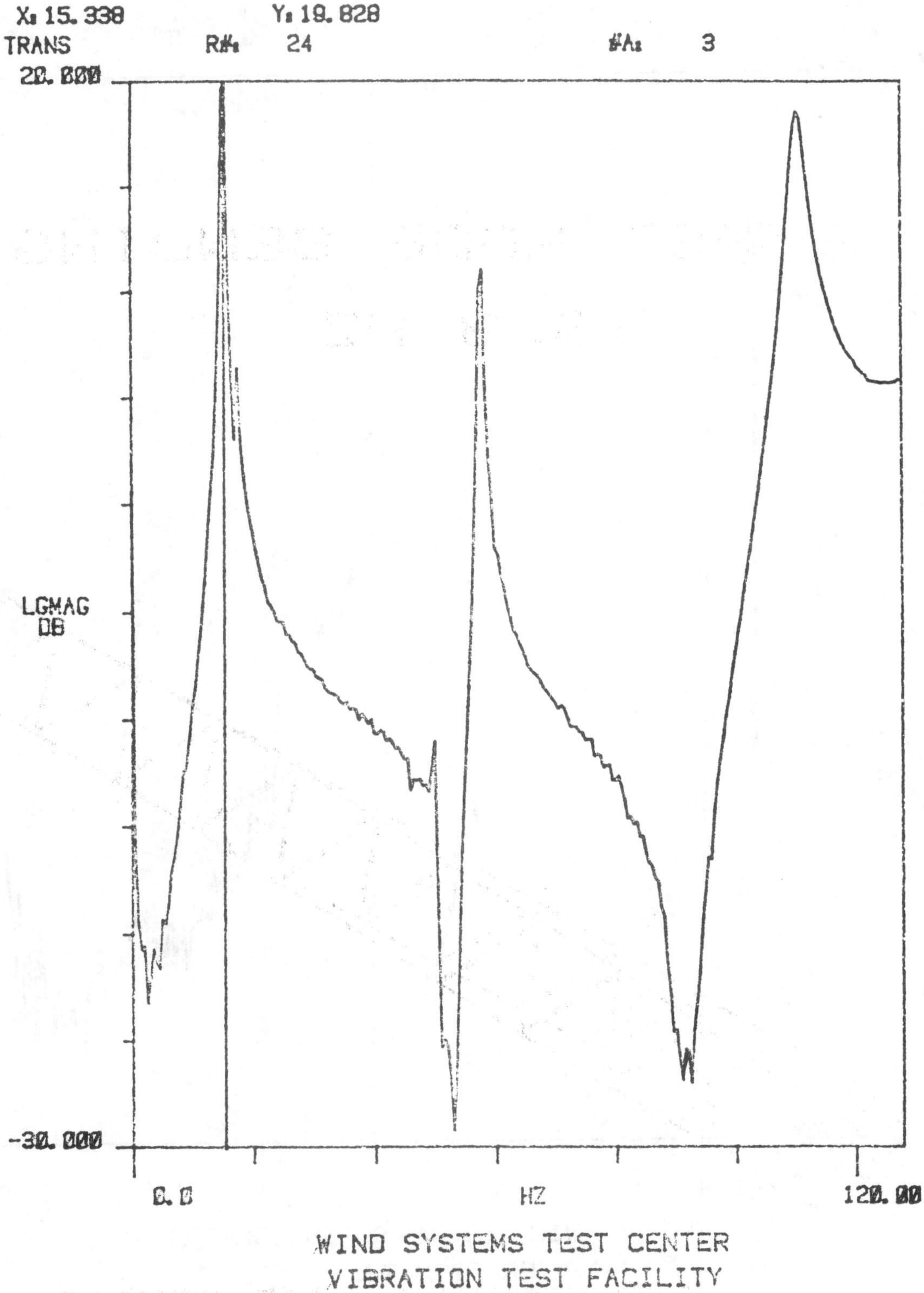

FIGURE 4

Transfer Function

FIRST MODE BENDING

15.3 HZ

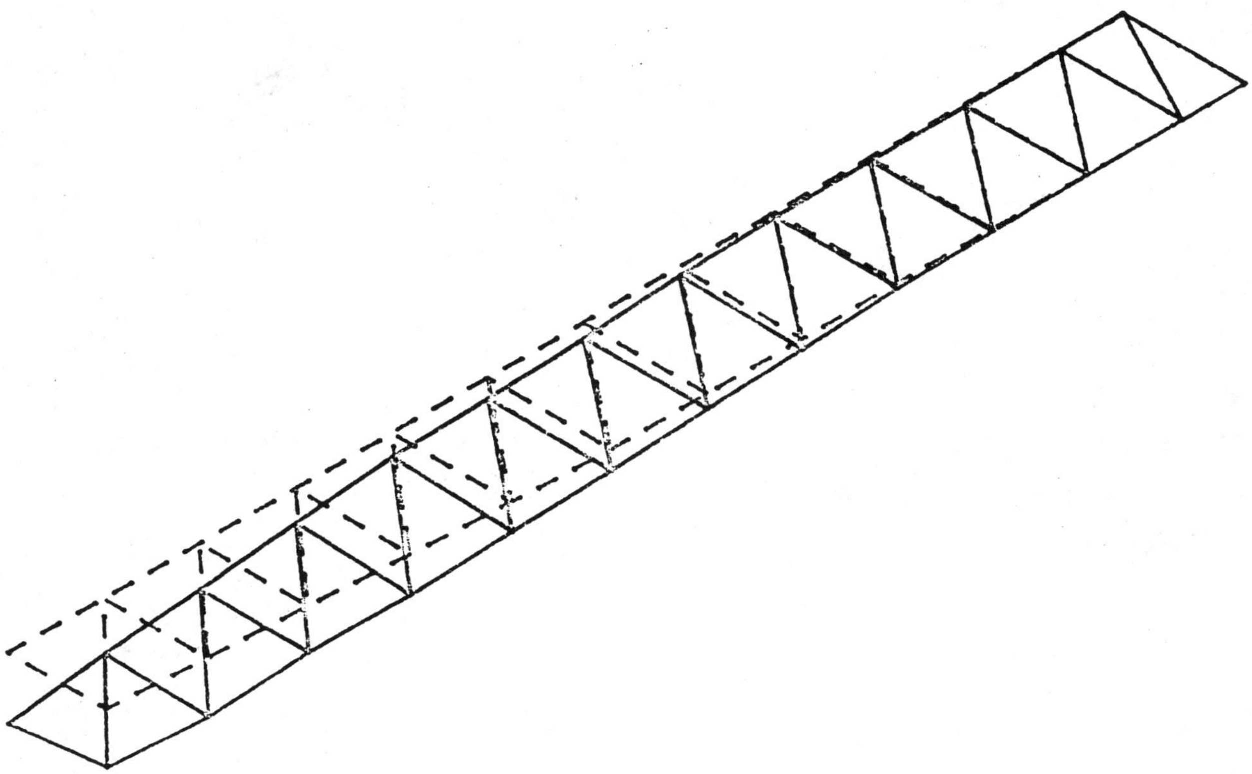

WIND SYSTEMS TEST CENTER
VIBRATION TEST FACILITY

FIGURE 5

Blade Mode Shape 1

SECOND MODE BENDING

54 HZ

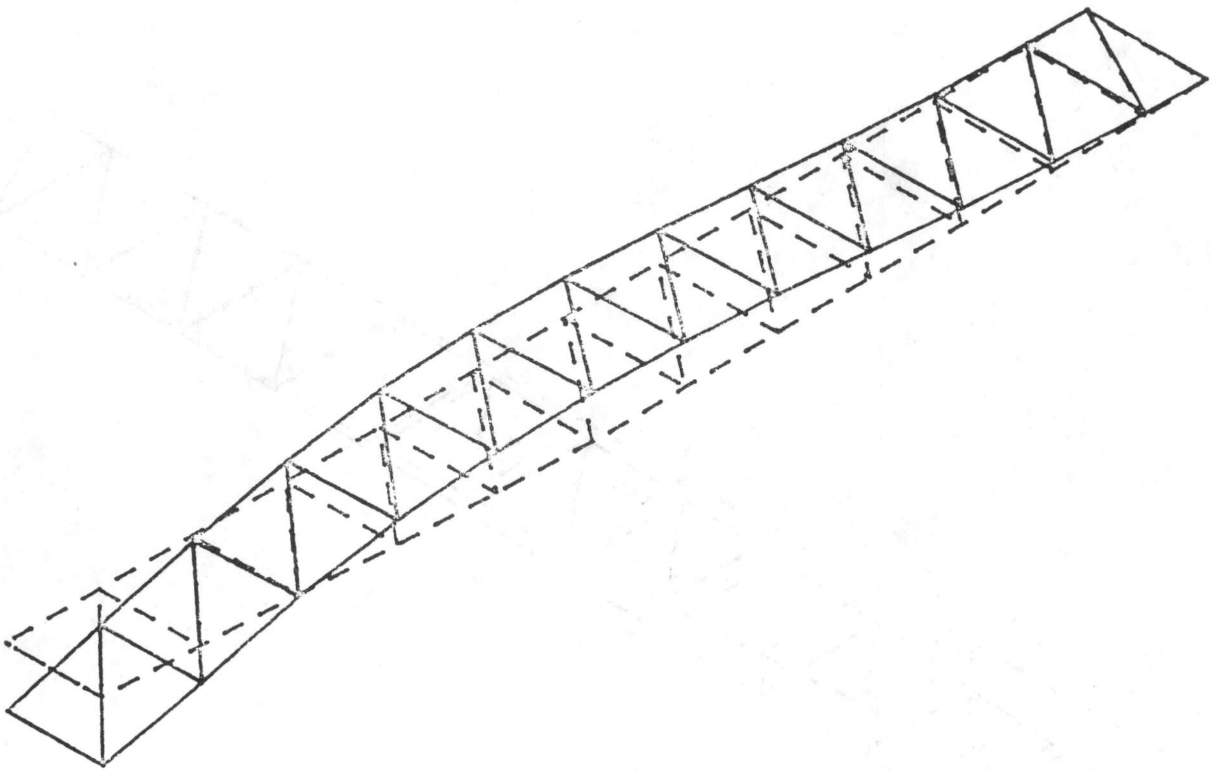

WIND SYSTEMS TEST CENTER
VIBRATION TEST FACILITY

FIGURE 6

Blade Mode Shape 2

FIRST MODE TORSION
105.5 HZ

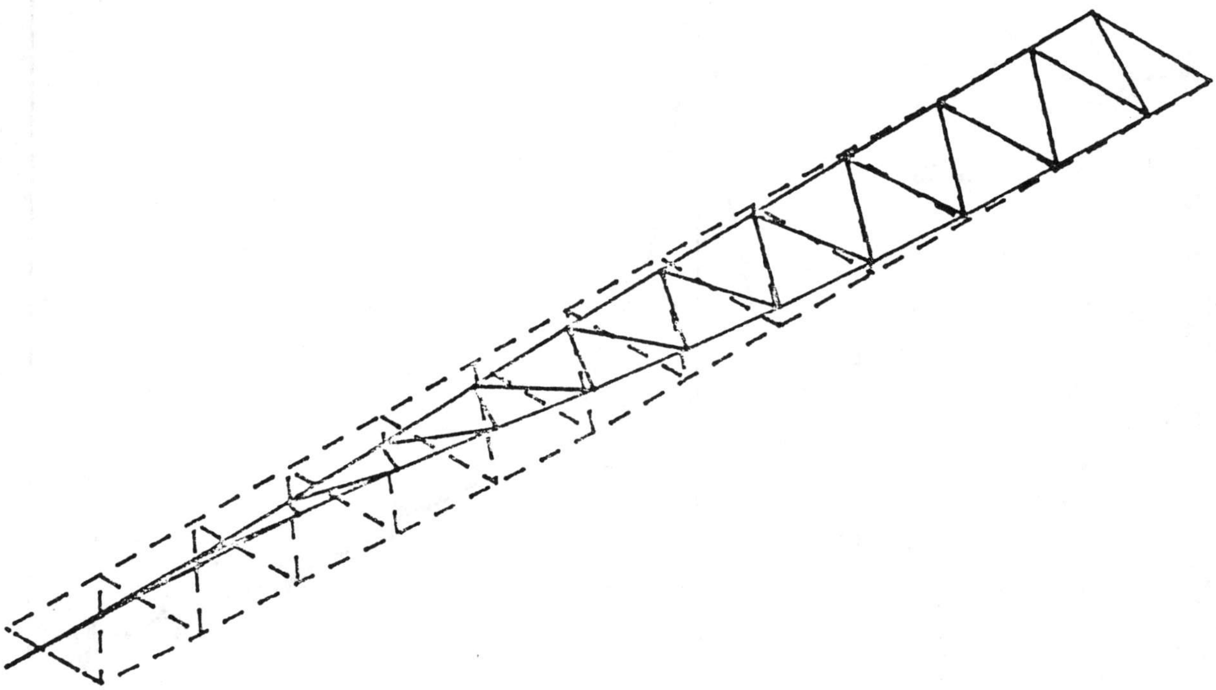

WIND SYSTEMS TEST CENTER
VIBRATION TEST FACILITY

FIGURE 7

Blade Mode Shape 3

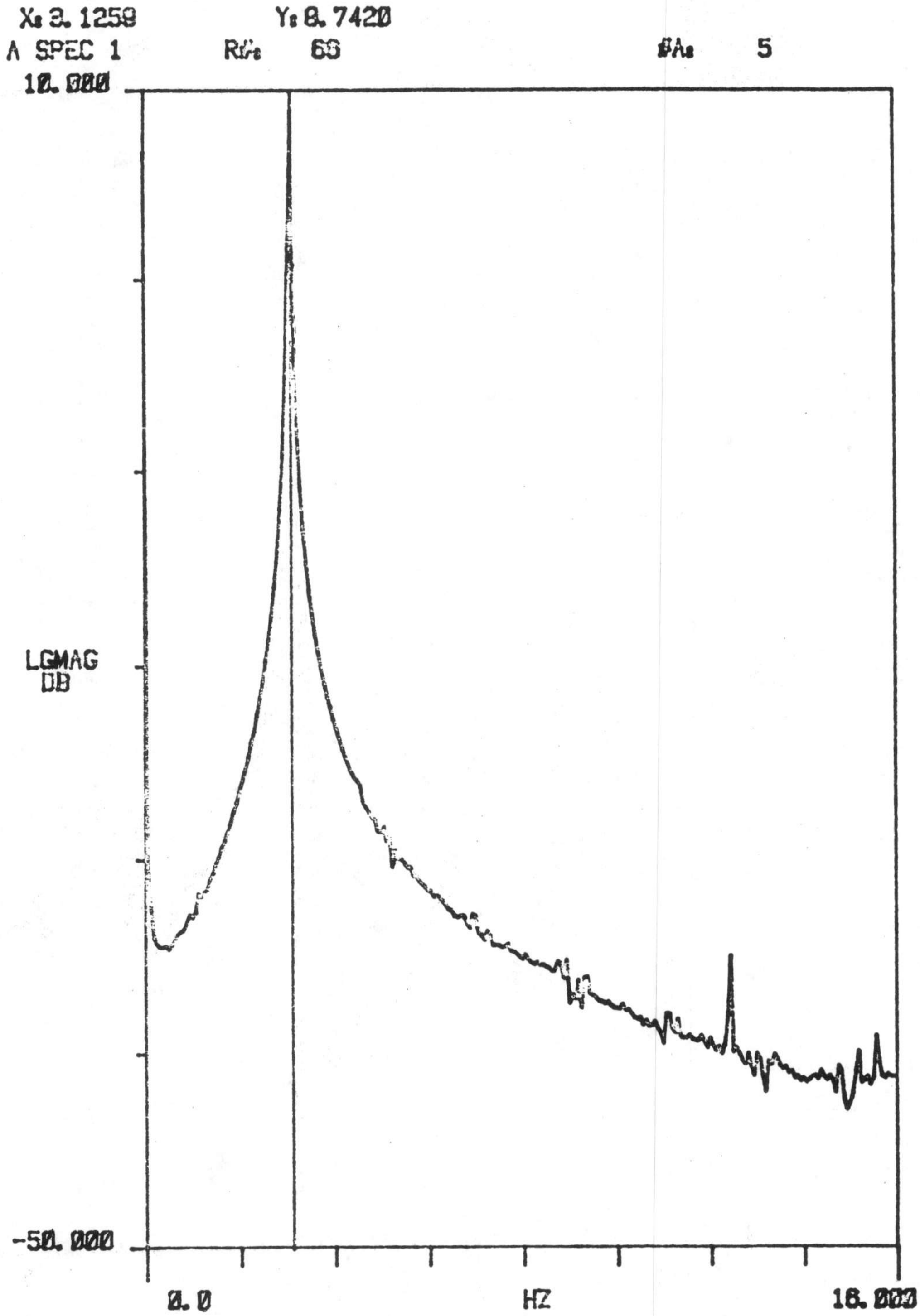

WIND SYSTEMS TEST CENTER
VIBRATION TEST FACILITY

FIGURE 8
Auto Spectrum (System)

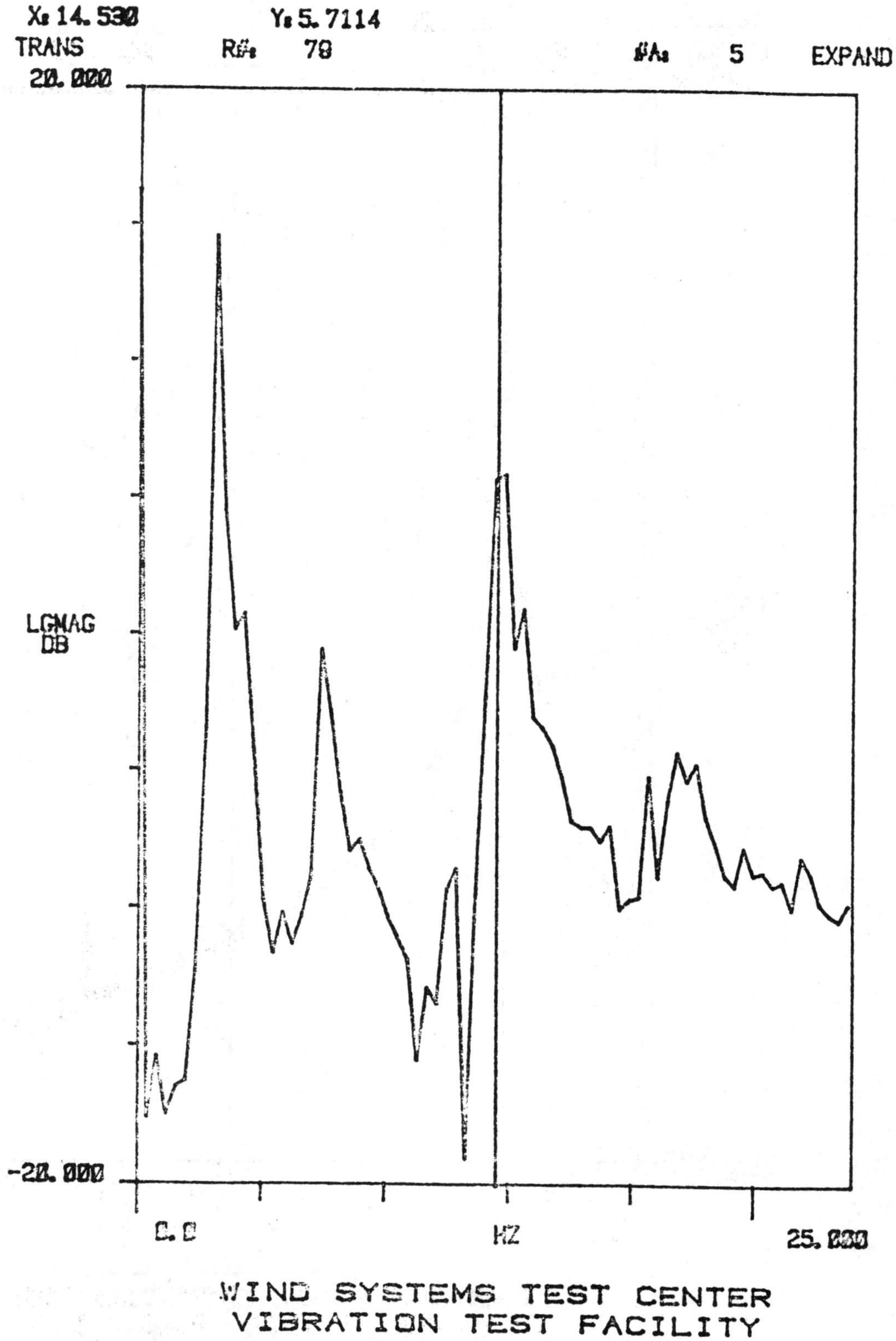

FIGURE 9

Transfer Function (System)

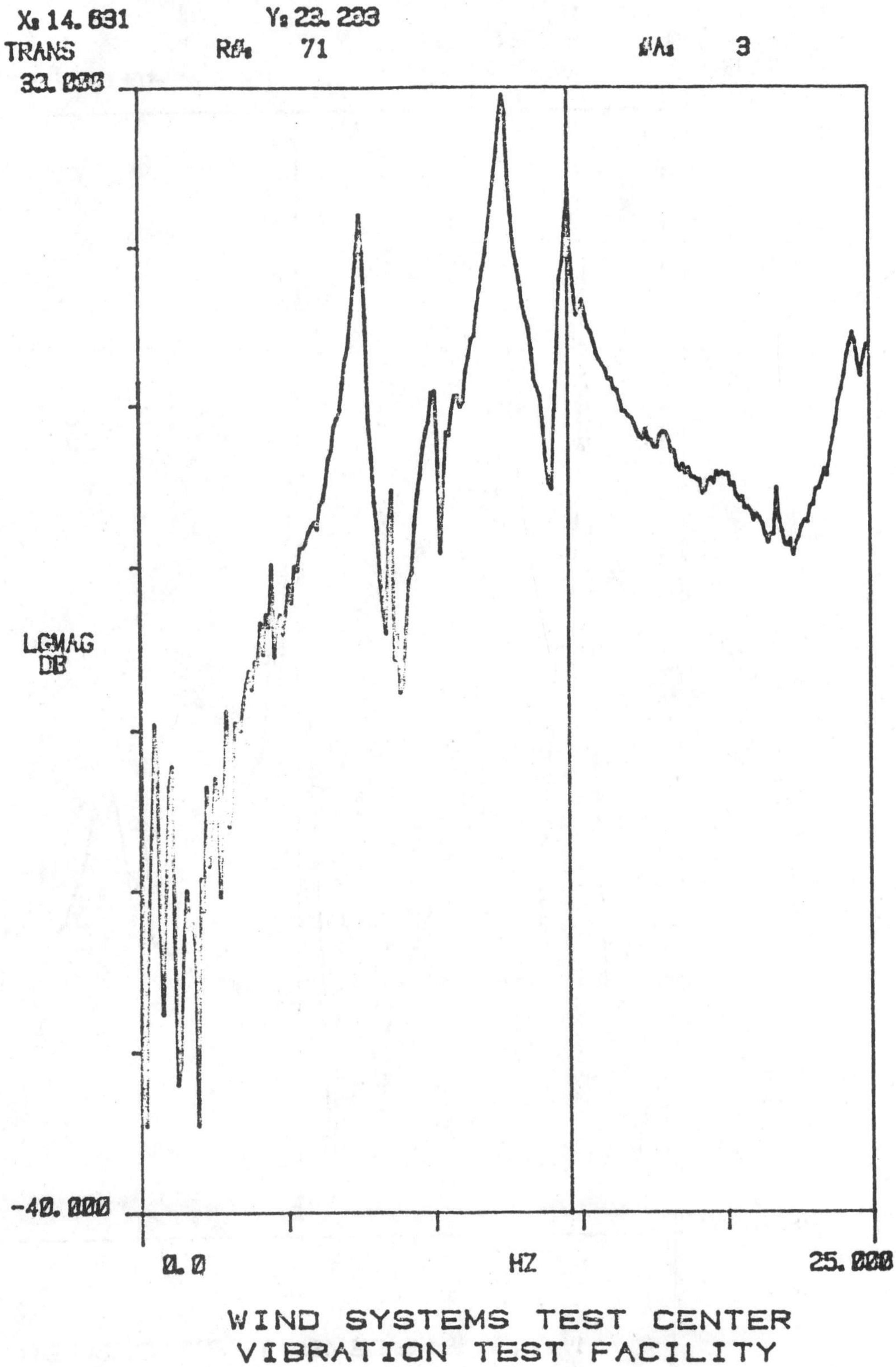

FIGURE 10

Transfer Function (Blade)

Blade 2 was tested, Blade 1 was also excited. The energy transfer between the two blades was visually observed during the test.

System Blades Removed (S5):

Based on the results of the previous two series of tests, a decision was made to remove the blades from the hub, thereby obtaining a clearer picture of the second mode of the system. As can be seen from Figure 11, the second was found to be 13.2 Hz.

TABLE II

SUMMARY OF TEST RESULTS

Component	Frequencies	Comments
Blade 1	FMB 14 Hz	Blade rigidly attached to test fixture.
Blade 2	FMB.15.3	Blade rigidly attached to test fixture.
	SMB 54 Hz	
	FMT 105.5 Hz	
Support Structure	FMB 6.2 Hz	
System (WTG/Tower)	FMB 3.1 Hz	Blades removed.
	SMB 13.2 Hz	
Blade 2	*FMT 7.5 Hz	Blades attached to hub atop the tower.
	FMB 12.3 Hz	

*Frequency of torsion arm and blade.

CONCLUSION/RECOMMENDATIONS

Based on the empirical data collected, the second bending of the system coincides too closely with first bending mode of the blades. This assessment is corroborated by observation of the WTG while in operation. The machine was seen to go through rather "violent" vibrations during operation. Figure 12 shows the machine's predominant modes of vibration while in operation, as can be seen 13.2 Hz was excited which was expected based on the previous tests.

It is the recommendation of the author that the support structure be reconfigured.

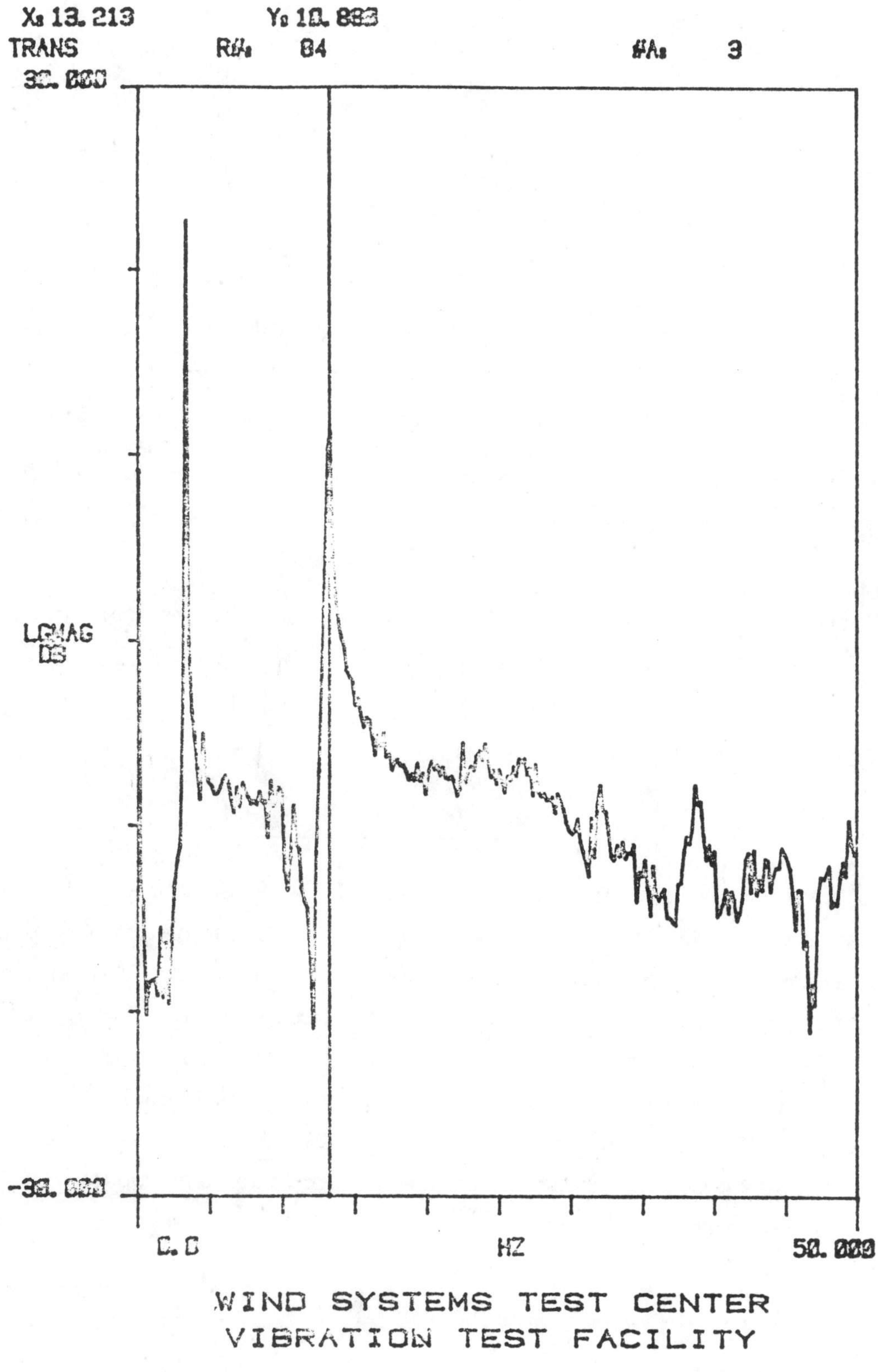

FIGURE 11

Transfer Function (System)

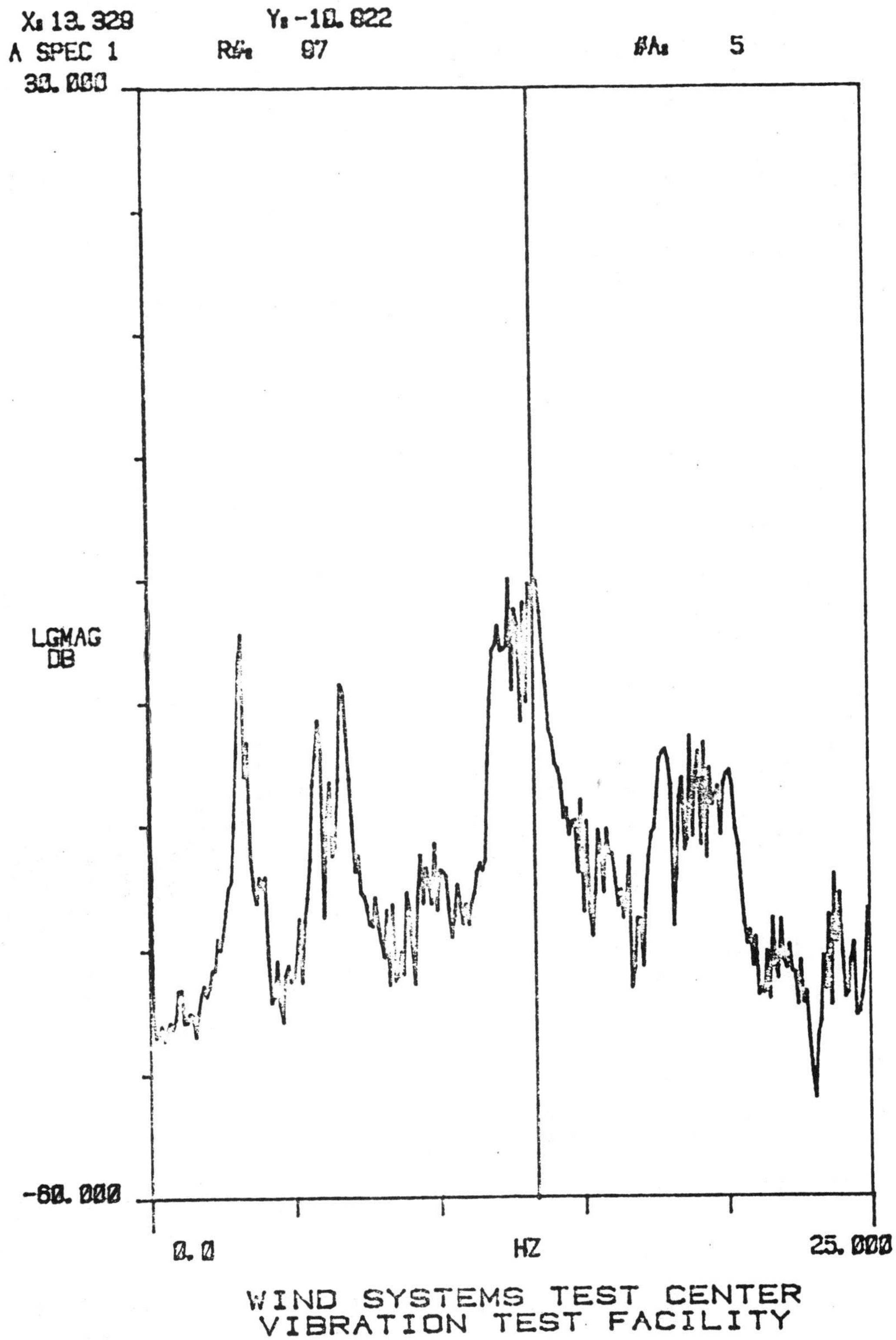

FIGURE 12

Auto Spectrum (WTG in Operation)

Possible options:

- Increase the tower height thereby reducing the first and (more importantly) the second mode resonant frequency.

- Increase weight at the tower top thereby reducing the first and second mode resonant frequencies.

- Change to a softer tower, perhaps a Rohn 45G. This would be done only after static loads were calculated.

Finally, it must be noted that these options are not all encompassing.

SYMBOLS

Auto	Auto Spectrum
DB	Decibel
FFT	Fast Fourier Transform
Hz	Hertz
LG	Log
Mag	Magnitude
S( )	Test Series (Number)
Trans	Transfer Function
ω	Frequency in Hertz

INDUCTION GENERATORS

G. P. Minges

November 5, 1979

INDUCTION GENERATORS

INTRODUCTION

Induction generators are being used in increasing numbers for wind turbine generator applications. This Technical Note describes some of the induction generator characteristics.

DISCUSSION OF RESULTS

The induction generator has several attractive features when a need for (non-stand alone) cogeneration exists. An induction generator does not normally require synchronization to put it on the line. Induction machines are cost effective since there is little or no difference between the induction generator and the mass produced induction motor. The induction generator is inherently safe from energizing a dead line since it draws its excitation for generation from the line.

The line supplied excitation of an induction machine allows the induction machine to automatically assume the line voltage and frequency and therefore, eliminates the need and cost of voltage and frequency controls. In a multiple phase application, care must be taken to assure proper phase rotation. Phase rotation of the induction machine does not automatically assume the line phase rotation. An induction generator draws leading magnetizing or excitation current from the line and it must be realized that this excitation can be supplied by other sources connected in the induction circuit. These sources might be static power factor, correction capacitors, motor start or run capacitors, and other synchronous machines. Any source of leading current connected to the terminals of an induction generator could cause it to build up and maintain a terminal voltage when supplied by a mechanical shaft input of almost any speed. In this case, it would be operating in a stand-alone mode with its terminal voltage and frequency determined by the prime mover speed.

An induction generator, as the name might imply, does have an inductive quality in that the moment its external source of excitation (normally the local utility) is removed, its terminal voltage decays over a finite period of time. During this time, line synchronization is lost. Also during this time, a reapplication of the line will lead to coupling of two non-synchronized sources resulting in above full rated mechanical and electrical transient conditions. These conditions must be expected and will be due to normal momentary outages of the local utility.

RECOMMENDATIONS

Testing of WTG induction machines should include the machine equivalent circuit and circle diagram for predicting and checking of machine operating characteristics. The equivalent circuit is also handy for interaction or computer modeling studies. The circle diagram and equivalent circuit can be determined from three tests performed on the machine. These tests are: the no-load test, the blocked rotor test and the stator resistance test. By classical textbook methods, an equivalent circuit and circle diagram can be determined.

EXPANDED COMPUTERIZED DATA ACQUISITION SYSTEMS

(ECDAS)

A. C. Hansen

December 11, 1979

ECDAS POLL INTERVAL

INTRODUCTION:

Some time ago, we decided that the ECDAS data poll rate should be reduced in light winds to reduce the annual data volume. I have re-evaluated the method discussed and this memo will summarize my findings. I feel the sampling should be done at two different rates. At wind speeds above the SWECS start-up speed, sampling should be at the standard 1 Hz rate. At speeds below start-up, the sample rate is not critical, 1 minute sample would be adequate if the right control strategy is used. The lowest start-up speed I can foresee is approximately 2.5 m/s (5.6 mph). At Rocky Flats, we can expect the wind to be above 2.5 m/s, roughly 60-75% of the time. Thus a 1 sec/1 minute sample rate strategy would reduce total data volume by 25-40%.

Control Options:

Several options are available for control of the poll rate. The table below lists four options along with their advantages and disadvantages.

RECOMMENDATIONS:

Based upon the advantages and disadvantages listed in the table, I would recommend we proceed in two steps: a) to bring the system on-line as soon as possible, we should begin with option IV (constant 1 Hz sample rate and storage of all data). The data volume will not pose a problem for several months and we will retain maximum control and flexibility. b) after the ECDAS is well established and we have broad experience with the data, we should implement option II. This option retains excellent control over the data and minimizes overhead on the Eclipse. If the NOVAs are not fast enough to do the averaging of light wind data, then option III should be pursued.

POLL RATE CONTROL OPTIONS

STRATEGY	ADVANTAGES	DISADVANTAGES
I. Change poll rate at NOVA based upon previous poll wind speed. (Original method)	o Most programming completed o Minimize work load on NOVA o Minimize data volume	o Minimal control means good data may be lost o Frequent switching of poll rates makes data analysis difficult
II. Poll at constant 1 Hz rate and let NOVA average low wind data before transmitting to Eclipse.	o Minimize Eclipse work load o Minimize data volume o Post-processing precludes loss of good data	o May over-burden NOVA o Greatest software effort
III. Poll at constant 1 Hz rate and transmit all data to Eclipse. Average low wind data before storing on tape	o Post-processing precludes loss of good data o Minimizes data volume o Places "number crunching" burden on the best "number cruncher"	o Increases Eclipse work load (and decreases analysis time availabi ity).
IV. Poll at constant 1 Hz rate and store all values	o Simplest to implement o Highest raw data retention	o High data volume

ADJUSTMENT OF SWECS POWER CURVES FOR AIR DENSITY VARIATIONS

A. C. Hansen

March 19, 1980

TABLES

FIGURES

ADJUSTMENT OF SWECS POWER CURVES FOR AIR DENSITY VARIATIONS

SUMMARY

Past methods for correcting SWECS power curves to standard sea level conditions have been shown to be inadequate. A new method is described which consists of adjustment to wind speeds near cut-in and adjustment to power output at all other wind speeds. Reynolds number and rotor/load matching effects, though possibly of significance in special limited situations, are not treated in the present density correction method.

INTRODUCTION

Air density affects the dynamic pressure and kinematic viscosity of the wind, and hence the power output performance of SWECS. When reporting SWECS performance, it is desirable that all test organizations report the performance that would be observed under standard density conditions. Thus, a method is needed to adjust Rocky Flats WSTC performance measurements to "standard day" conditions. This paper will discuss the density variations that will be observed at Rocky Flats, effects that air density variations will have on SWECS performance, possible methods for mathematically adjusting test results to standard conditions, and finally, the method that will be implemented at Rocky Flats.

DENSITY EFFECTS IN SWECS PERFORMANCE

The dynamic pressure and power density in the wind are both directly proportional to air density. That is:

$$\text{Dynamic pressure} = 1/2\, \rho V^2$$

$$\text{Power density} = 1/2\, \rho V^3$$

Where:

ρ = Air density.
V = Wind speed.

If a SWECS runs at constant efficiency (or power coefficient) the power output is also directly proportional to density.

$$P/A = Cp\ (1/2\, \rho V^3)$$

Where:

Cp = System power coefficient.
A = Rotor swept area.
P = System power output.

The dynamic pressure (and hence density) affects lift and drag forces on a rotor, and hence performance of a system, and must be considered when presenting performance testing results. But density can also affect the system power coefficient in at least two ways. To a first order approximation, a rotor power coefficient depends only upon the rotor tip speed ratio for a given rotor geometry. Thus, to first order, the power coefficient is independent of the density. But the Reynolds number of the flow through the rotor is linearly proportional to air density and airfoil lift, and drag coefficients are at least mildly influenced by Reynolds number. Therefore, the rotor efficiency can be mildly influenced by density variations. Under typical SWECS operating conditions, an order-of-magnitude change in Reynolds number is required to observe a significant impact on performance. The exception would be a small rotor (3-5 m diameter) operating very near its critical Reynolds number. In that situation, a 10-20% change in density could produce a similar change in power coefficient. It must be noted, however, that a rotor should not be designed to operate near the critical Reynolds number. Thus, Reynolds number effects should not be significant for systems designed to operate efficiently in the varied climate across the continental United States.

The second means by which density can influence system power coefficient could conceivably be important in some variable speed SWECS. A match between rotor power output and load (the generator load on the rotor) is critical to optimum rotor performance. Over- or under-loading a rotor will cause it to run at a nonoptimum tip speed ratio and can, in extreme cases, essentially stop the rotor. Since the generator load depends only upon rotor speed (for a given generator control system) and the rotor power depends upon air density as well as rotor speed, density variations can result in rotor/load mismatch. This rotor/load match effect is highly dependent upon the specific system configuration and not amenable to generalized adjustment techniques.

Since the Reynolds number effects are generally of second order importance, and the rotor/load match effects, though possibly important in special cases, are not amenable to a generalized density adjustment, the remainder of this document will treat only the density corrections due to dynamic pressure effects.

EXPECTED DENSITY VARIATIONS

The Rocky Flats Test Center is at 1,860 m (6,100 ft) MSL and has a standard atmosphere pressure of 23.90 in.Hg. Seasonal and daily variations in air temperature and pressure result in significant variations in ambient air density (referred to simply as density in the remainder of this paper) over the period of test of any given SWECS. Table I shows the range of densities that are observed at Rocky Flats and some ratios between commonly observed Rocky Flats and standard-day sea level conditions. The standard-day conditions at sea level have a density ranging from 1.1 to 1.4 times the observable Rocky Flats conditions. This wide variation provides an opportunity for eventually testing the density correction method proposed later in this report.

ALTERNATIVE CORRECTION METHODS

The method in past common use assumes that the power at a given wind speed can be adjusted by simple multiplication of the power by the density ratio. That is:

$$P_1 = P_2 (\rho_1/\rho_2).$$

TABLE I

Density Variations at Rocky Flats WSTC

Condition	Temp. (°C)	Pressure (in.Hg)	Density (kg/m^3)	Density Ratio Sea Level/ Rocky Flats
Standard (sea level)	15	29.92	1.226	1.0
Standard (1,860 m)	3	23.90	1.022	1.20
Typical Day	15	23.9	.977	1.25
Summer Extreme	38	23.0	.873	1.40
Winter Extreme	-18	25.0	1.156	1.06
Typical Summer Day	30	24.0	.932	1.32
Typical Winter Day	0	24.0	1.033	1.19

This means that power output measured on a typical day at Rocky Flats must be multiplied by 1.25 to determine the output that would be measured on a standard day at sea level. Though simple to apply and understand, this method has two major drawbacks. First, though it is known that cut-in speed is a function of density, the common adjustment method changes only the power. Clearly the cut-in speed cannot be adjusted by a power correction multiplier. Second, the maximum output of many SWECS is limited by controls or generator capacity rather than aerodynamic limits. Thus, the common power multiplier method may predict a maximum power output greater than the system capacity. It can be concluded that the common correction method is always inaccurate at speeds near the SWECS cut-in speed and often inaccurate near the cut-out speed.

An alternative to an adjustment to the power output would be an adjustment to the wind speed for a given power output. The adjustment might consist of shifting the power curve along the wind speed axis by an amount calculated from the slope of the measured power/wind speed relationship. This method would change the cut-in speed and would not over-predict power in high winds. But the method has one serious flaw for SWECS whose maximum power output is limited by aerodynamic rather than generator capacities. Many stall-controlled rotors are aerodynamically limited and would produce greater power in air at standard conditions. The second method of density correction would not predict this increase due to density change at the maximum power point of the power curve. Thus, the second method is not universally applicable to all SWECS.

At this writing, there is no apparent single, simple, universal method for adjusting a power curve to standard sea level conditions. The only method which offers sufficient accuracy does so at the expense of lost simplicity.

THE PRESENT ADJUSTMENT METHOD AT ROCKY FLATS

The sea level correction method which will be used on all SWECS at Rocky Flats WSTC is a composite of the methods previously discussed. The new method is summarized in Figure 1.

Each SWECS has a maximum power output capability regardless of air density. This maximum power (P_{max}) will generally be limited by the generator size and controls. The correction method must not yield a power output greater than P_{max}. At wind speeds above the speed at which 10% of P_{max} is generated ($V_{10\%}$), the common power correction method is used, provided P_{max} is not exceeded. Hence for:

$$V > V_{10\%}$$

$$P_{s.c.} = P_{r.f.} \times \frac{(\text{Density})s.c.}{(\text{Density})r.f.}$$

<u>or</u>

$$P_{s.c.} = P_{max}, \text{ whichever is less.}$$

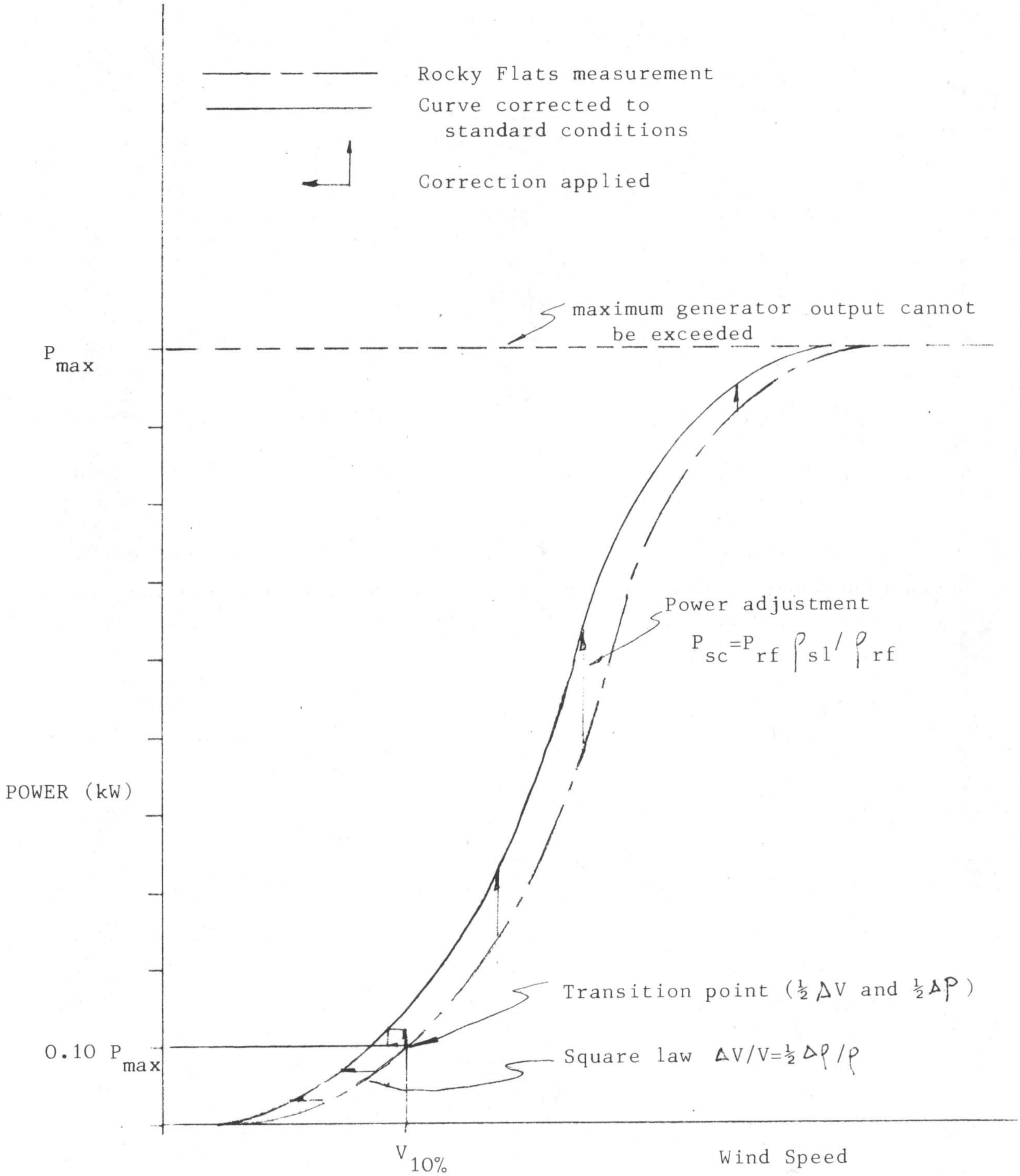

Figure 1

Correction of Rocky Flats
power curves to standard sea level conditions.

Where:

$P_{s.c.}$ = Power corrected to standard conditions.

$P_{r.f.}$ = Power measured at Rocky Flats.

$Density_{s.c.}$ = 1.226 kg/m^3.

$Density_{r.f.}$ = Actual density at Rocky Flats when $P_{r.f.}$ was measured.

P_{max} must be obtained from dynamometer testing or long term atmospheric testing for each SWECS. At wind speeds near cut-in ($V < V_{10\%}$) the wind speed rather than the power output must be adjusted. Since startup of a SWECS rotor depends on the dynamic pressure of the wind, a V^2 correction is applied. To maintain a constant dynamic pressure when a density change, $\Delta\rho$, is applied, a change of wind speed, $\Delta V \approx -(1/2\ \Delta\rho/\rho)V$, must be applied. Hence for:

$$V < V_{10\%}$$

$$\frac{V_{s.c.} - V_{r.f.}}{V_{r.f.}} = \frac{-1}{2}\left[\frac{Density_{s.c.} - Density_{r.f.}}{Density\ r.f.}\right]$$

To smooth the transition between the two correction methods at $V_{10\%}$, a correction equal to one-half the standard velocity correction and one-half the standard power correction is applied at $V = V_{10\%}$.

DYNAMOMETER TEST RESULTS

OF THE

1/3 UTRC INDUCTION GENERATOR AND GEARBOX

G. D. Price

April 1980

TABLES

FIGURES

DYNAMOMETER TEST RESULTS

OF THE

1/3 UTRC INDUCTION GENERATOR AND GEARBOX

SUMMARY

The dynamometer test of the 1/3 UTRC induction generator system provided data to determine machine output and performance curves. The two horsepower induction motor will generate up to two thousand watts of power into a three-phase utility system when driven above its synchronous speed of 1,800 revolutions per minute. A system efficiency (gearbox and generator) of 73 percent was attained. The generator draws excitation current from the utility system. Power factor remained at or below 66%. 1,827 reactive volt amperes was measured at 1,595 watts output, which is approximately rated output. 520 inch pounds of torque was required to drive the system at rated output. Other performance data is shown in curves included with this report.

INTRODUCTION

This report covers the dynamometer test of the United Technologies Research Institute (UTRC) 1/3-scale wind generator system. The generator is a standard three-phase induction motor with a squirrel cage rotor. The system is designed to interface directly with a 208-, 230-, or 480-volt (V) line-to-line three-phase utility system. An electrical contactor between the induction generator and utility system closes when the wind velocity is sufficient to drive the generator above synchronous speed (1,800 rpm). A speed sensor on the generator shaft will brake the wind system if it overspeeds (approximately 1,900 rpm). A gearbox with a 5.25:1 ratio steps up the input shaft speed to the generator.

Nameplate data for the induction generator and gearbox is listed in Table I. This information is as stamped on the equipment and does not reflect test results. Discrepancies are shown in test results.

Code rating determines the expected maximum current inrush when starting motor from standstill or under locked rotor. "Code H" rates the induction motor at 6.30 to 7.09 kVA per horsepower.[1]

Service factor requires the induction motor to operate safely at 115% of rated horsepower.[2] The motor must also be protected by an overcurrent device rated to trip at no more than 125% of rated current.[3] Class A insulation allows an operating temperature of 105°C (40°C ambient + 65°C rise).[4]

Synchronous speed of the four pole machine is 1,800 rpm (Ns = 120 x F/P). The phase rotation is A-B-C. A ratchet on the generator shaft permits rotation in only one direction. The nameplate gearbox ratio of 5.06 was found to be incorrect and measured at 5.25:1. The speed sensor on the rear generator shaft was damaged. It was removed because of an unbalanced slotted wheel.

---

[1] NEC (National Electric Code) 1978, Art. 430-7, Table 430-7(b), p. 290.
[2] NEMA (National Electrical Manufacturers Association) 1970, MGI-12.47a.
[3] NEC 1978, Art. 430-32(a)(1), p. 297.
[4] NEMA, 1970, NGI-12.41.

TABLE I

NAMEPLATE DATA

FOR

1/3 UTRC INDUCTION GENERATOR

Generator:	Baldor Industrial Motor (induction type)
	Cat. No. VWM 3157 T
	Spec. No. 35BOS-754
	Frame 145TC Ser. 1078
	3 Phase, 9 Leads
	Rating: 2 hp
	Volts: 208-230/460
	Amps: 6.8-6.4/3.2
	Rpm: 1,725
	Full Load Efficiency: 80%
	Power Factor: 71%
	Class: A
	Code: H
	Ser F: 1.15
Gearbox:	Dresser, Electra Motors
	Model 8E 640676 QI
	Frame 6410C5
	Ratio - 5.06:1

OBJECTIVES

The objectives of the dynamometer test are to determine the electrical operating characteristics of the induction generator. The gearbox ratio and efficiency are measured. Balance and vibration at operating speeds are checked. Locked rotor and no load motor tests are performed to develop an equivalent circuit and plot a circle diagram. The circle diagram may be used to give a quick reference to voltage, current, power factor, and efficiency at any motor or generator operating point. Output curves are plotted from the following test data: speed, watts, vars, horsepower, power factor, torque, and efficiencies of the generator and gearbox.

TEST DESCRIPTION

The initial motor test was set up as in Figure 1. The induction machine was uncoupled and operated at full voltage (208 line-to-line) and no load. The motor ran freely until bearings and windings were warmed up to a normal operating temperature and conditions were stable. The no load speed was 1,795 rpm. Average line current was 3.16 amps. Total watt input was 164.

The locked rotor test was performed by reversing two leads to the motor and using the ratchet to prevent rotation. Reduced voltage was applied through variacs to limit the current to rated values; 5.53 amps was measured per line (average) with 41 volts applied (line to line). Power flow was 242 watts. The power factor was 62% or 52° lagging (watts/ $\sqrt{3}$ VI = Cos θ). Figure 2 shows generator test set up.

RESULTS

The equivalent resistance of 2.63 ohms was calculated from blocked rotor tests.

$$r_e = 242/3(5.53)^2 \text{ ohms per phase}$$
$$r_e = W_{BR}/3(I_{BR})^2 \text{ ohms per phase}$$

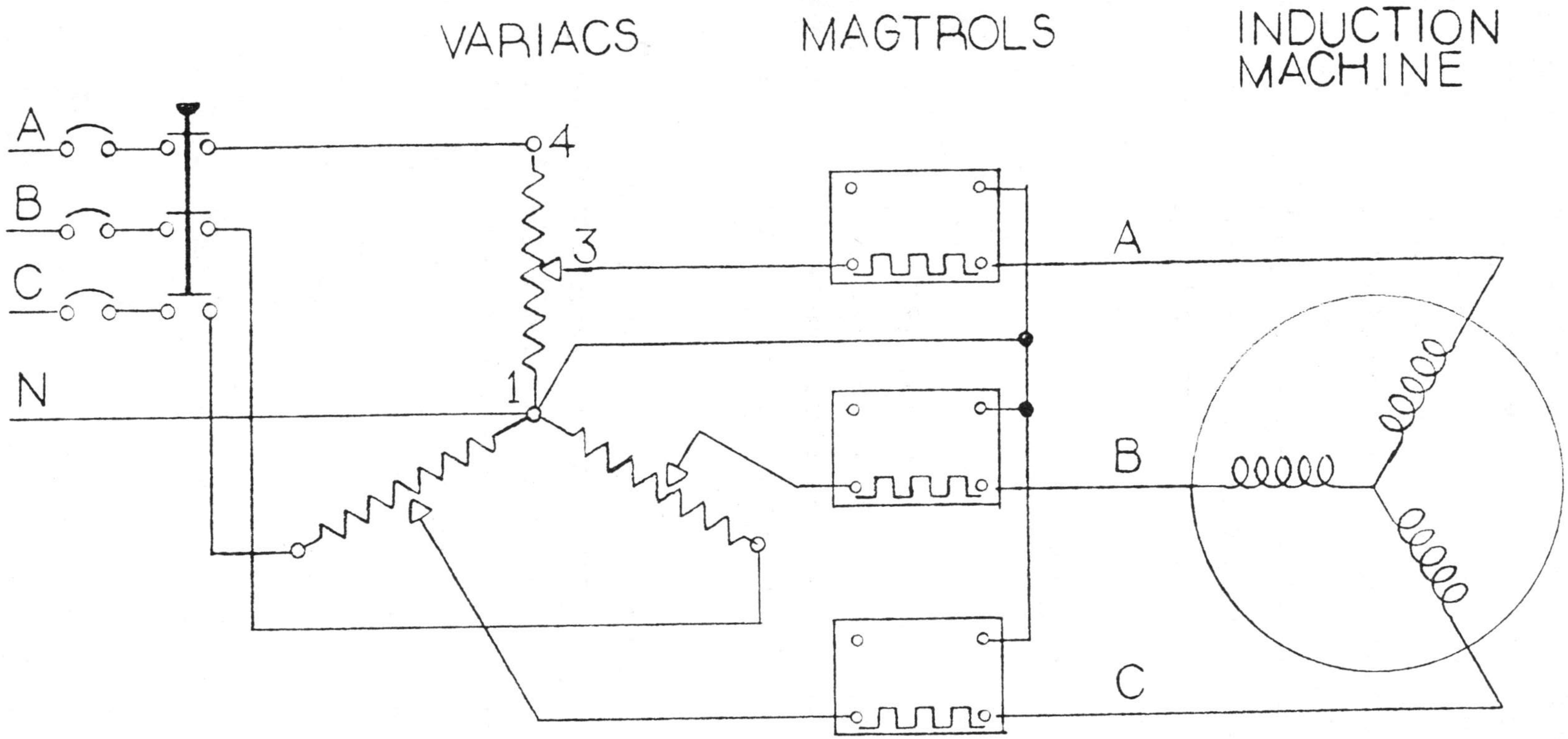

FIGURE 1

INDUCTION GENERATOR TEST

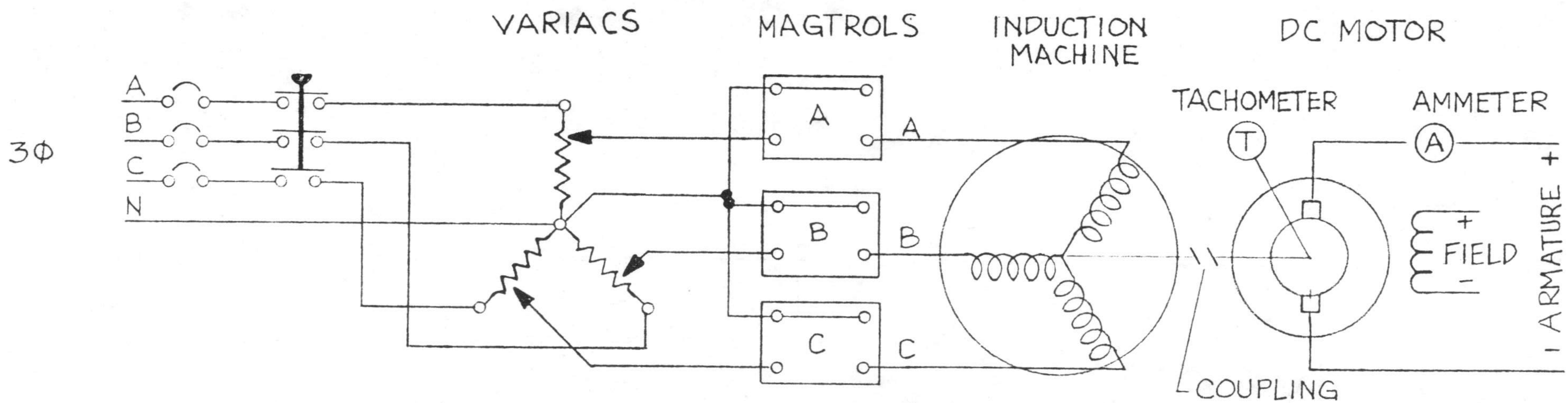

FIGURE 2

INDUCTION GENERATOR TEST

Stray power losses are constant and independent of machine speed or output. Friction and windage losses are included in stray power; 85 watts of stray power was calculated from the no load test data.

$$SP = 164 - 3(3.16)^2\ (2.63) \text{ watts}$$
$$SP = W_{NL} - 3(I_{NL})^2\ r_e \text{ watts}$$

The static stator resistance was determined by applying a dc voltage, measuring the current flow and applying ohms law. The winding was assumed to be wye connected.

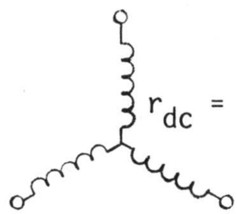

r_{dc} = 1.4 ohms per phase

AC resistance may be estimated to be 1.4 times dc resistance.[5] r_{ac} = 2.0 ohms per phase.

An equivalent circuit is derived from the resistance, no load, and blocked rotor tests. Voltage E, and current I, shown in Figure 3 are at the machine stator terminals. E_2 and I_2 are the voltage and current in the rotor. "a" is an operator equivalent to $1\angle 120°$ and "a^2" is equal to $1\angle 240°$. They represent the phase shift between the stator and rotor. "j" is another operator of unit magnitude and +90° ($1\angle 90°$). "s" is the slip and equal to $(N_s - N)/N_s$ where N_s is the synchronous speed and N is the operating speed.

AC resistance per phase R_1 was determined to be 2.0 ohms. The stator iron resistance R_{fe} is calculated from no load test data. Total no load power per phase was 54.7 watts ($W_{NL}/3$). Power in R_1 was 20.2 watts ($I_{NL}^2\ R_1$). The remaining power was dissipated in R_{fe}:

$$P = 54.7 - 20.2 = 34.5 \text{ watts}$$
$$R_{fe} = \frac{V\phi^2}{P} = (117)^2/34.5 = 397 \text{ ohms}$$

[5] Direct and Alternating Current Machinery, Rosenblatt, Friedman, 1963, p. 242.

EQUIVALENT CIRCUIT

1/3 UTRC INDUCTION GENERATOR

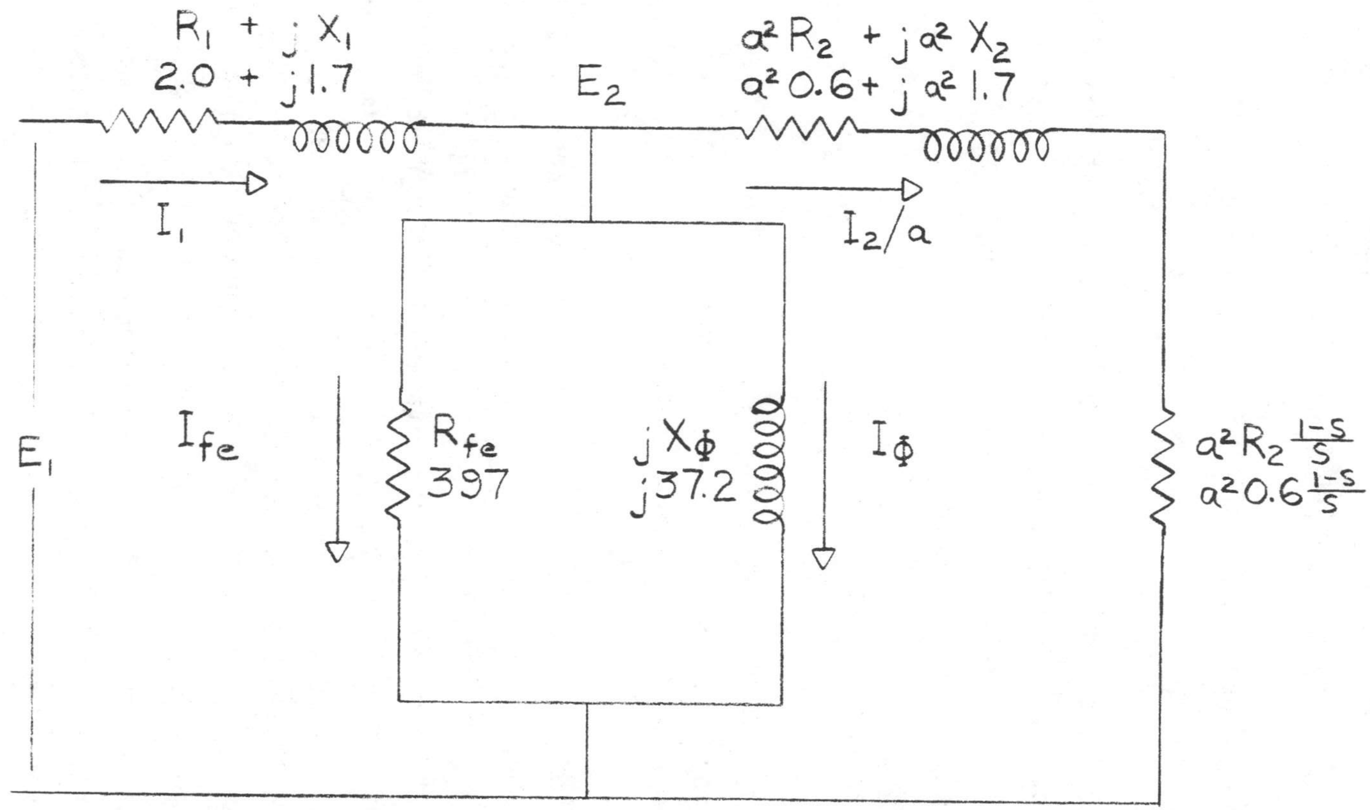

FIGURE 3

Current in R_{fe} was 0.29 amps (34.5 watts/117 volts), the magnetizing current $I\emptyset$ was 3.15 amps,

$$I_{\emptyset} = [I_{NL}^2 - I_{fe}^2]^{1/2}$$

and $X\emptyset$ is 37.2 ohms.

$$X_{\emptyset} = \frac{V\emptyset}{I\emptyset}$$

Blocked rotor test data was used to determine the rotor equivalent circuit. Equivalent impedance Zeq was 4.3 ohms.

$$Z_{eq} = V_{BR}/\sqrt{3}(I_{BR})$$

Equivalent resistance r_{eq} was 2.62 ohms.

$$r_{eq} = W_{BR}/3\ I_{BR}^2$$

Then equivalent reactance X_{eq} was 3.36 ohms.

$$X_{eq} = [Z_{eq}^2 - r_{eq}^2]^{1/2}$$

The rotor and stator reactances are assumed to be equal $X_1 = X_2 = 1/2\ X_{eq} = 1.7$ ohms. Rotor resistance is the equivalent resistance r_{eq} less the stator resistance $(R_2 = r_{eq} - R_1)$.

The circle diagram was constructed from no load and blocked rotor data. It is shown in Figure 4. Vector $\overline{ON}$ represents no load current magnitude and angle $\emptyset$ is the no load power factor angle.

$$\text{p.f.} = \frac{W}{\sqrt{3}VI} \qquad \emptyset = \cos^{-1}(\text{p.f.})$$

$$\overline{ON} = 3.16\ \angle 82^\circ \text{ amps}$$

Vector $\overline{OB}$ is the blocked rotor current magnitude. Angle θ is the blocked rotor power factor angle.

$$\text{p.f.} = \frac{W}{\sqrt{3}VI} \qquad \theta = \cos^{-1}(\text{p.f.})$$

$$\overline{OB} = 28.2\ \angle 52^\circ \text{ amps}$$

CIRCLE DIAGRAM

1/3 UTRC INDUCTION GENERATOR

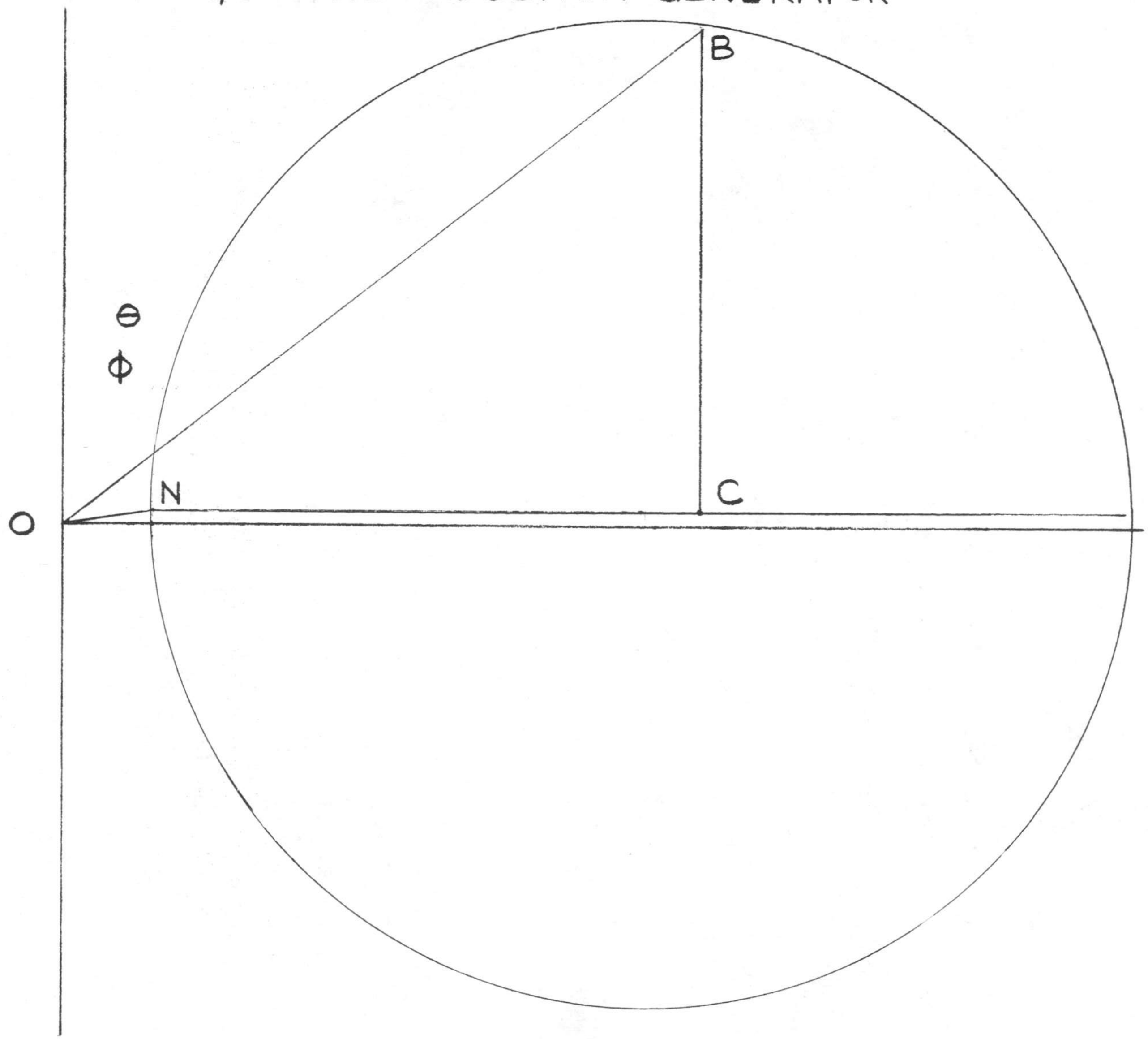

FIGURE 4

28.2 amps at 208 volts was extrapolated from the blocked rotor data of 5.53 amps at 41 volts. From points B and N which are points on the circumfrence and line NC on which lies the center, the circle is constructed.

Efficiency of the generator is the ratio of watt output over watt input. The output power is read directly from the Magtrols in the generator output circuit. Input power is output power plus calculated losses.

$$Win = Wout + \text{copper losses} + \text{stray power losses}$$

Stray power losses are a constant 85 watts. Copper loss varies with current squared.

$$C.L. = 3\ I^2\ r_{eq}\ \text{watts}$$

Efficiency of the gearbox was determined from measured torque input, speed, and generator input.

$$Win = hp \times 746 \text{ watts and}$$
$$hp = \text{torque} \times rpm/63{,}024$$

Gearbox efficiency is equal to the ratio of generator input watts to gearbox input in watts. System efficiency is the ratio of generator watt output to gearbox watt input. At rated output, gearbox, generator, and system efficiency was 94%, 78%, and 73%, respectively. Efficiency curves are plotted versus speed in Figure 5.

Output curves are plotted in Figure 6. At rated output of 6.8 amps, the machine generated 1,595 watts or 2.1 horsepower. Reactive volt-amperes (VARS) at rated output was 1,827 and supplied by the utility. The power factor therefore was 66% or 49 degrees lagging.

$$p.f. = \text{watts}/\sqrt{3}VI = \cos\theta$$

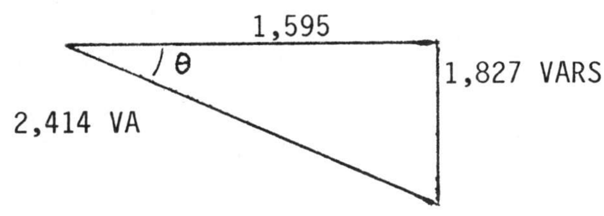

EFFICIENCY CURVES

1/3 UTRC INDUCTION GENERATOR

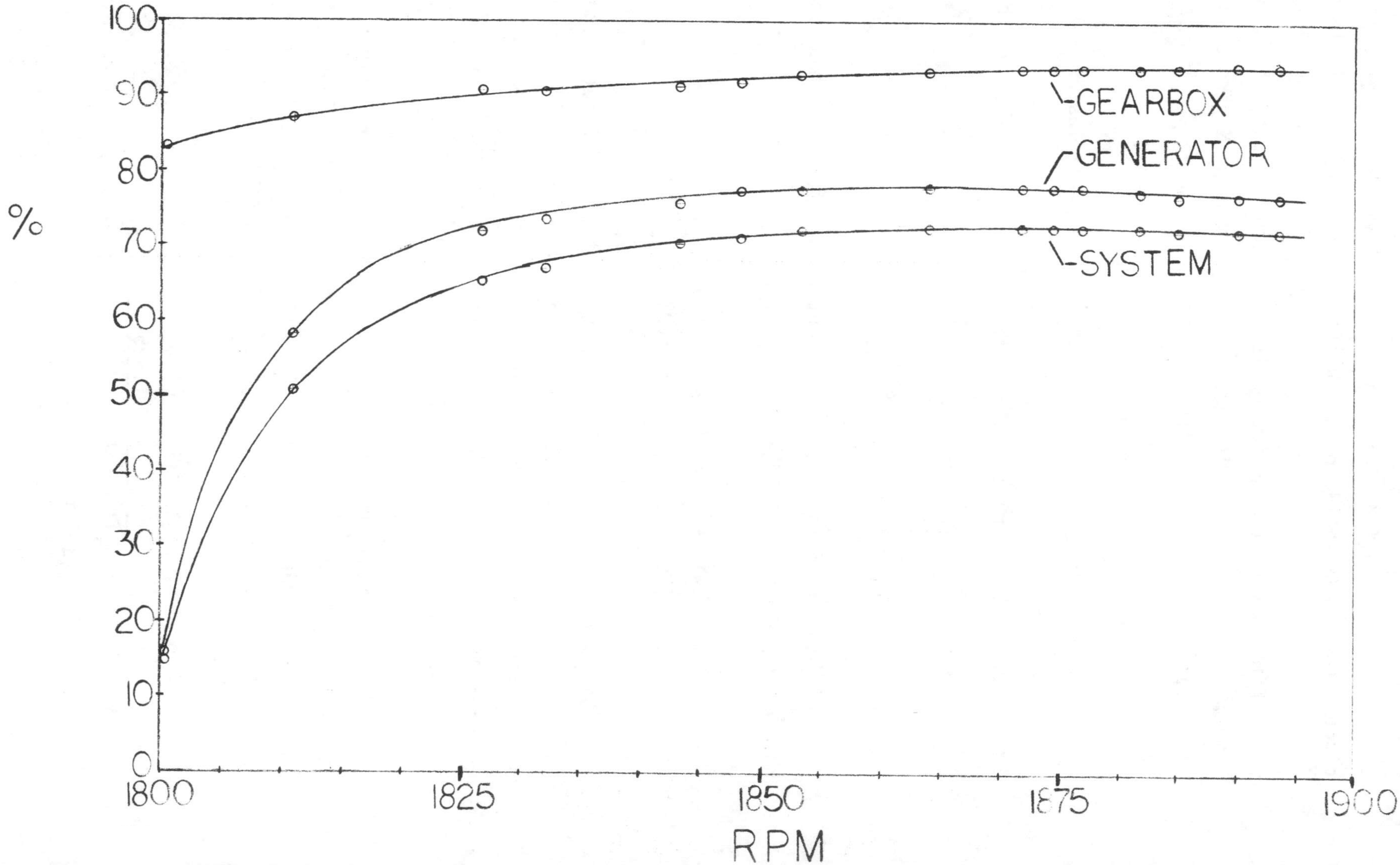

FIGURE 5

OUTPUT CURVES
1/3 UTRC INDUCTION GENERATOR

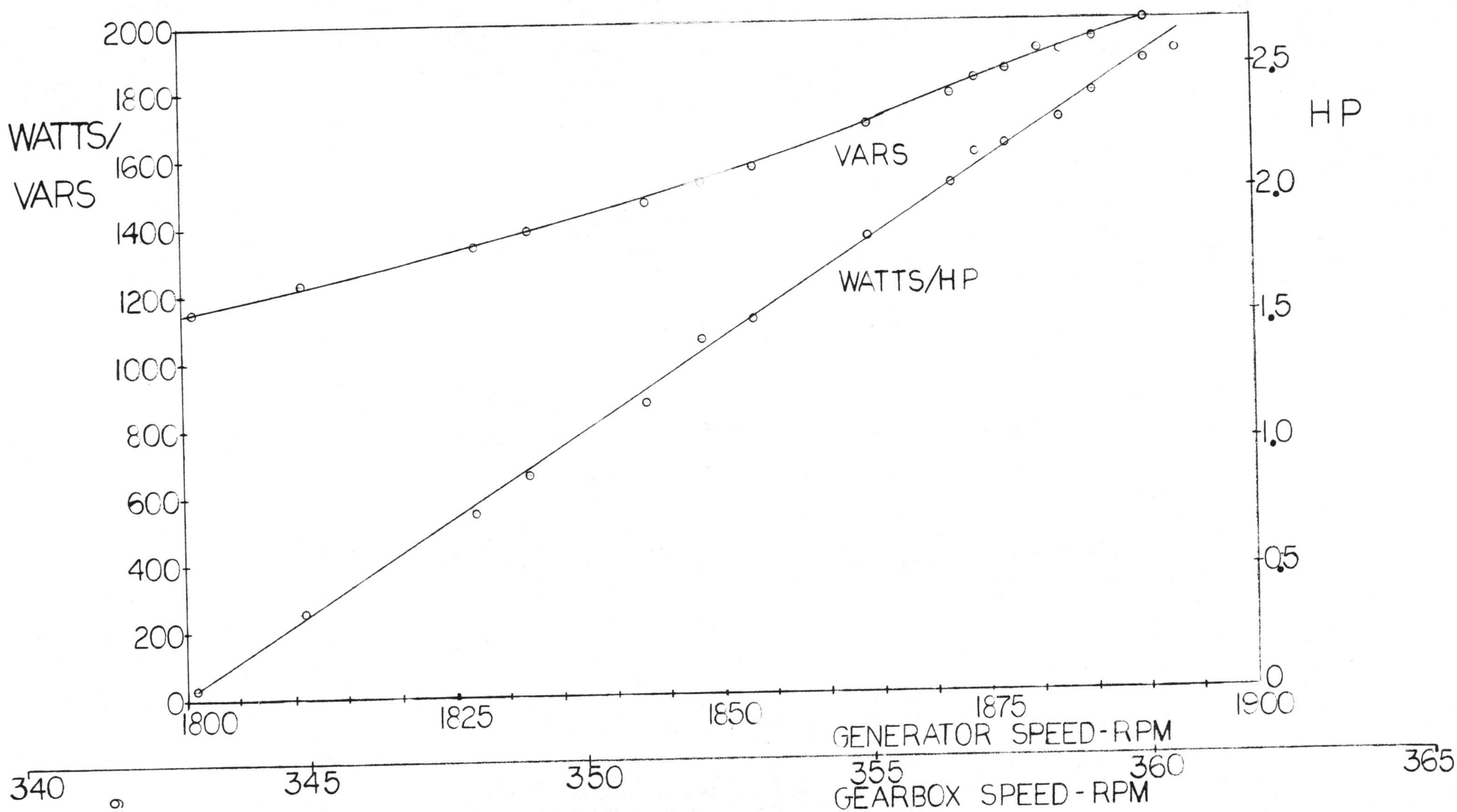

FIGURE 6

A power factor curve is plotted in Figure 7. Speed at rated output was 1,874 rpm or 357 rpm at gearbox input shaft. Power losses are shown in Figure 8 with the output versus speed curve. A copper loss of 370 watts and stray power loss of 85 watts was calculated at rated speed.

The torque speed curve in Figure 9 shows the measured torque input versus generator speed. The relationship was nearly linear in the operating speed range. 520 inch pounds was required to drive the gearbox and generator at rated output.

CONCLUSIONS

The induction generator used with the 1/3 UTRC wind system operated closely to its motor nameplate data. The power factor was 8% less than nameplate. Efficiency of 78% was close to the 80% nameplate data. It must be kept in mind these comparisons are generator operation to motor operation at rated motor input values.

The gearbox operated at 94% efficiency at rated speed and about 83% at cut-in speed (1,800 rpm). The gear ratio was incorrectly listed on the nameplate and found to be 5.25 to 1. The overspeed sensor caused a vibration on the generator shaft and should be balanced on the shaft before operation.

POWER FACTOR
1/3 UTRC INDUCTION GENERATOR

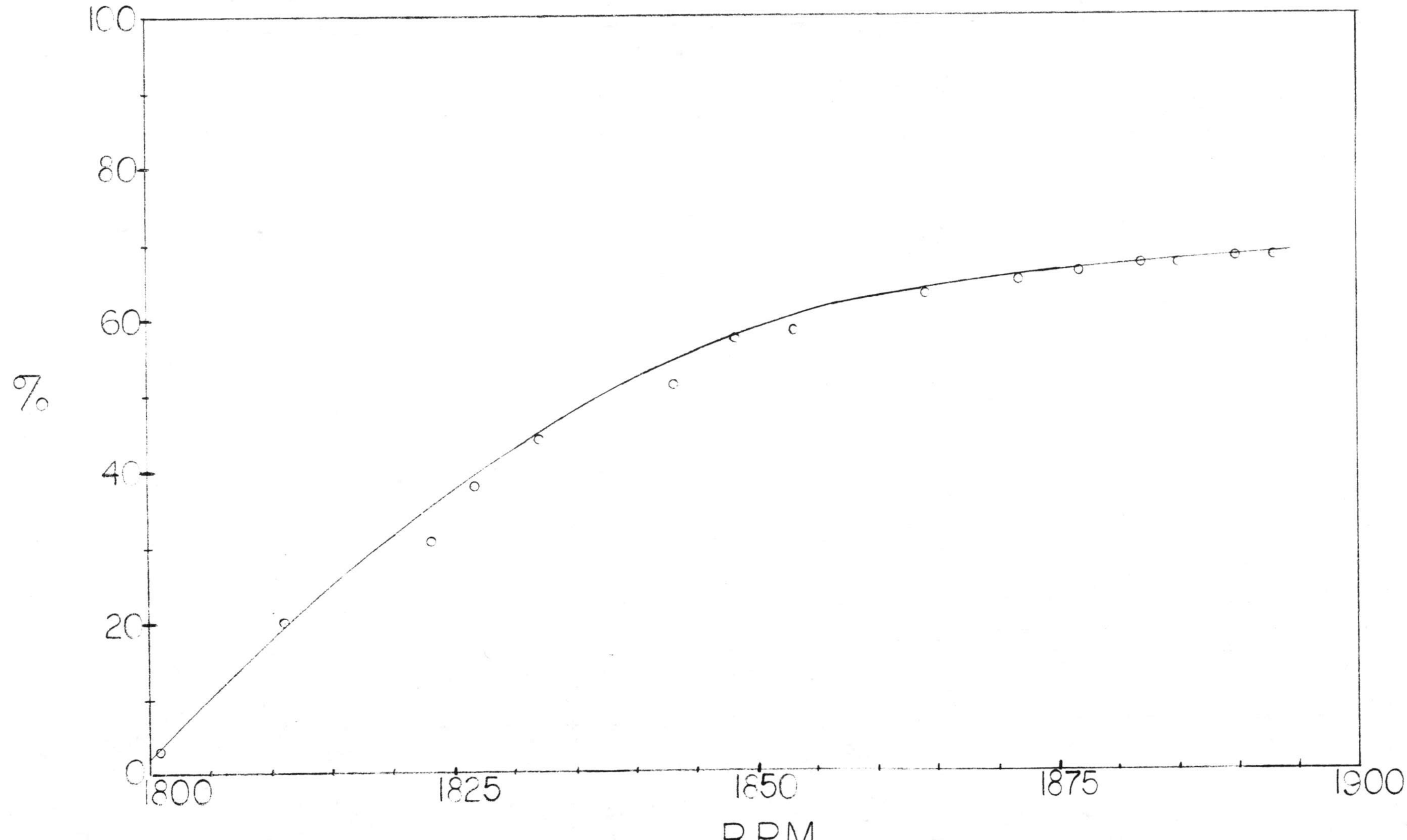

FIGURE 7

POWER CURVES

1/3 UTRC INDUCTION GENERATOR

FIGURE 8

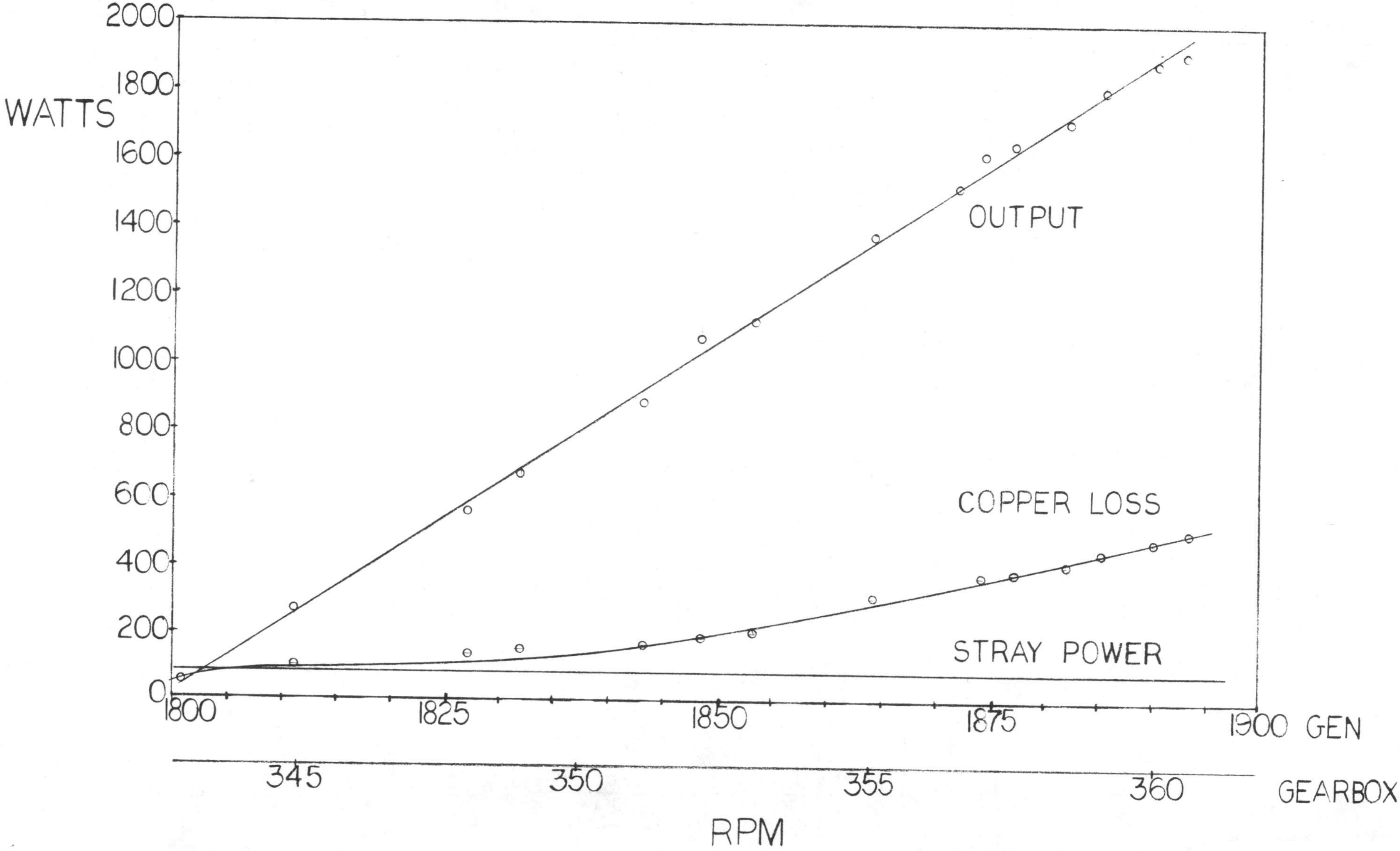

TORQUE-SPEED CURVE

1/3 UTRC INDUCTION GENERATOR

FIGURE 9

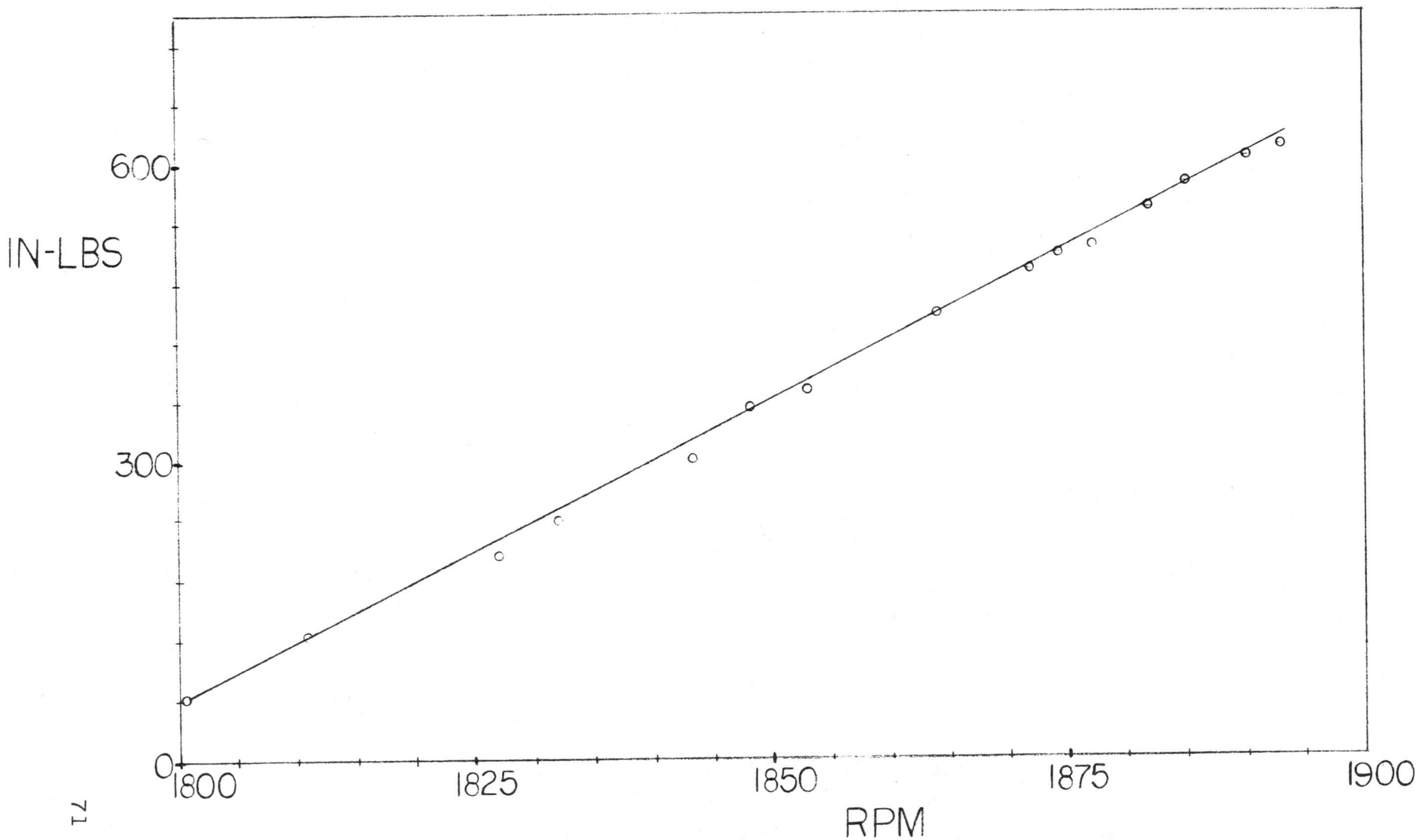

SYMBOLS

Ø	-	Magnetizing or reactive component of electrical current or impedance.
a	-	An operator equal to unity and phase angle of 120 electrical degrees.
a^2	-	An operator equal to unity and phase angle of 240 electrical degrees.
j	-	An operator equal to unit magnitude and a phase angle of 90 electrical degrees.
N	-	Speed.
S	-	Slip or ratio of the difference in speed and synchronous speed to synchronous speed.
θ, Φ	-	Phase angle of current to reference voltage.
	-	Shunt element.
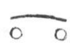	-	Circuit breaker.
PF	-	Power factor.
T	-	Torque in inch pounds.
VARS	-	Reactive volt-amperes.

OPTICAL RPM SENSORS

S. L. West

June 1980

FIGURES

OPTICAL RPM SENSORS

INTRODUCTION

Optical sensing devices are presently being used at the Rocky Flats Small Wind Systems Test Center (WSTC) for the collection of wind turbine generator (WTG) rpm data. These sensors, along with magnetic pickup transducers, are the primary source of rpm data at the WSTC. Optical sensors are readily available and inexpensive with high sensitivity that permits direct interface with TTL logic.

DISCUSSION OF RESULTS

Optical sensors work on interrupted or reflective light principles (Figures 1 and 2). The interrupted light method requires the installation of a slotted disc on a revolving shaft, while the reflective device senses white surfaces against a black background in a subdued ambient light environment. The reflective mode has the advantage of durability, as it can be mounted up to 1.0 cm from a rotating shaft or coupling. The electronic circuitry required for both techniques is simple and straightforward through the use of a Schmidt trigger (7413 chip with inherent hysteresis). The 7413 is a dual chip that allows dual outputs: one for data collection and one for digital displays, printers, etc. Its output is a "clean" 5 volt squarewave signal (Figure 3). The electronics developed for the optical sensors can also lend themselves to the wave-shaping of magnetic pickup transducers. This quality is demonstrated by the Dakota WTG which is presently collecting rpm data with a magnetic pickup using a waveshaping trigger originally fabricated for an optical sensor on the Enertech 1500.

Optical sensors are presently used at the WSTC in the following applications:

1) An interrupted light sensor with 60 slotted disc is used for high resolution rpm readout in the Dynamometer Testing Facility (Figure 4).

2) An interrupted light sensor using 30 slotted disc is mounted on the high speed side of the Storm Master WTG gearbox.

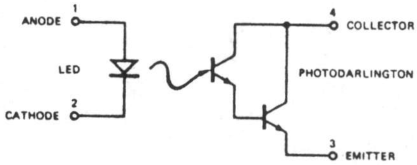

Figure 1

Interrupted Light Sensor

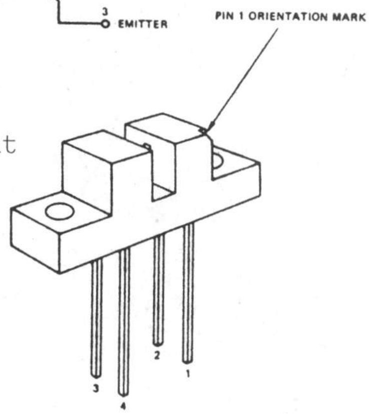

Figure 2

Reflective Object Sensor

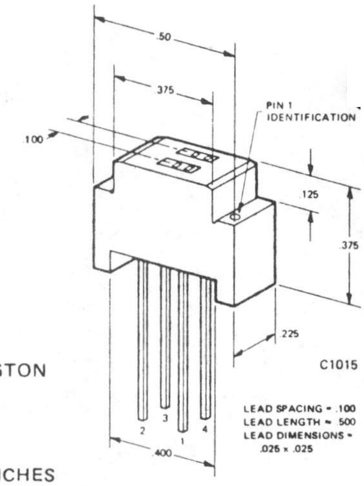

PIN 1 ANODE } LED
2 CATHODE
3 COLLECTOR } PHOTO-DARLINGTON
4 EMITTER

ALL DIMENSIONS ARE IN INCHES

Figure 3

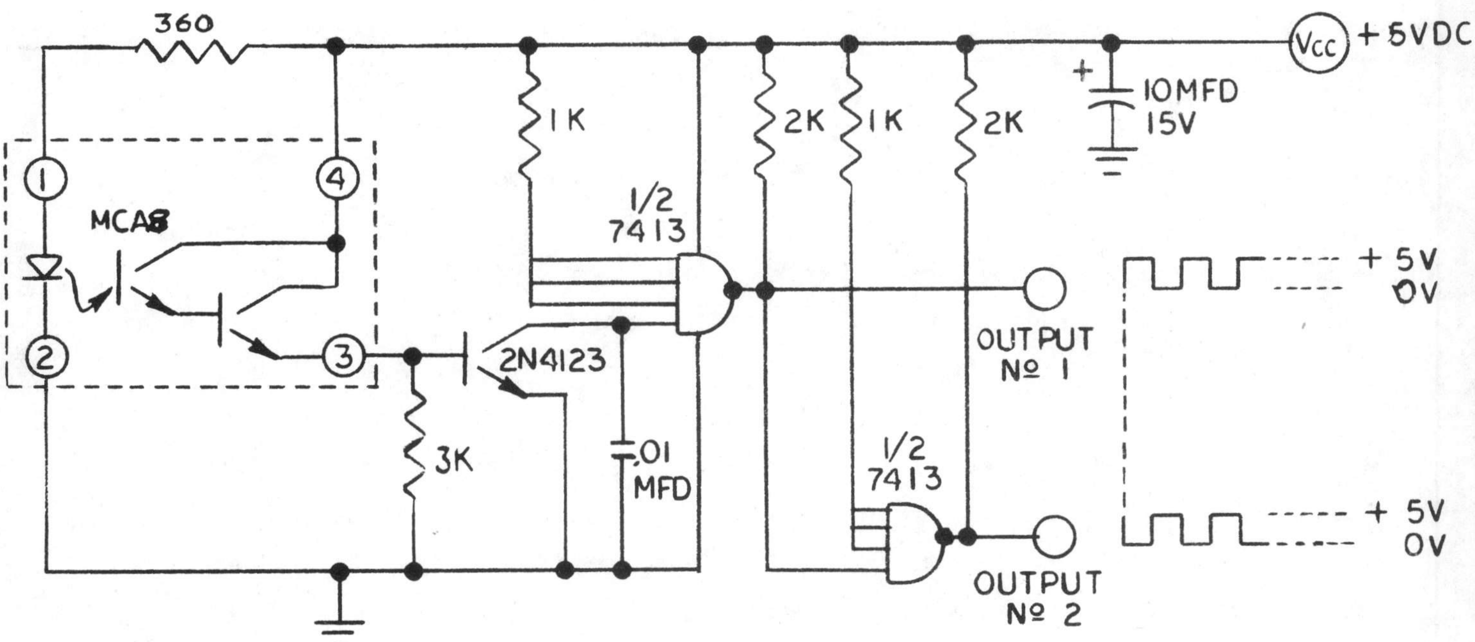

Figure 4

Light Sensor

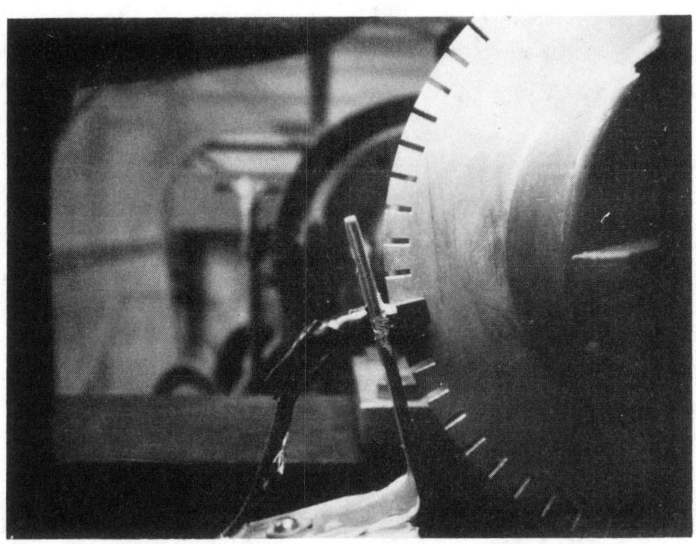

3) The Enertech 1500 has an inspection hole over the coupling between the gearbox and motor. This coupling was given a black paint job with the addition of six white stripes. Then, a simple holding bracket for the reflective sensor was inserted through the inspection hole, thereby, placing the sensor approximately 0.5 cm from the revolving coupling.

RECOMMENDATIONS:

In some situations, especially where magnetic transducers with their geartooth requirements prove to be cumbersome due to space limitations and labor requirements, optical sensing devices can be more feasible than magnetic pickup transducers. They have proven to be reliable and durable while in use at the WSTC.

DYNAMOMETER TEST RESULTS OF THE NORTH WIND HIGH-RELIABILITY PROTOTYPE WIND TURBINE GENERATOR

G. D. Price

June 1980

FIGURES

DYNAMOMETER TEST RESULTS OF THE NORTH WIND HIGH-RELIABILITY PROTOTYPE WIND TURBINE GENERATOR

INTRODUCTION

Dynamometer testing of the North Wind High Reliability Prototype Number 1 has been completed at the dynamometer test facility at Rocky Flats. During atmospheric testing the rotor shaft was damaged. The bent shaft was cut off close to the frame for further stress testing. A coupling had to be fabricated which fastened to the shaft stub. The alternator rotor did not appear to be otherwise damaged and turned freely. This paper will discuss the results of the dynamometer tests and performance observations of the alternator and control unit only.

The North Wind HR system includes a Lundell alternator and a control unit manufactured by Magnetics Products, Inc. The low speed alternator was designed as a 24-volt battery charger and rated at a speed of 250 rpm. It is a 3-phase alternator rated at 2.2 kVA. The field is wound on the rotor with slip rings and brushes for remote control. A full wave rectifying circuit is built into the rear alternator housing. The model SMC-10 control unit contains a field regulator and reverse current diode. A current shunt and current limit circuit were not included as shown on the schematic. A switching regulator (dump load control) was also not included with the prototype. The voltage regulator was adjustable from 22 to 32 volts dc.

RESULTS OF POWER TESTING

Field cut-in by the voltage regulator occurred at 240 rpm. The residual magnetism is small and does not cause voltage to build until near rated speed. The field cut-out is around 70 rpm. At rated speed of 250 rpm and voltage regulation at 27.0 volts, the generator produced 2,024 watts* of dc power. The dc shunt and flukemeter measured 70.5 amps. Power curves showing watts output and dc amps are shown in Figures 1 and 2.

Torque input at rated speed was 918.6 inch pounds. Horsepower input, therefore, was 3.64 (hp = rpm X T ÷ 63,024). Efficiency of the alternator, regulator, and rectifier was 74.3% at rated speed and 27.0 dc volts.

$$\text{EFF (\%)} = W_{out}/W_{in} \times 100$$

$$= 2{,}024/(3.64)(746) \times 100 = 74.3$$

Torque and efficiency curves are shown in Figures 3 and 4.

* Watts are measured on an OSI transducer which read consistently higher than the volt and amp product as measured separately.

2T-14:skp

OUTPUT POWER
NORTH WIND HR

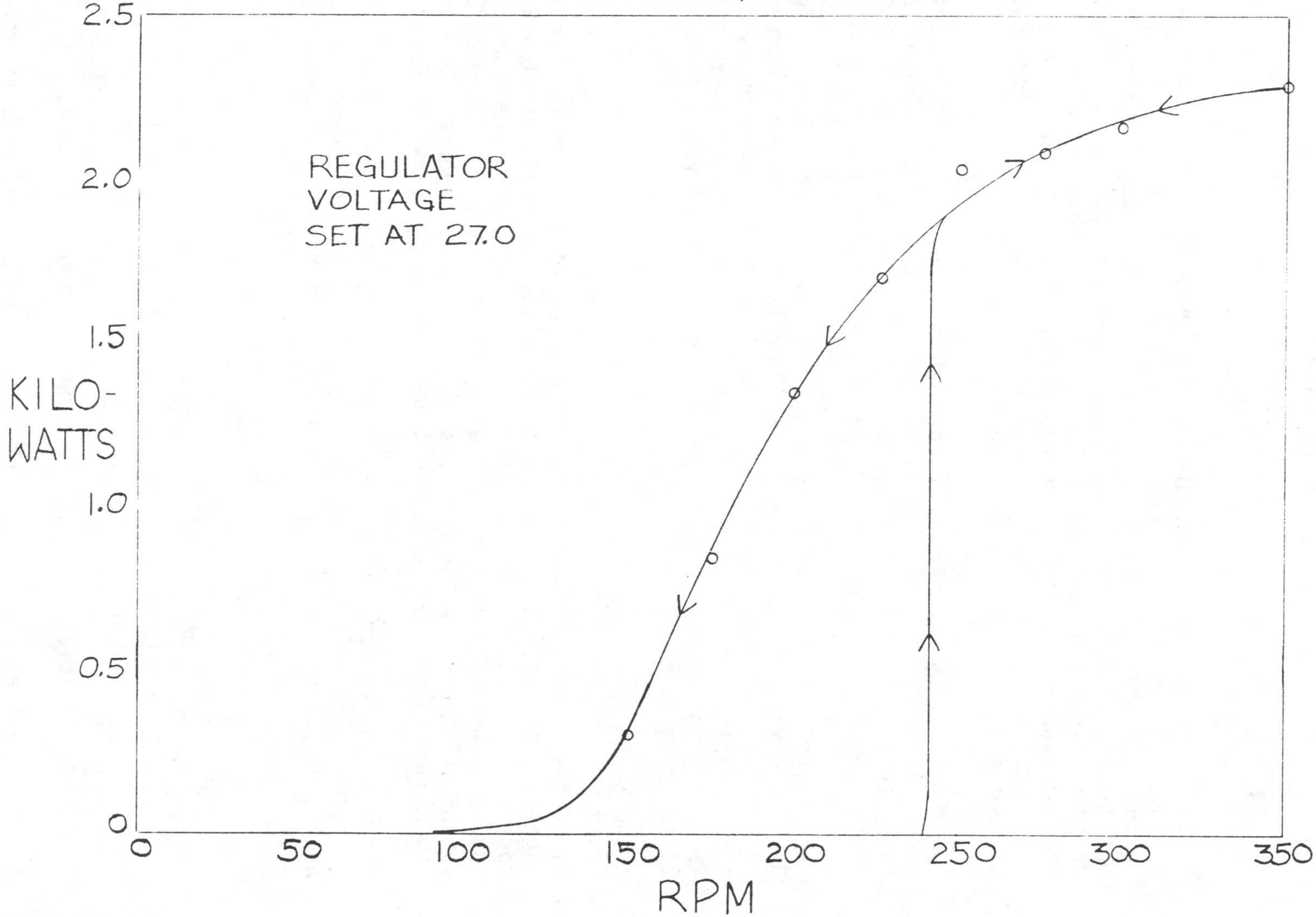

FIG 1

OUTPUT CURVE

NORTH WIND HR

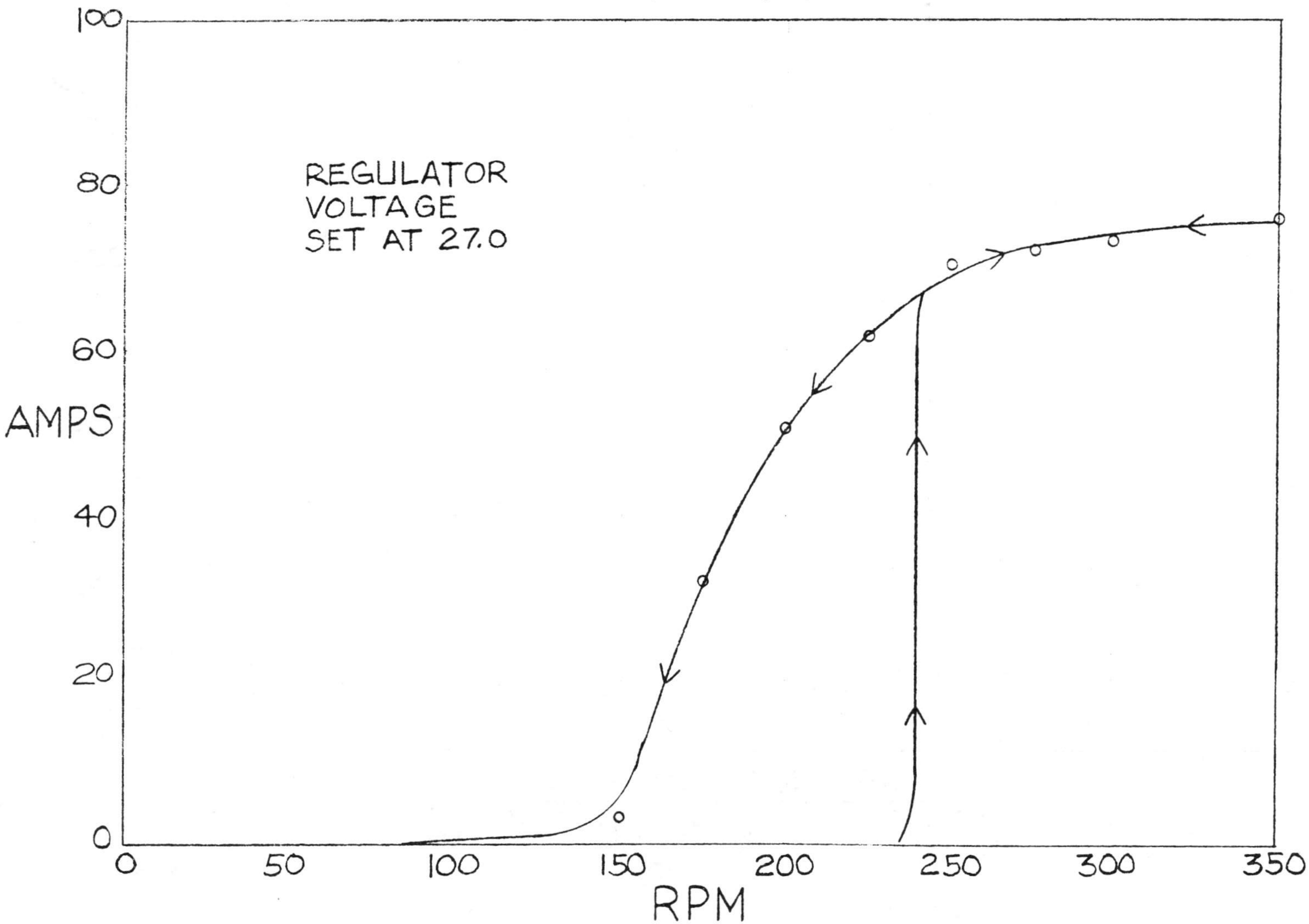

FIG 2

TORQUE / SPEED CURVE

NORTH WIND HR

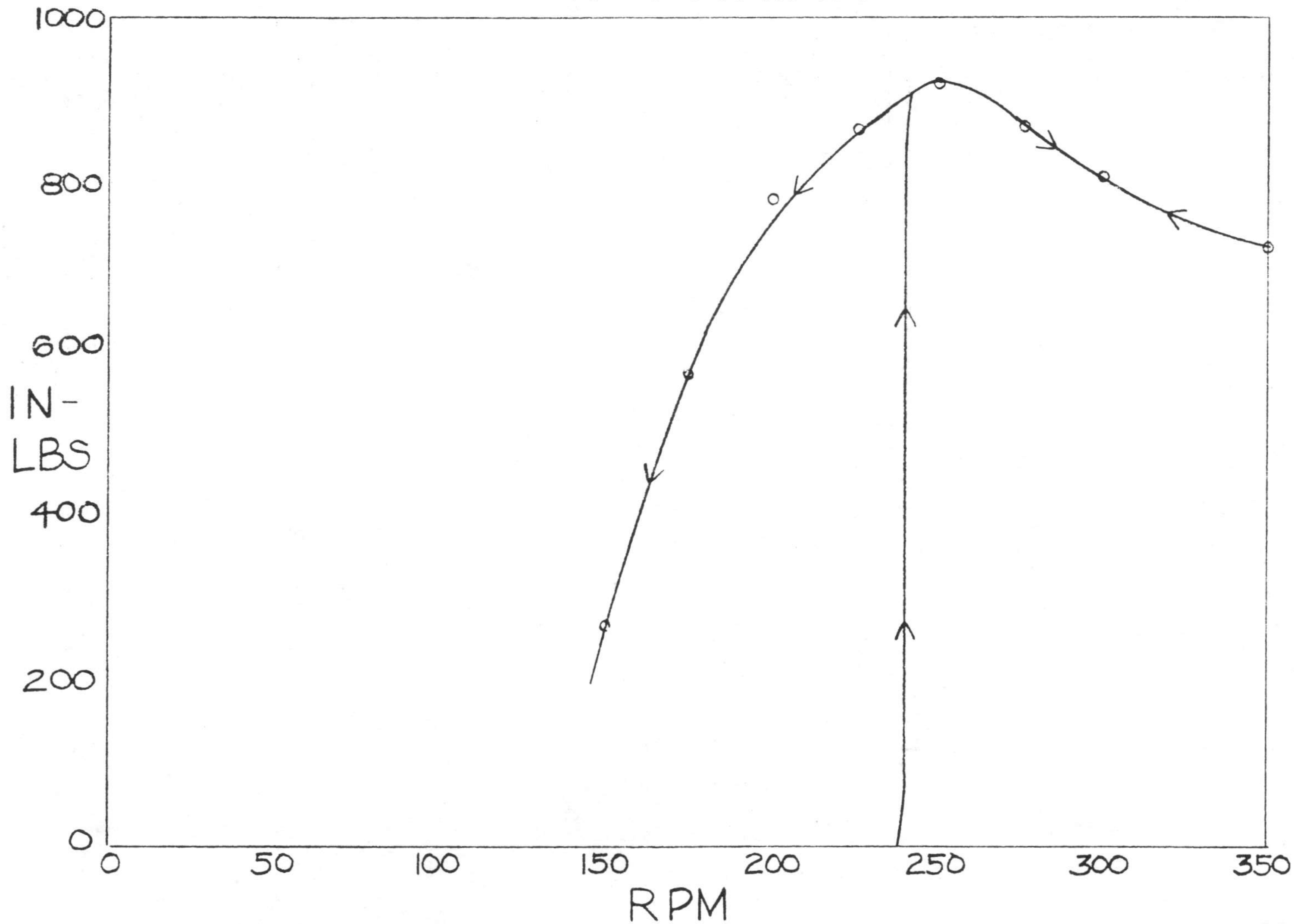

FIG 3

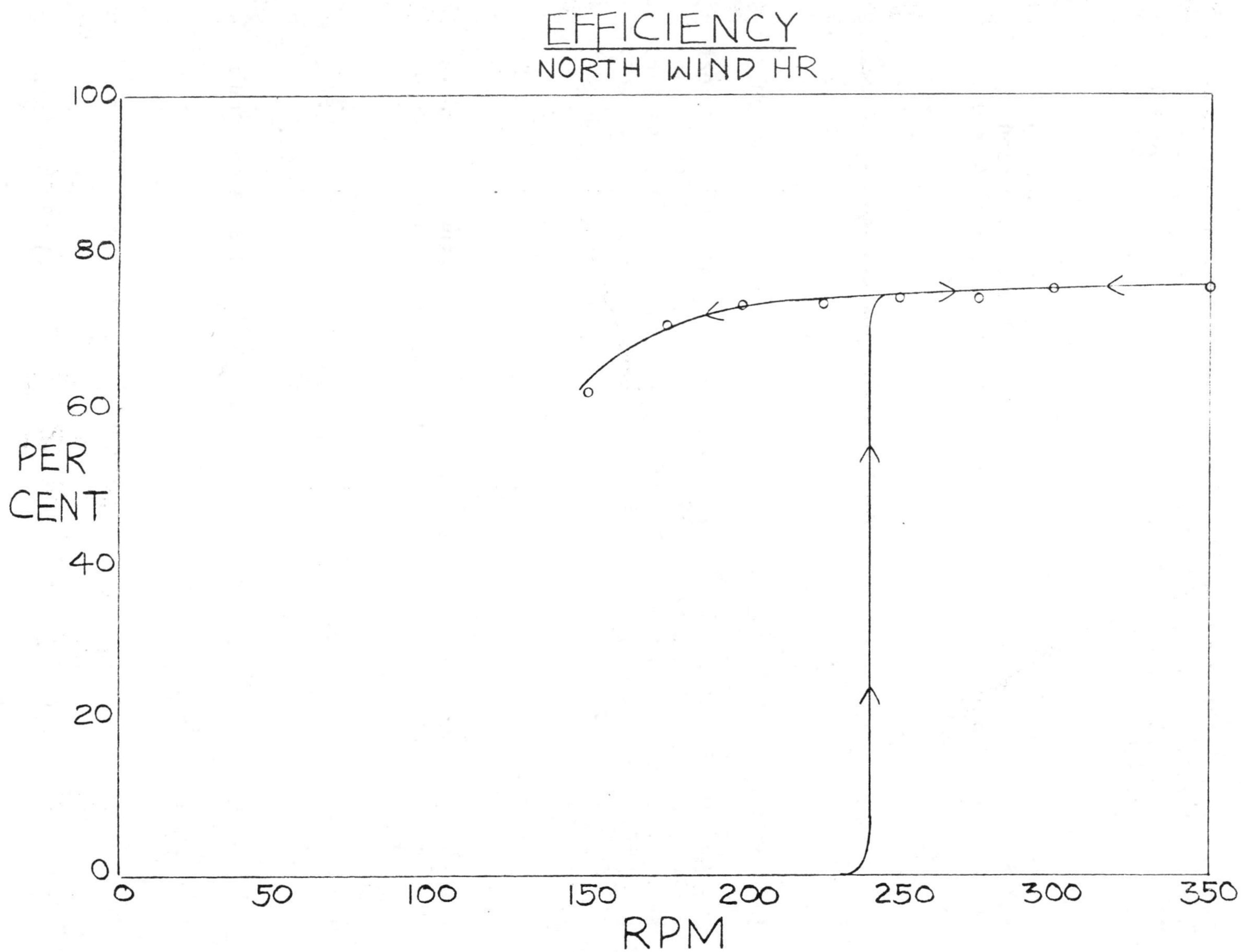
EFFICIENCY
NORTH WIND HR
100
80
60
PER CENT
40
20
0
0
50
100
150
200
250
300
350
RPM
FIG 4

Maximum output attained at 350 rpm was 3,672 watts and 116.6 dc amps. The dc voltage was not regulated, but maintained at 30 volts by controlling the load. 1,318 inch pounds of torque or 7.32 horsepower was required as input. The efficiency was 67%.

VOLTAGE REGULATION

Short circuit and saturation tests were performed to determine synchronous impedance. At a field current of 5.94 amps, the open circuit voltage was 32.5 volts and the short circuit current was 94 amps. The synchronous impedance is 0.200 ohms per phase.

$$Z_s = \frac{V_{o.c.}}{\sqrt{3}\, I_{s.c.}}$$

Test curves are shown in Figure 5. Speed was constant at 250 rpm.

Resistance measurements of the windings were made by applying dc battery voltage and measuring current. Field resistance was 3.08 ohms. The stator winding was assumed to be wye connected. DC stator resistance was .08 ohms between terminals or .04 ohms per phase. Effective ac resistance is then .056 ohms.

$$r_{\emptyset} = 1.4 \times R_{dc}$$

Synchronous impedance is the resultant of the quadrature components of synchronous reactance and ac resistance. The calculated synchronous reactance is 0.19 ohms.

$$X_s = (Z_s^2 - r_{\emptyset}^2)^{1/2}$$

Regulation is calculated from no load voltage (V_o) and rated terminal voltage (V_t). I is rated stator current.

$$V_o = [(V_T + I \cdot r_{\emptyset})^2 + (I \cdot X_s)^2]^{1/2}$$

$$= [(12.9 + (52.4)(.056))^2 + ((52.4)(.19))^2]^{1/2} = 18.7$$

$$\text{Percent Regulation} = \frac{V_o - V_T}{V_T}(100) = 44.8\%$$

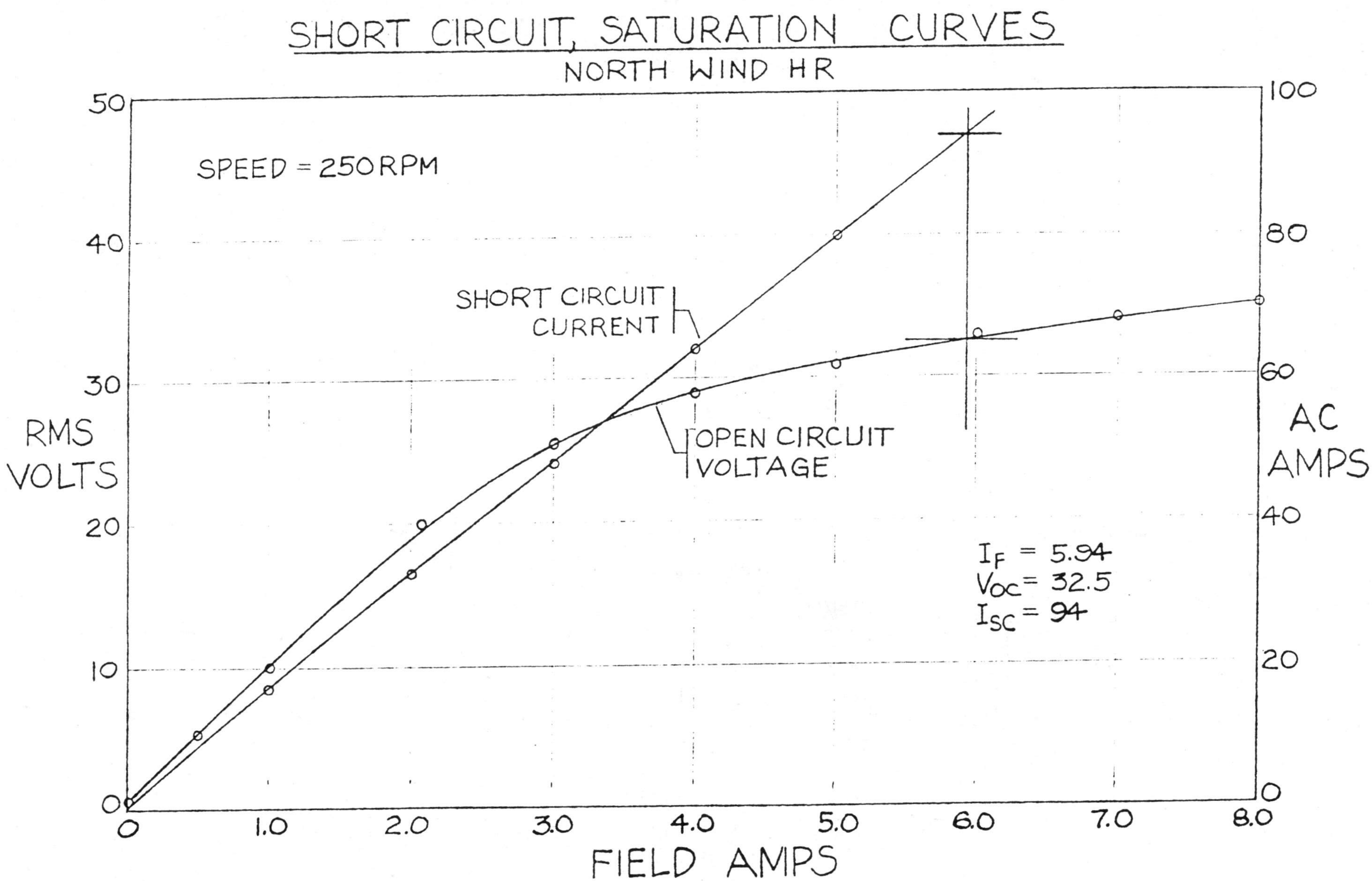
SHORT CIRCUIT, SATURATION CURVES
NORTH WIND HR
SPEED = 250 RPM
SHORT CIRCUIT CURRENT
OPEN CIRCUIT VOLTAGE
RMS VOLTS
AC AMPS
I_F = 5.94
V_{OC} = 32.5
I_{SC} = 94
0
10
20
30
40
50
100
80
60
0
1.0
2.0
3.0
4.0
5.0
6.0
7.0
8.0
FIELD AMPS

FIG 5

DYNAMOMETER TEST SCHEMATIC

NORTH WIND HR

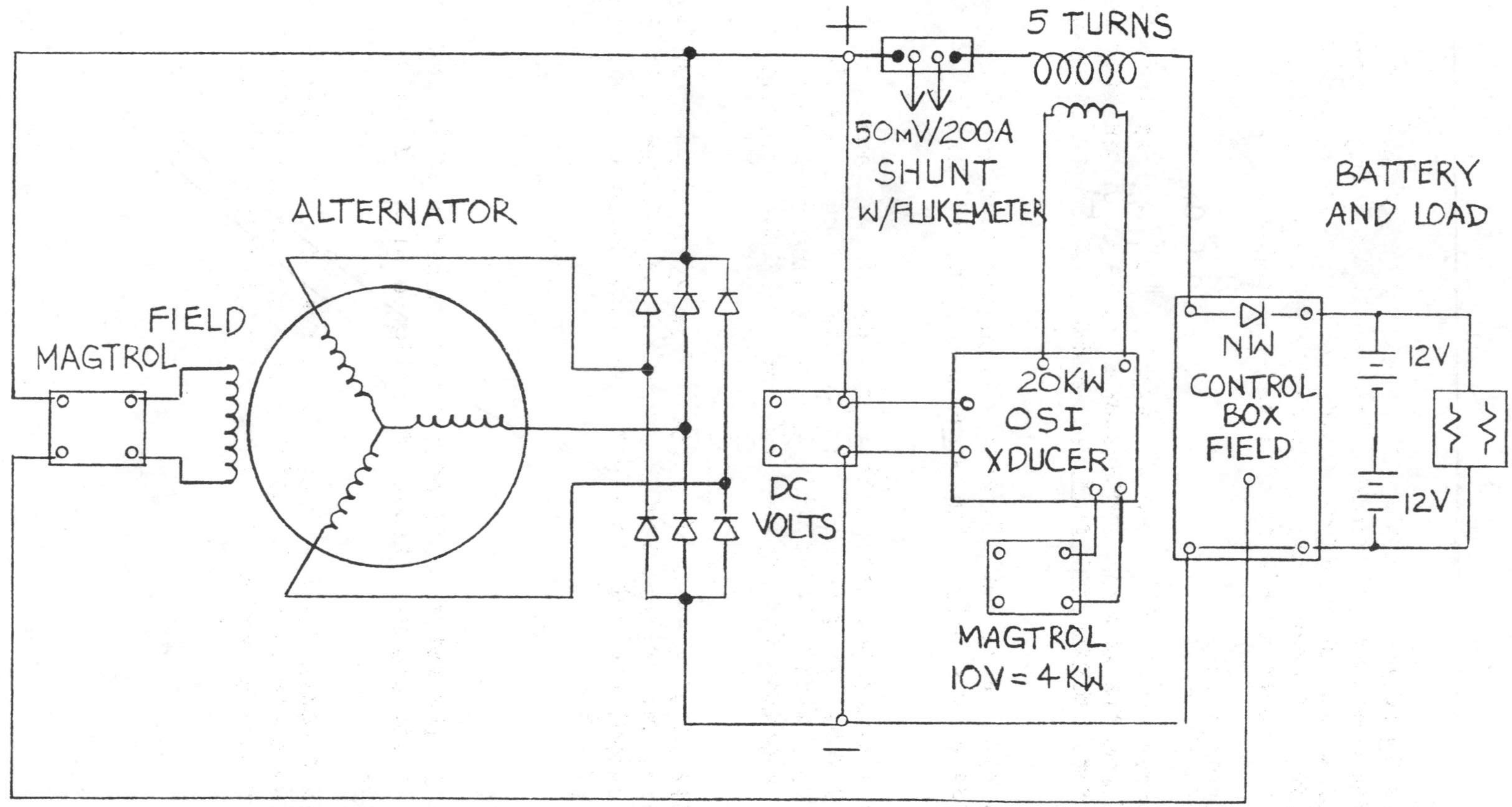

Figure 6

The synchronous impedance method used to determine voltage regulation is often called the pessimistic method. Other methods using a synchronous motor as a load to the alternator produce lower and more realistic regulation values. However, the synchronous impedance method is satisfactory when used consistently to compare alternators.

OPERATING CHARACTERISTICS

Operating temperature of the frame reached 31.0°C. Rectifying diodes were at 32.5°C and the ambient temperature was 24°C. Operating conditions were intermittent. Higher temperatures would occur under continuous duty.

The field slip rings were out of round and caused constant brush movement. The brushes were also poorly aligned and not properly seated on the slip rings.

The alternator rotated smoothly with no noticeable vibration or bearing noise up to 400 rpm. Frequency of the dc output ripple was 150 cycles per second at 250 rpm, which signified a 12-pole stator construction. DC current ripple averaged 4.4 amps or 6.3% of total current at rated output.

The control unit regulates the dc voltage from 22 to 32. When set at 27 volts at 250 rpm, the voltage varied from 22.7 at 150 rpm to 28.5 at 350 rpm. Current output was not limited by the control unit. The test schematic is shown in Figure 6.

RECOMMENDATIONS

The slip rings on the rotor shaft need to be machined to be concentric with the shaft. The brushes should be realigned with the slip rings and properly seated.

A current limit circuit may be necessary to protect the alternator from overloads or short circuits. Capability to equalize and float charge should be added to the regulator for efficient battery storage.

RESULTS OF VIBRATION TESTING

UNITED TECHNOLOGIES RESEARCH CENTER (UTRC)

8 KW PROTOTYPE WIND TURBINE GENERATOR

J. H. Sexton

June 1980

Additional available reports on the United Technologies Research Center (UTRC) 8 kW prototype wind turbine generator are listed below and are available from National Technical Information Service.

1. Development of an 8 kW Wind Turbine Generator for Residential Type Applications, Phase I - Design and Analysis, June 25, 1979, M. C. Cheney, et al., United Technologies Research Center, Volume I - Executive Summary, 10 pp., (RFP-3006-1): Volume II - Technical Report, 202 pp., (RFP-3006-2).

2. UTRC 8 kW Wind System, Phase II - Fabrication and Test, February 4, 1981, R. B. Taylor and M. C.Cheney, United Technologies Research Center, Executive Summary, 13 pp., (RFP-3232-1): Technical Report, 93 pp., (RFP-3232-2)

3. United Technologies Research Center 8 kW Prototype Wind System, Final Test Report, September 1981, K. K. Higashi, 26 pp., $6.00. (RFP-3294).

TABLES

FIGURES

FIGURES (Continued)

RESULTS OF VIBRATION TESTING

UNITED TECHNOLOGIES RESEARCH CENTER (UTRC)
8 kW PROTOTYPE WIND TURBINE GENERATOR

SUMMARY

This note contains the results of vibration tests conducted at the Rocky Flats Small Wind Systems Test Center on the UTRC 8 kW wind system. The machine is a prototype machine developed under U.S. Department of Energy funding.

Vibration tests indicate that the first and second bending modes of the tower are excited during normal machine operation. At the present time, excitation of the first bending mode is not considered a serious problem. However, the second bending mode has been observed to be excited in two situations: 1) if the machine is unloaded (i.e., a power outage); and 2) when the machine synchronizes with the utility grid, thereby, creating a "hammer-type" vibration. The point of greatest deflection has been visually observed to be where the tower sections are bolted together. It is felt, therefore, that bolts on the tower flange should be checked for tightness and structural integrity on a routine schedule. The accelerometers located at the tower top and midsection should be carefully monitored for any change in frequencies.

INTRODUCTION

As the wind industry becomes increasingly aware of the vital role dynamics and frequency considerations occupy in the overall design of SWECS, dynamic analysis of structures and components has become more important in the design process. In order to define the dynamic qualities and requirements of SWECS, the Rocky Flats Small Wind Systems Test Center (WSTC) has developed vibration testing capabilities.

This note presents data generated from dynamic testing of the UTRC 8 kW prototype wind system developed under U.S. Department of Energy (DOE) funding. These data are pertinent to the forthcoming UTRC design report (to be published by DOE) and will assist developers involved in possible attempts to produce a system using the UTRC design. In addition, this note is intended to underscore the importance of dynamic testing as one effective method to help insure that wind turbine generators, support structures and their components meet design performance expectations and behave in a predictable manner in a dynamic operating environment.

The type of structural dynamics testing referred to in this note is called "modal analysis." Modal analysis is the process of characterizing the dynamic properties of an elastic structure by identifying its modes of vibration. Each mode has a specific natural frequency and damping factor. Also, each mode of vibration has a characteristic "mode shape" which is defined spatially over the entire structure.

Actual measurements of the dynamic properties and behavior of a wind system are an essential part of any dynamic analysis. The dynamic properties of a component or structure may be determined by using finite element computer modeling techniques; however, most structures still require further experimental verification of analytical results.

TEST DESCRIPTION/THEORY

A technique currently being used at the WSTC for dynamic testing is commonly known as impact testing. The structure can be excited with a hammer. With a load cell attached to the hammer, the input force can be accurately recorded. The response (output) of the structure is measured with the use of an accelerometer. A generalized test setup is depicted in Figure 1. Techniques have been developed which allow the modes of vibration of an elastic structure to be identified from measured transfer data. Once a set of transfer (frequency response) functions relating to points of interest on the structure have been measured and recorded, they may be operated on to obtain modal parameters, i.e., the natural frequencies, damping factors and characteristic mode shapes for predominant modes of vibration of the structure.

Components tested are listed in Table I.

TABLE I. Components Tested

Component Tested	Comments
Blades 1 and 2	Cantilever vertical position rigidly supported
Flexbeam	Cantilever horizontal position rigidly supported
Blades/Flexbeam	Cantilever horizontal position rigidly supported
WTG Atop Tower	Impact excitation
WTG Atop Tower	Machine running

The instrumentation used in testing the UTRC components is listed in Table II.

TABLE II. Instrumentation List

Instrument	Manufacturer	Model No.
Load Cell	PCB	086B20/20BA03
Charge Amplifier	PCB	482A10
Accelerometer	ENDEVCO	2262C-25
Signal Conditioning	Cyber	9320
Calculator	Hewlett-Packard	9825A
Plotter	Hewlett-Packard	9872A
Digital Analyzer	Hewlett-Packard	5420A
Digital Scope	Nicolet	201

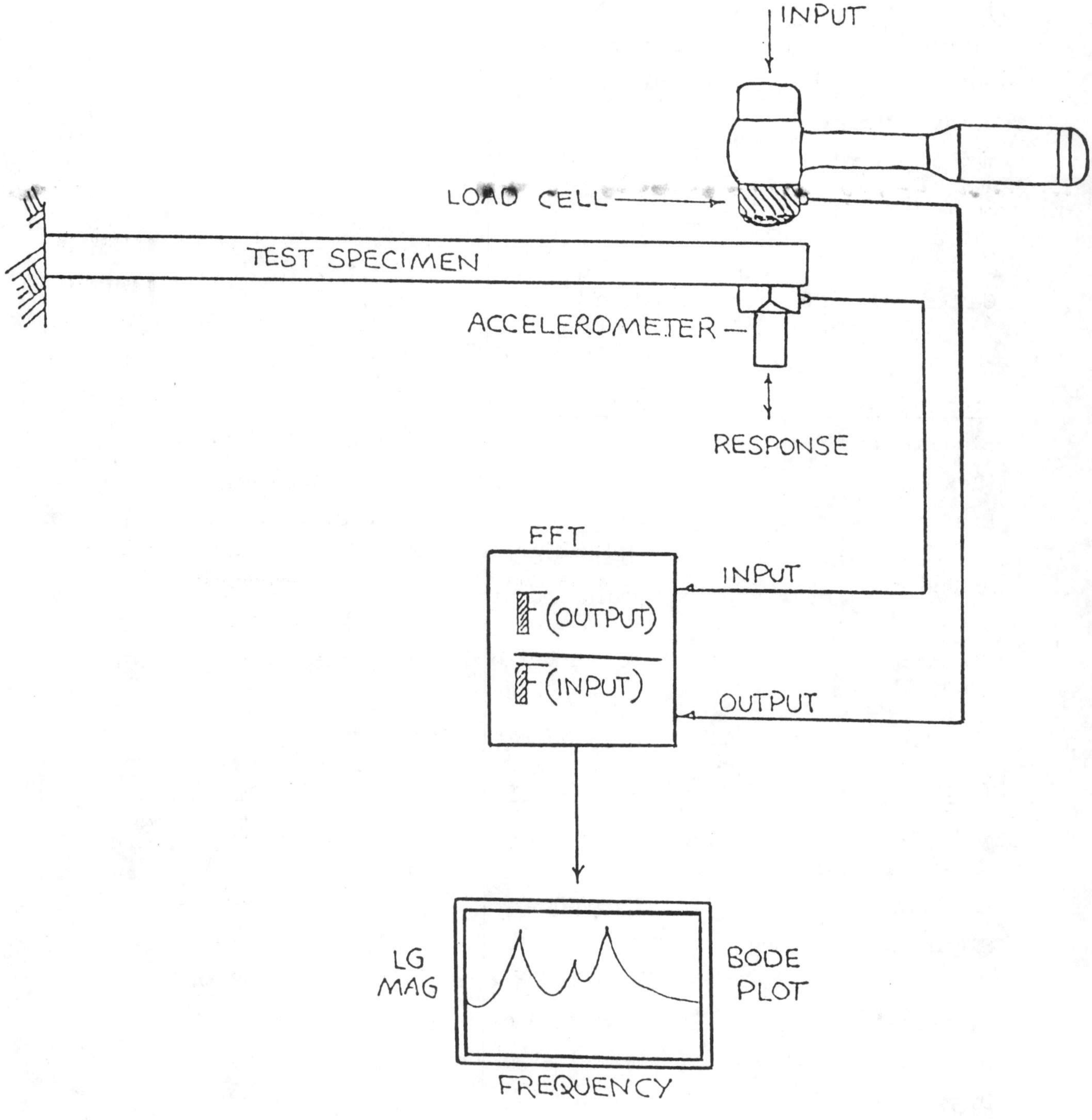

Figure 1

Driving Point Measurement

RESULTS

Blade Vibration Tests

Each blade was rigidly attached to a fixture. The setup is similar to that depicted in Figure 1. The frequency response of the test fixture was determined to be over 250 Hz, well above the frequencies of interest for the UTRC blades. Using the impulse techniques described earlier, the first six modes of vibration were determined. It is important to note that the blades were not attached to the flexbeam during these tests. Figure 2 shows the first bending mode of Blade #1. The first bending mode of Blade #2 is shown in Figure 3. Both Figures 2 and 3 depict the results of blade responses when excited at the tip. Figure 4 depicts the transfer function showing the first six predominant modes of vibration for Blade #1. Figures 5 through 10 portray the associated mode shapes of Blade #1. A summary of blade tests is given in Table III.

TABLE III. Summary of Blade Vibration Tests

Component	Predominant Modes	Type of Excitation
Blade #1	1.4 Hz FMB	Handshake
Blade #2	1.5 Hz FMB	Handshake
Blade #1	1.4 Hz FMB	Impact
	9.0 Hz SMB	
	22.0 Hz FMT	
	25.0 Hz TMB	
	46.0 Hz FtMB	
	68.0 Hz SMT	
Blade #2	1.5 Hz FMB	Impact
	9.4 Hz SMB	
	23.0 Hz FMT	
	25.4 Hz TMB	
	46.5 Hz FtMB	
	68.3 Hz SMT	

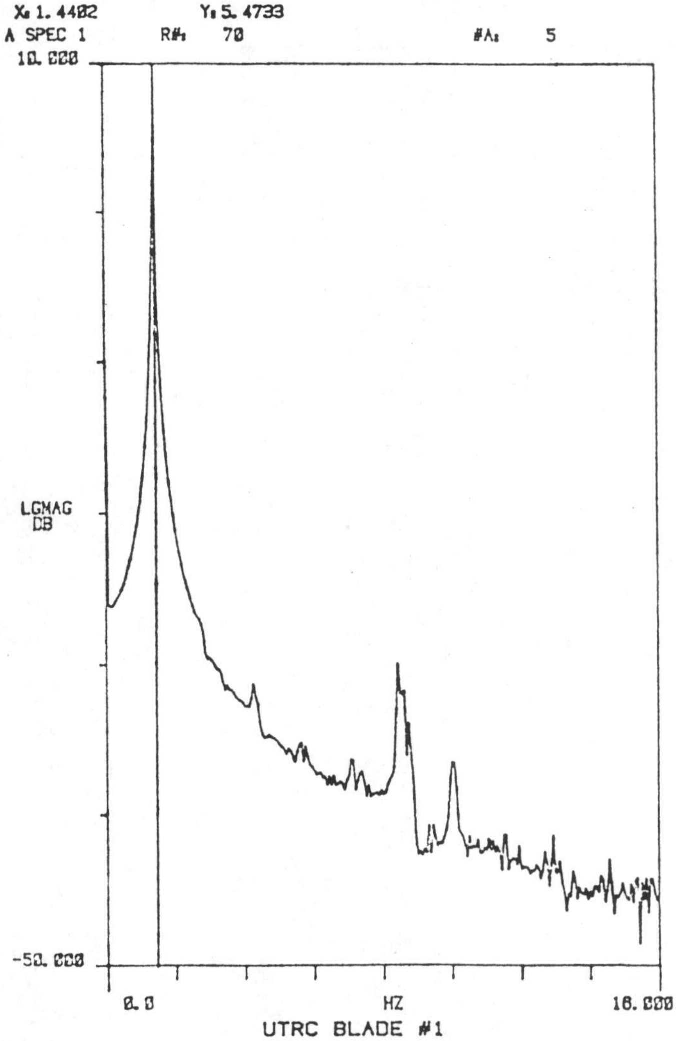

TYPE OF EXCITATION HAND SHAKE
LOCATION OF INPUT BLADE TIP
LOCATION OF RESPONSE XDCR BLADE TIP
3/20/80

Figure 2
First Bending Mode of Blade #1

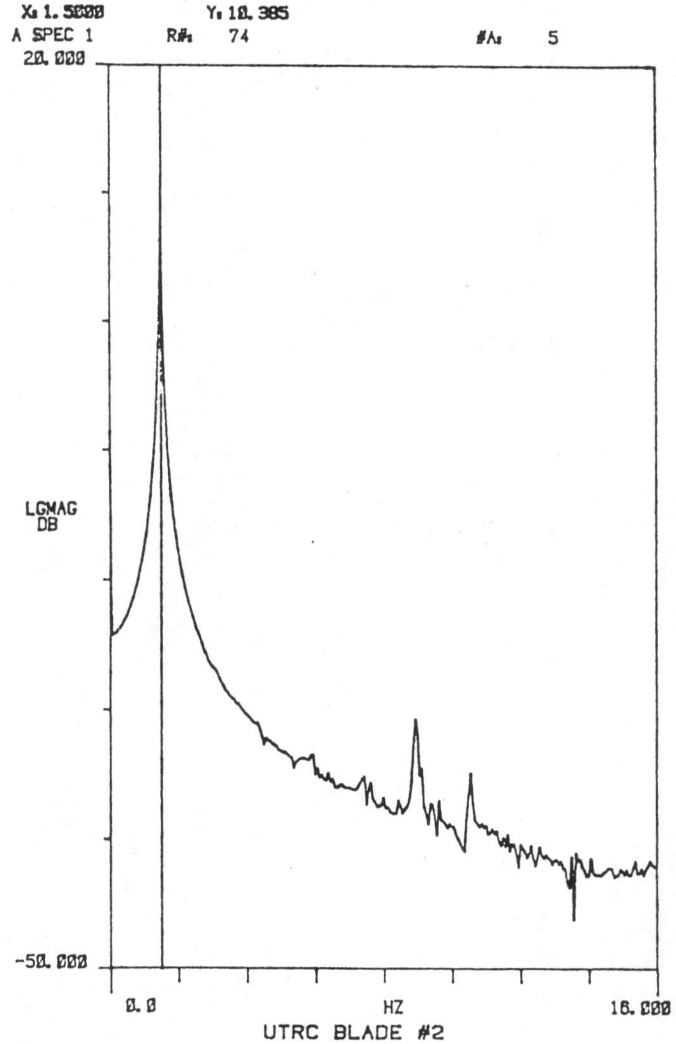

TYPE OF EXCITATION HAND SHAKE
LOCATION OF INPUT BLADE TIP
LOCATION OF RESPONSE XDCR BLADE TIP
3/20/80

Figure 3
First Bending Mode of Blade #2

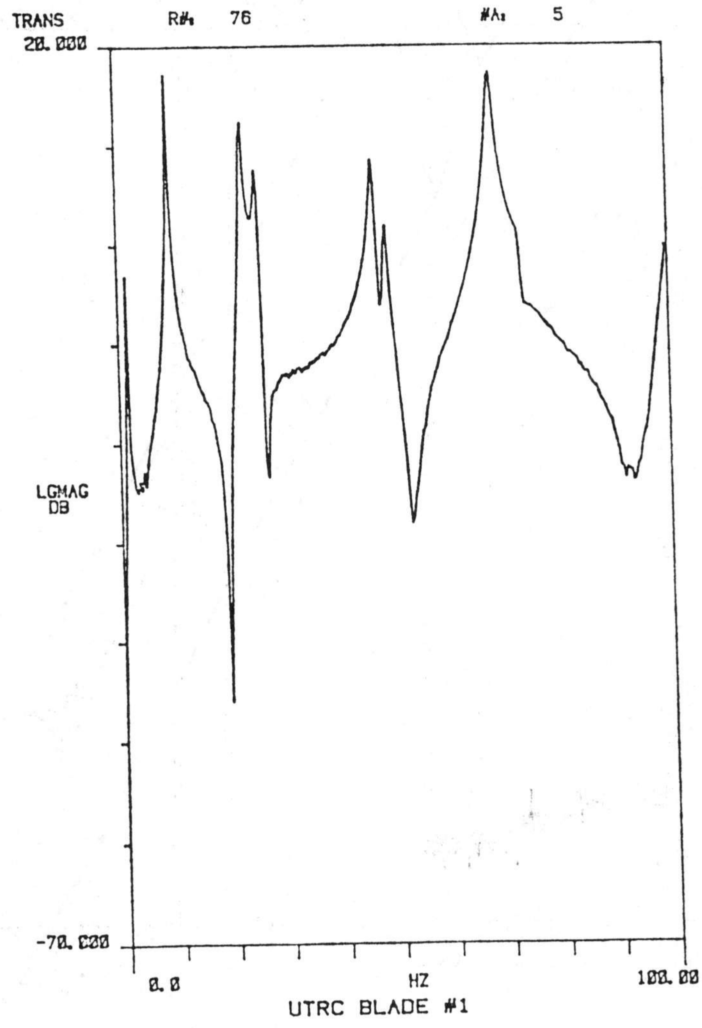

TYPE OF EXCITATION IMPACT
LOCATION OF INPUT DRIVING POINT
LOCATION OF RESPONSE XDCR DRIVING POINT
3/20/80

Figure 4
Transfer Function (Blade)

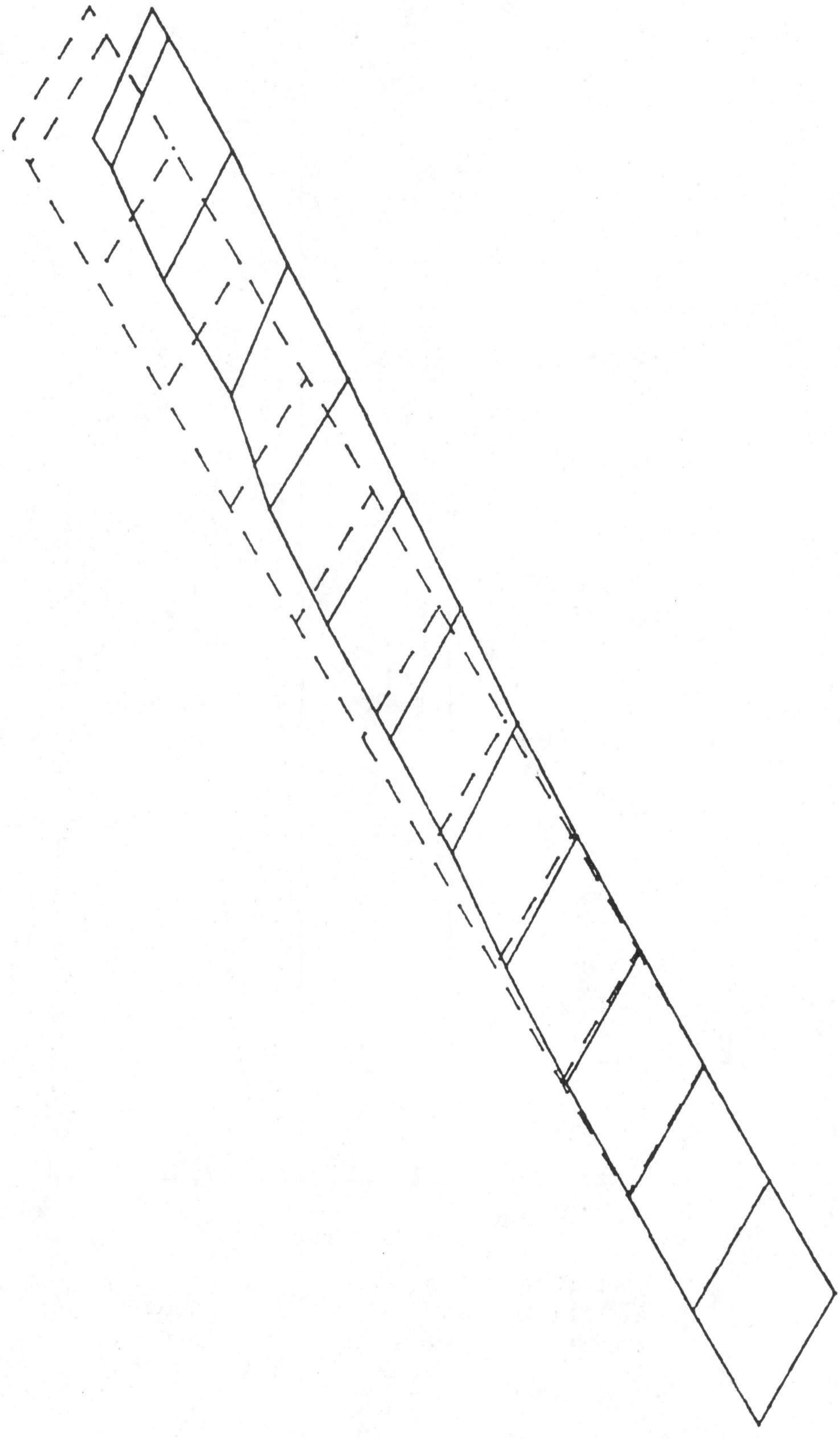

Figure 5

Blade Mode Shape 1

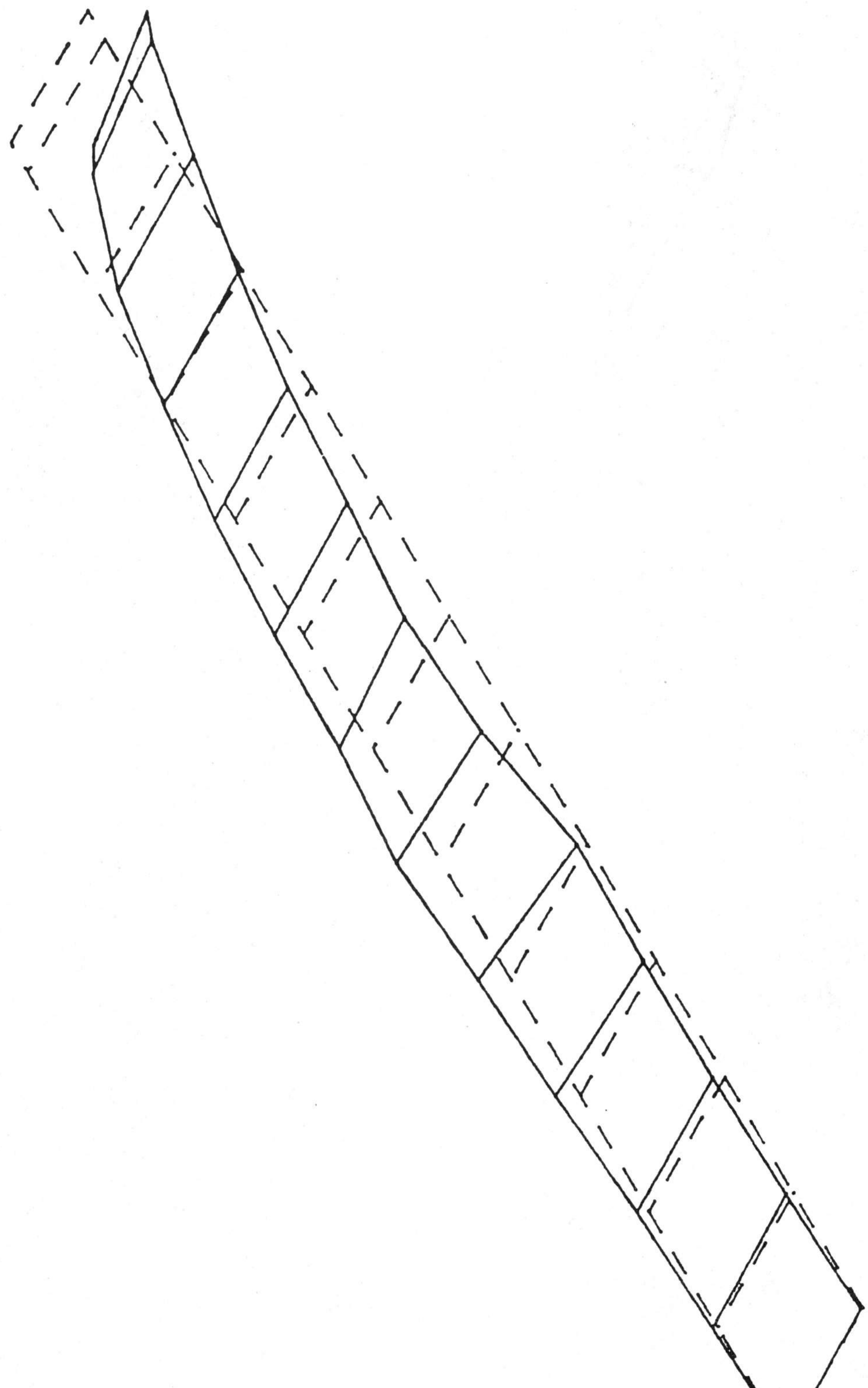

Figure 6
Blade Mode Shape 2

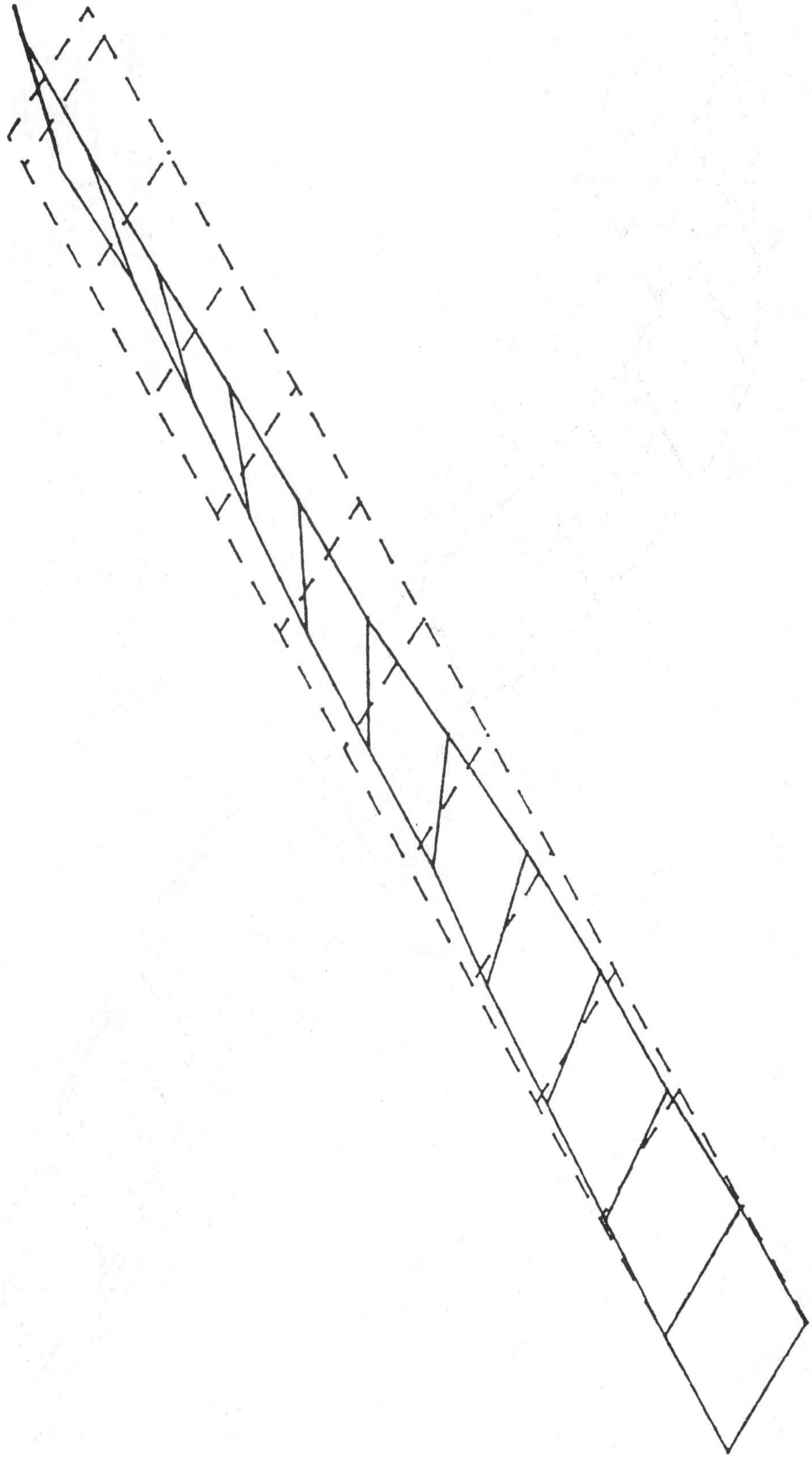

Figure 7
Blade Mode Shape 3

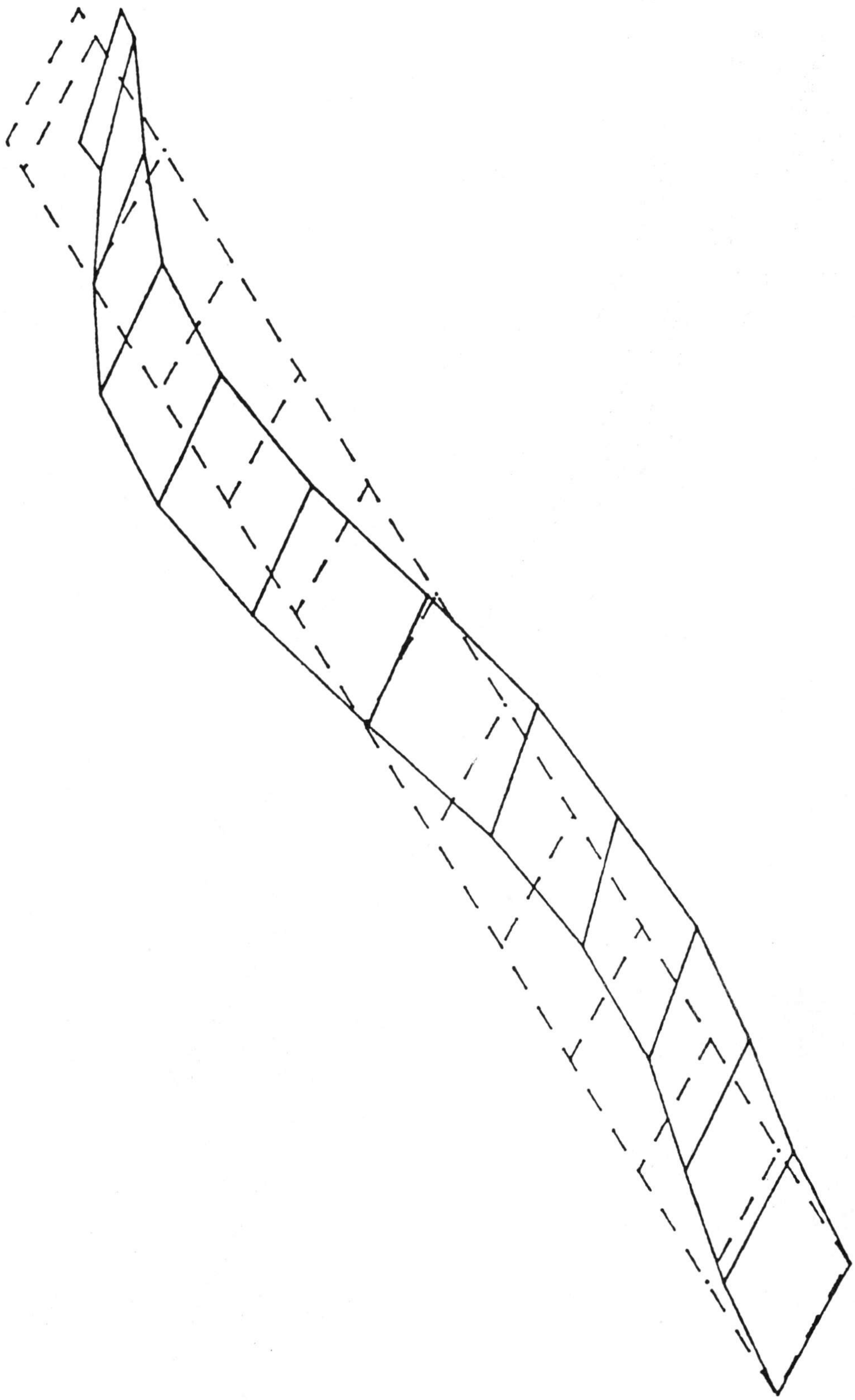

Figure 8

Blade Mode Shape 4

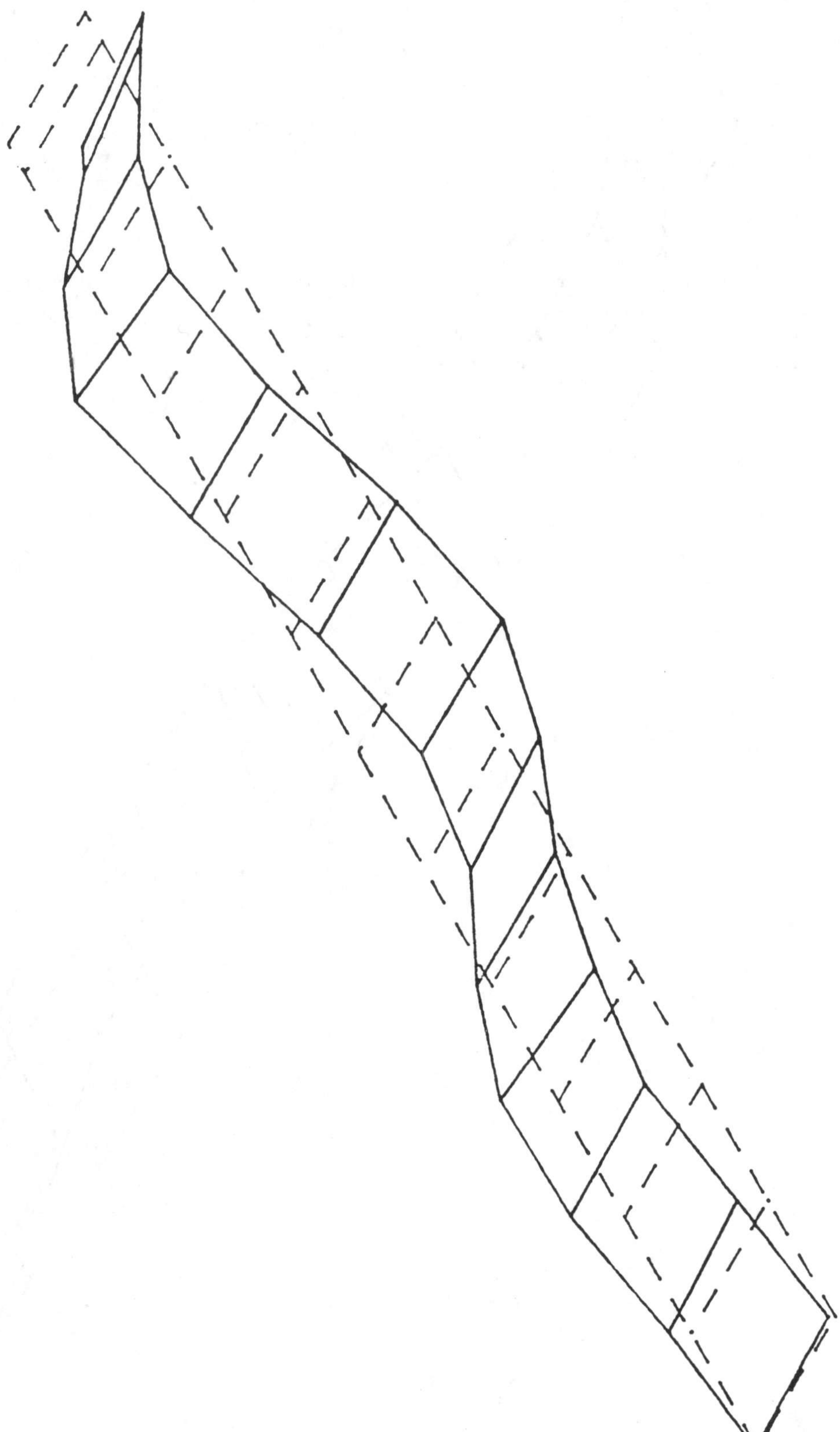

Figure 9

Blade Mode Shape 5

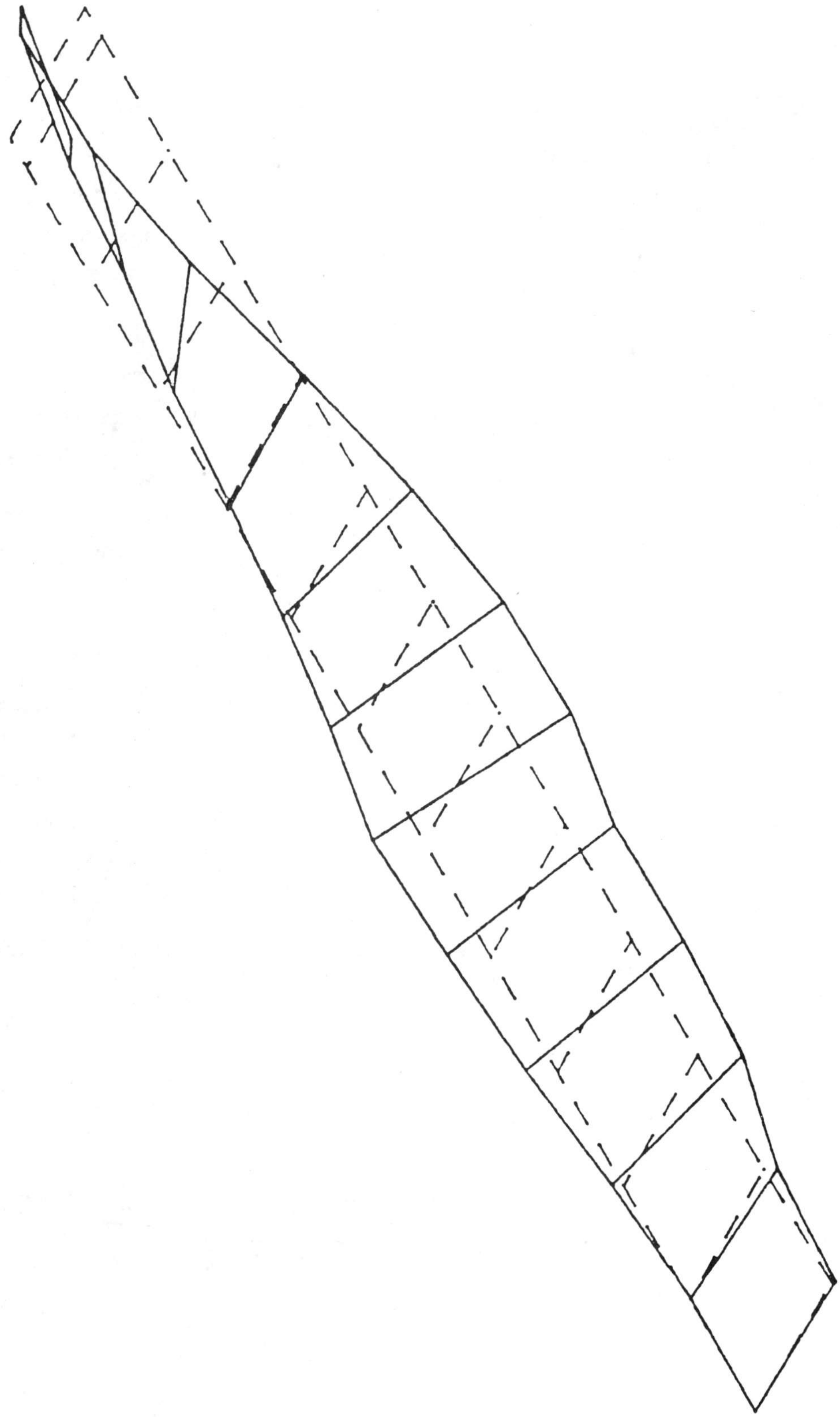

Figure 10

Blade Mode Shape 6

Flexbeam Vibration Tests

The flexbeam was rigidly attached to a fixture as shown in Figure 11. The frequency response of the test fixture was determined to be over 500 Hz, well above the frequencies of interest for the flexbeam. Using the impulse techniques described earlier, the first two modes of vibration were determined. The first bending mode of the flexbeam side #1 was 14 Hz (Figure 12). Side #2 of the flexbeam had a first bending mode of 13.6 Hz.

Side #1 of the flexbeam was then excited in the flatwise direction at the tip. As shown in Figure 13, two predominate modes were excited: 14 Hz and 85 Hz. Note that the most predominant of the two modes was 14 Hz.

Figure 14 shows the transfer function when side #2 was excited edgewise. In this configuration, the most predominate mode was 85 Hz. A summary of the flexbeam tests is contained in Table IV.

TABLE IV. Summary of Flexbeam Vibration Tests

Component	Predominant Modes	Type of Excitation
Flexbeam Side #1	14.0 Hz FMB	Handshake
Flexbeam Side #2	13.6 Hz FMB	Handshake
Flexbeam Side #1	14.0 Hz FMB	Handshake
	85 Hz First Edgewise	Impact
Flexbeam Side #2	13.6 Hz FMB	Handshake
	85 Hz First Edgewise	Impact

Figure 11

Flexbeam and Fixture

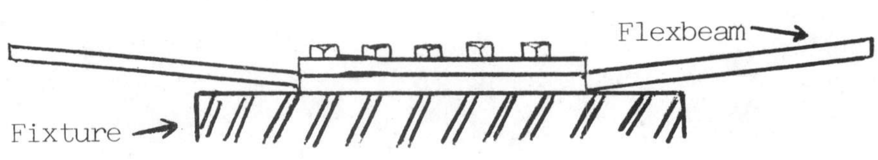

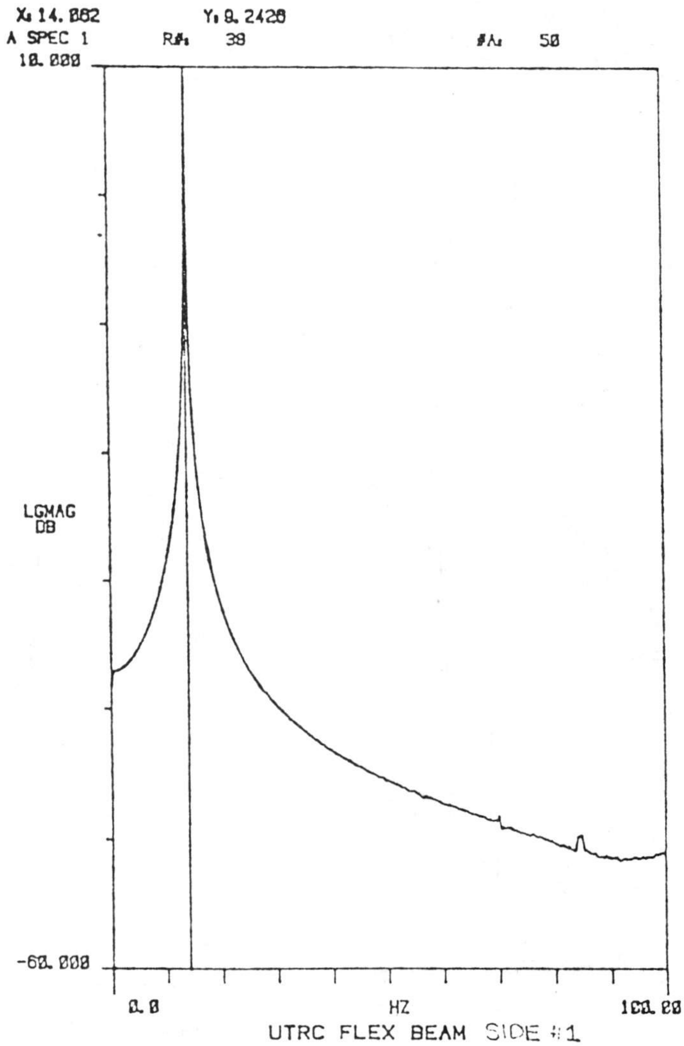

TYPE OF EXCITATION	HAND SHAKE
LOCATION OF INPUT	TIP
LOCATION OF RESPONSE XDCR	TIP

3/10/80

Figure 12

First Bending Mode - Flexbeam Side #1

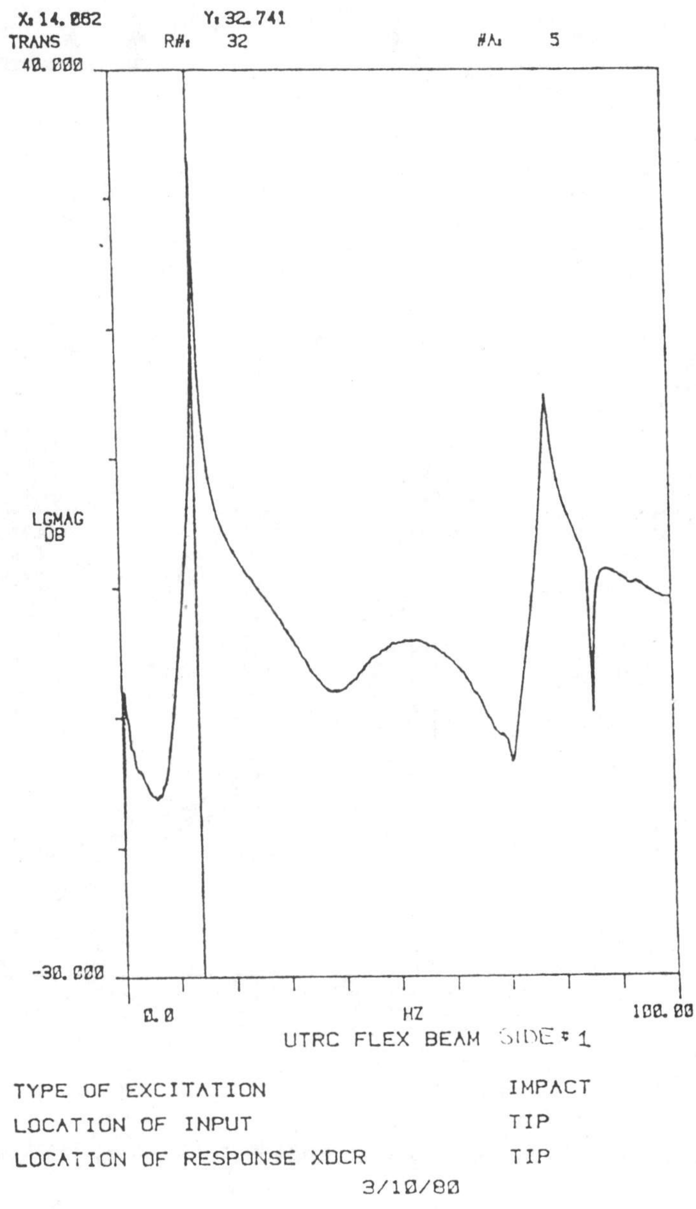

Figure 13

Predmoninant Modes

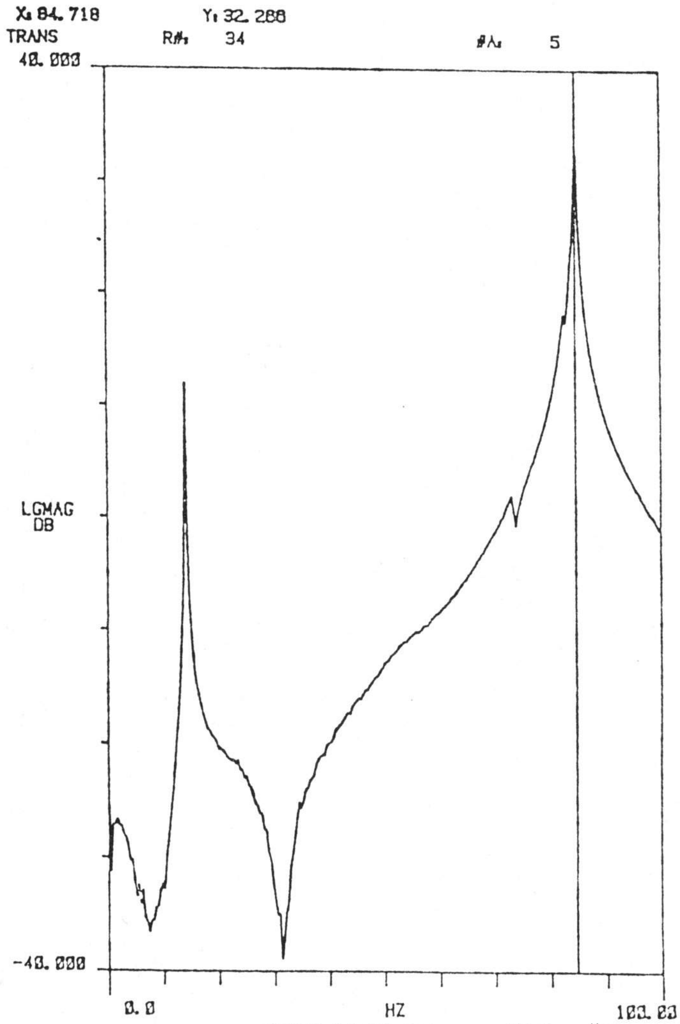

UTRC FLEX BEAM – Side #2

TYPE OF EXCITATION IMPACT
LOCATION OF INPUT EDGE
LOCATION OF RESPONSE XDCR EDGE
3/10/80

Figure 14
Transfer Function (Flexbeam)

Blade/Flexbeam Vibration Tests

The blades were attached to the flexbeam which was still rigidly attached to the fixture (Figure 11). The blades were then excited in the edgewise direction (Figures 15 and 16) and then excited in the flatwise direction (Figures 17 and 18). A summary of these tests is given in Table V.

TABLE V. Summary of Blades/Flexbeam Vibration Tests

Component	Predominant Modes	Type of Excitation
Blade #1 (Flexbeam)	0.7 Hz FMB	Handshake
	2.3 Hz First Edgewise	
Blade #2 (Flexbeam)	0.7 Hz FMB	Handshake
	2.4 Hz First Edgewise	

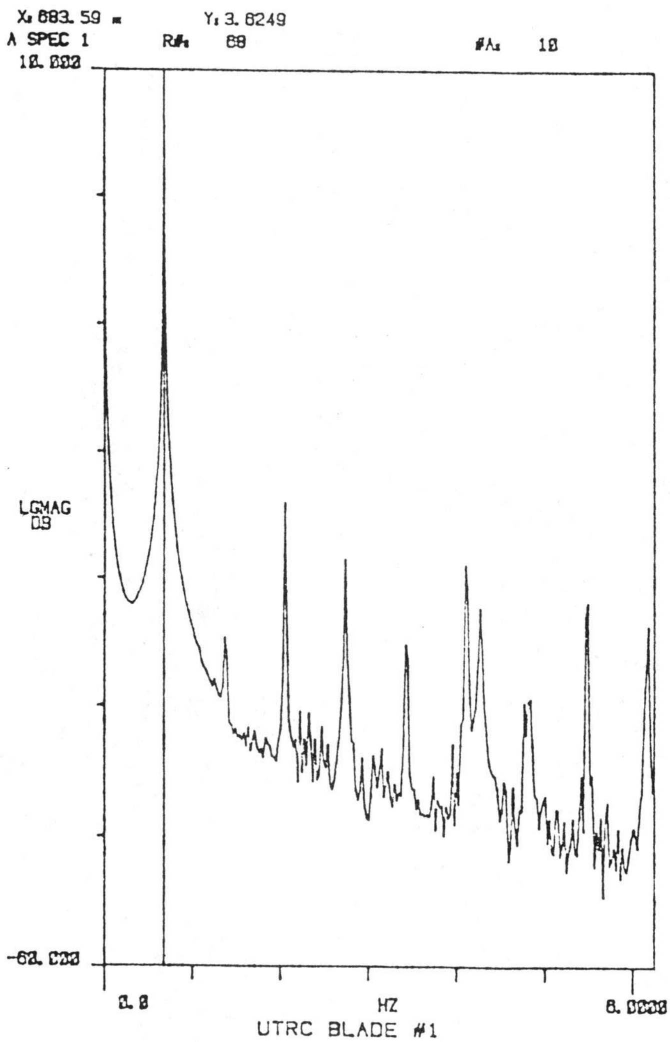

TYPE OF EXCITATION
LOCATION OF INPUT BLADE TIP
LOCATION OF RESPONSE XDCR BLADE TIP
3/11/80

Figure 15
Blade #1 Excited Edgewise

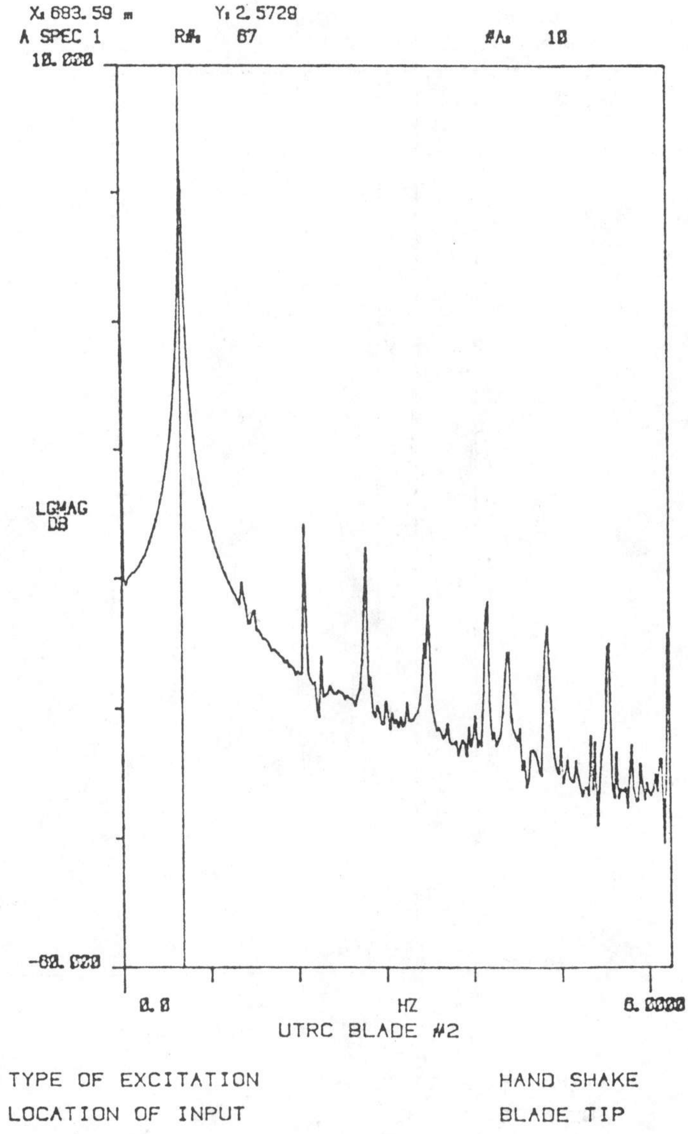

TYPE OF EXCITATION HAND SHAKE
LOCATION OF INPUT BLADE TIP
LOCATION OF RESPONSE XDCR BLADE TIP
3/11/80

Figure 16

Blade #2 Excited Edgewise

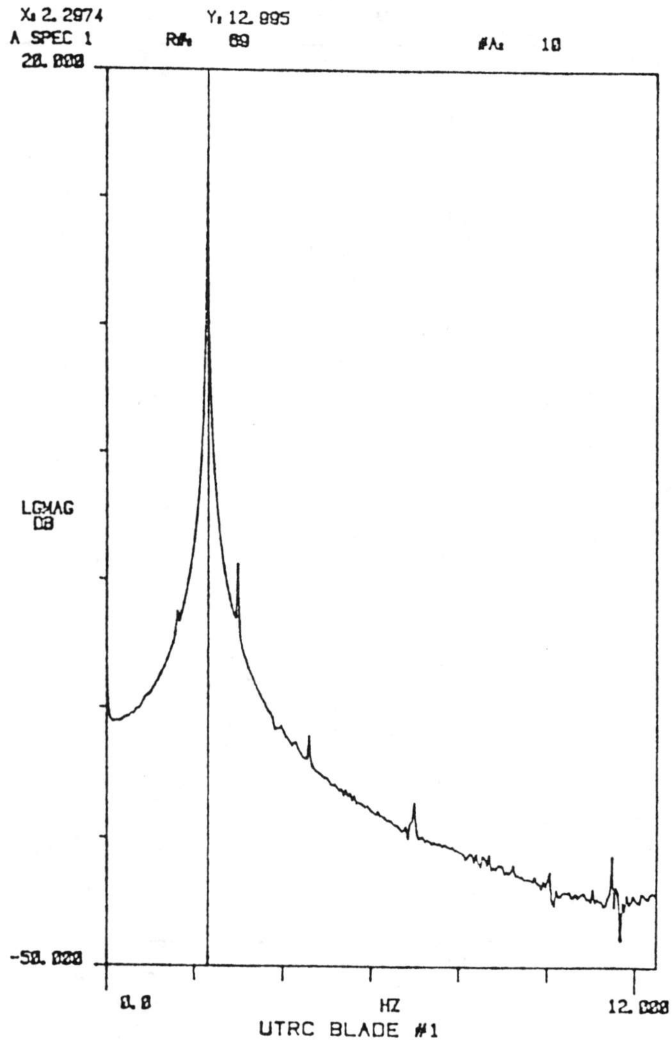

TYPE OF EXCITATION HAND SHAKE
LOCATION OF INPUT EDGE WISE
LOCATION OF RESPONSE XDCR L EDGE
3/11/80

Figure 17
Blade #1 Excited Flatwise

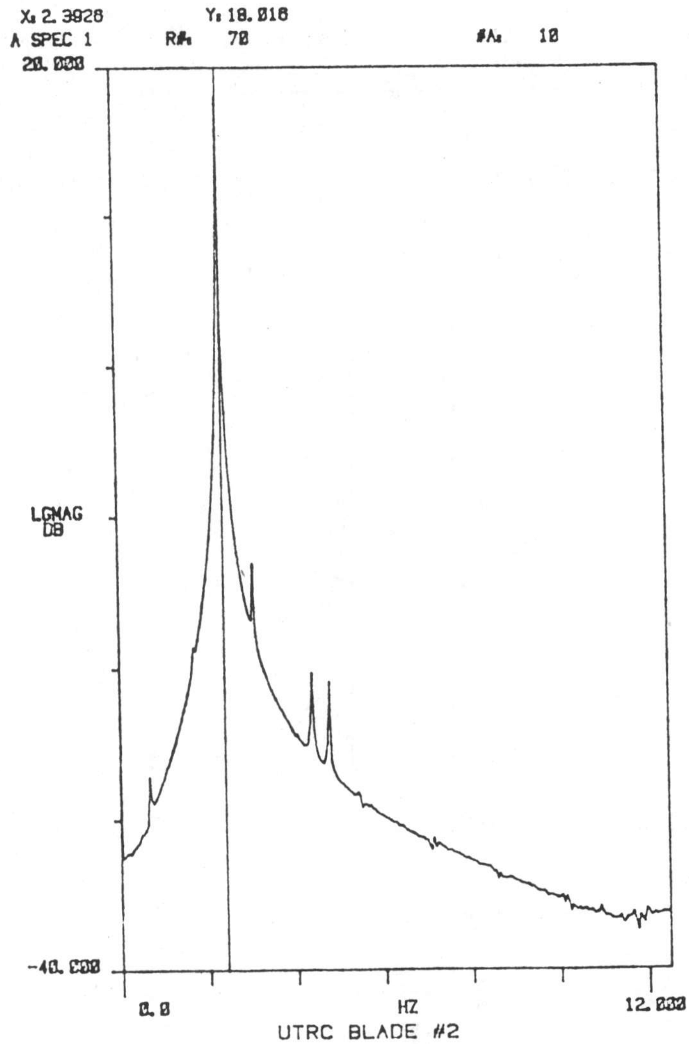

TYPE OF EXCITATION HAND SHAKE
LOCATION OF INPUT EDGE WISE
LOCATION OF RESPONSE XDCR L EDGE
3/11/80

Figure 18
Blade #2 Excited Flatwise

System (WTG/Tower) Vibration Tests

After the tower was plumbed, guy wires were tensioned, and the WTG minus the blades was put aloft for vibration tests. Figure 19 shows the results of handshake exciting of the system (in first bending mode) that resulted in a frequency of 1.5 Hz. Next, an impulse test was performed to determine the higher modes of vibration. The plot of the transfer function resulting from the impulse is shown in Figure 20. As can be seen, the second mode of vibration is 8.8 Hz. Figure 21 shows the coherence is quite high, above .9 at most frequencies, indicating a "good" measurement. Figures 22 through 27 are plots of the guy frequencies. A summary of the system tests is given in Table VI.

TABLE VI. Summary of System Vibration Tests

Component	Predominant Modes	Type of Excitation
System	1.5 Hz FMB	Handshake
System	1.5 Hz FMB	Impact
	8.8 Hz SMB	
	15.0 Hz TMB	
	16.0 Hz*	

Guy Wires

	Upper	Lower	Type of Excitation
South	3.7 Hz	5.5 Hz	Handshake
North	3.6 Hz	6.1 Hz	
East	4.0 Hz	5.3 Hz	

*Guy Frequency

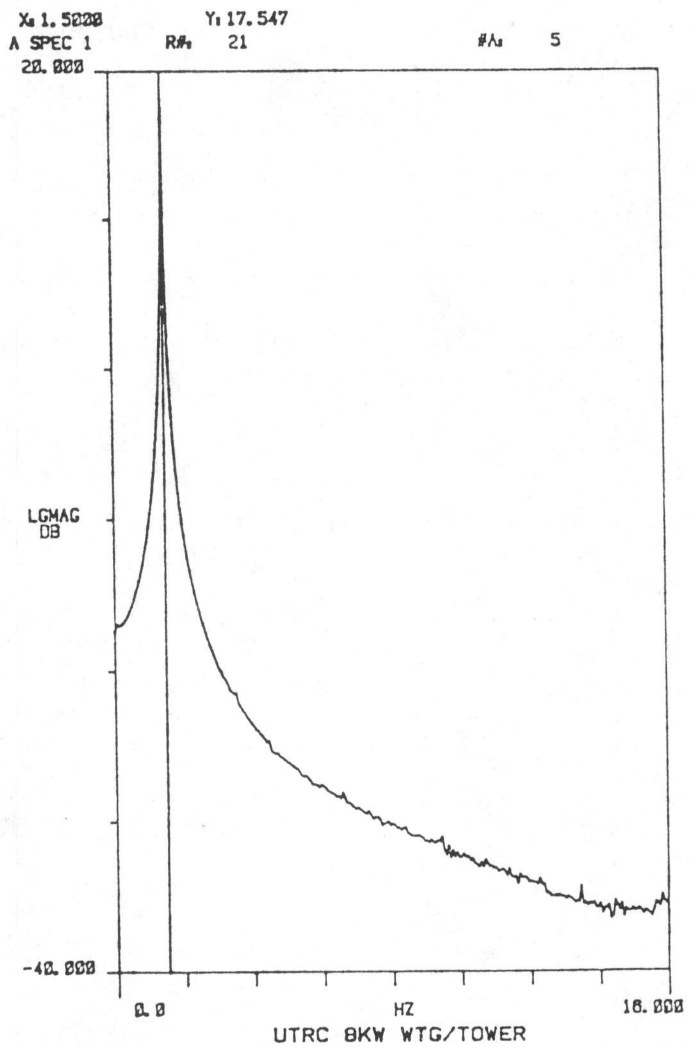

TYPE OF EXCITATION HAND SHAKE
LOCATION OF INPUT TOWER TOP
LOCATION OF RESPONSE XDCR TOWER TOP
4/2/80

Figure 19

Results of Handshake Exciting

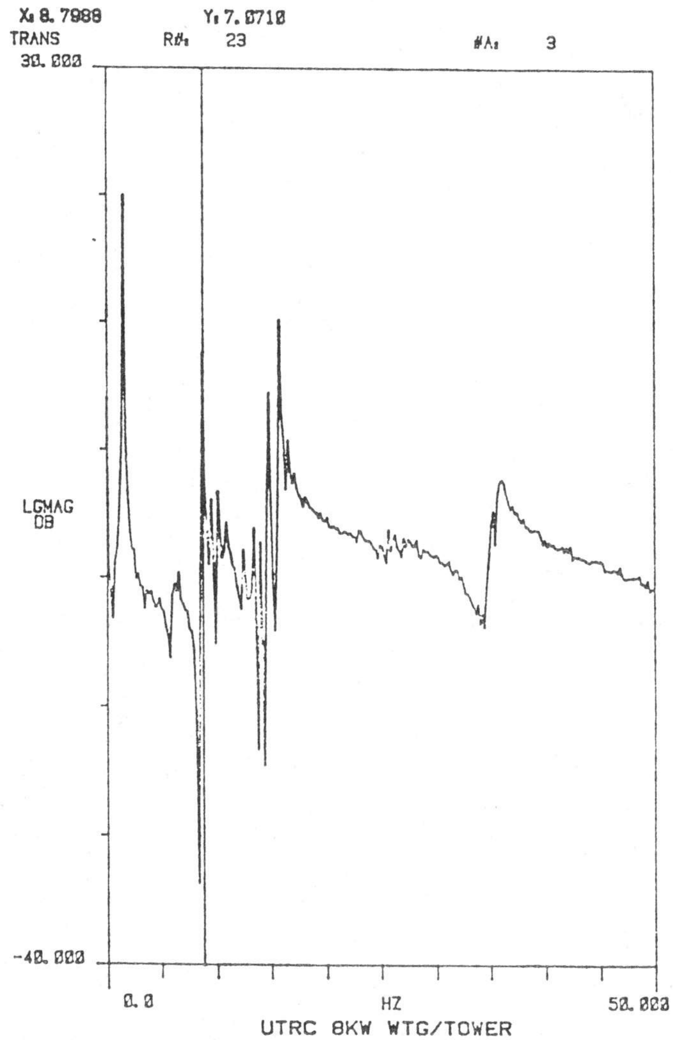

TYPE OF EXCITATION IMPACT

LOCATION OF INPUT TOWER TOP

LOCATION OF RESPONSE XDCR TOWER TOP

4/2/80

Figure 20

Transfer Function (WTG/Tower)

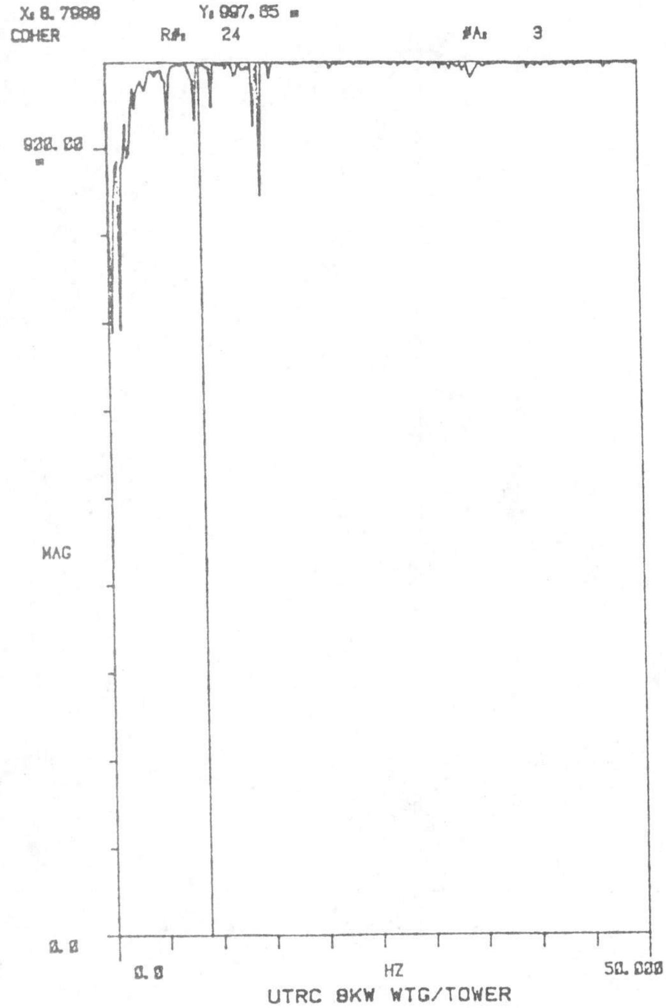

TYPE OF EXCITATION		IMPACT
LOCATION OF INPUT		TOWER TOP
LOCATION OF RESPONSE XDCR		TOWER TOP
	4/2/80	

Figure 21
Impact Test

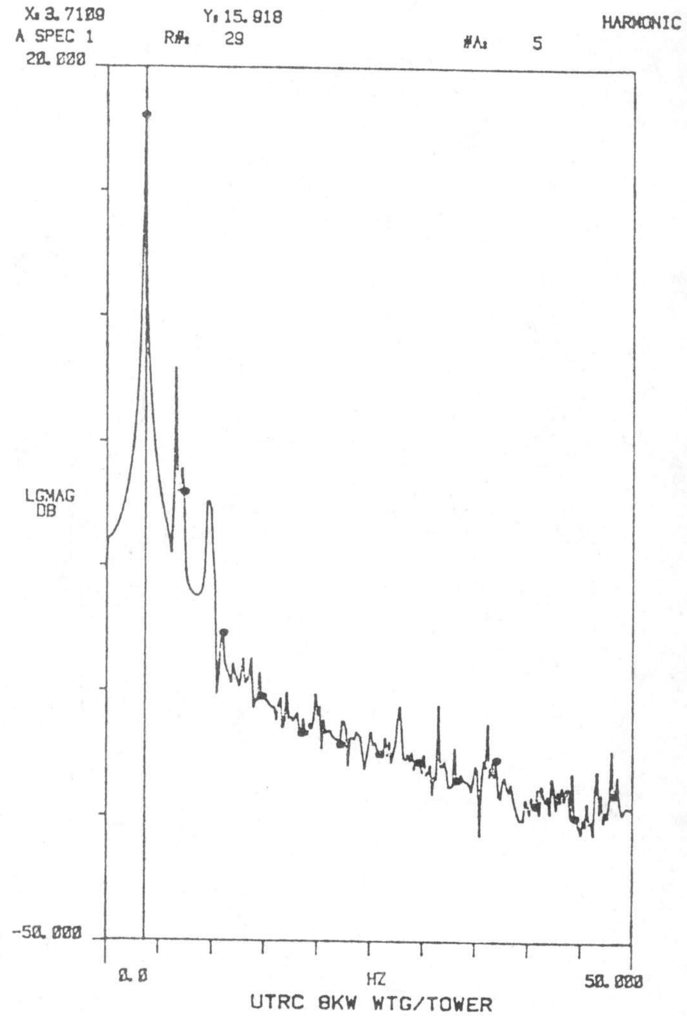

TYPE OF EXCITATION		HAND SHAKE
LOCATION OF INPUT		GUY SOUTH UPPER
LOCATION OF RESPONSE XDCR		GUY SOUTH UPPER
	4/2/80	

Figure 22
Guy Frequency

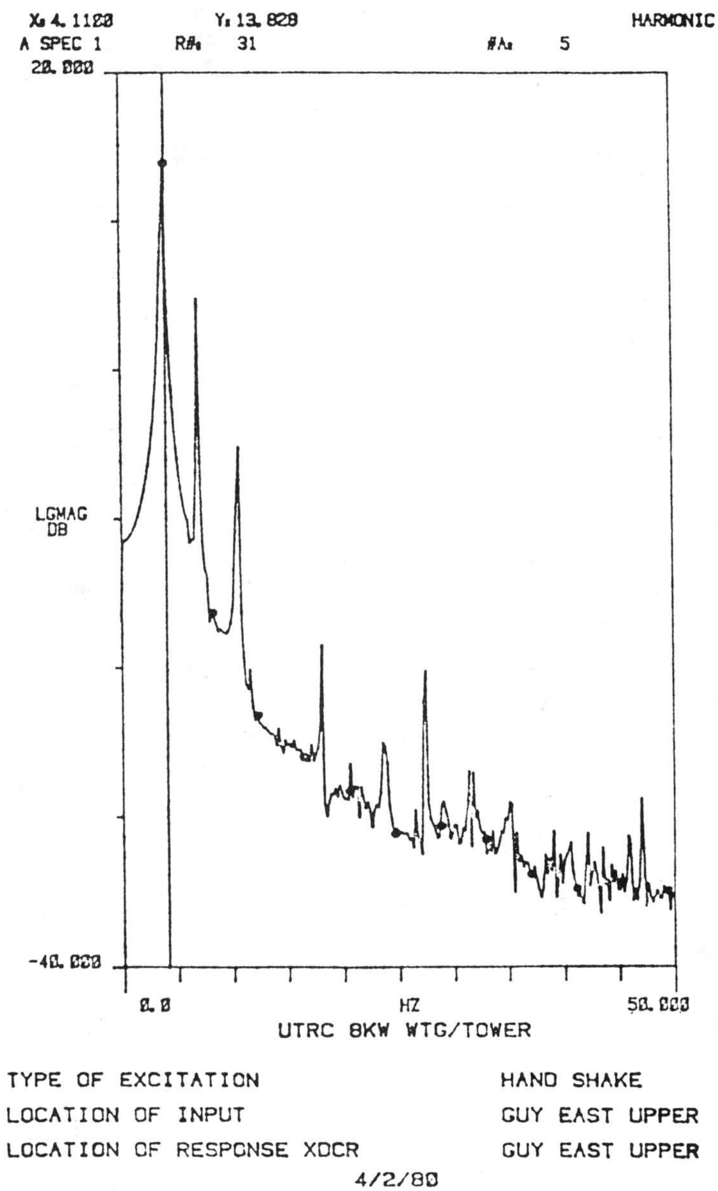

Figure 23

Guy Frequency

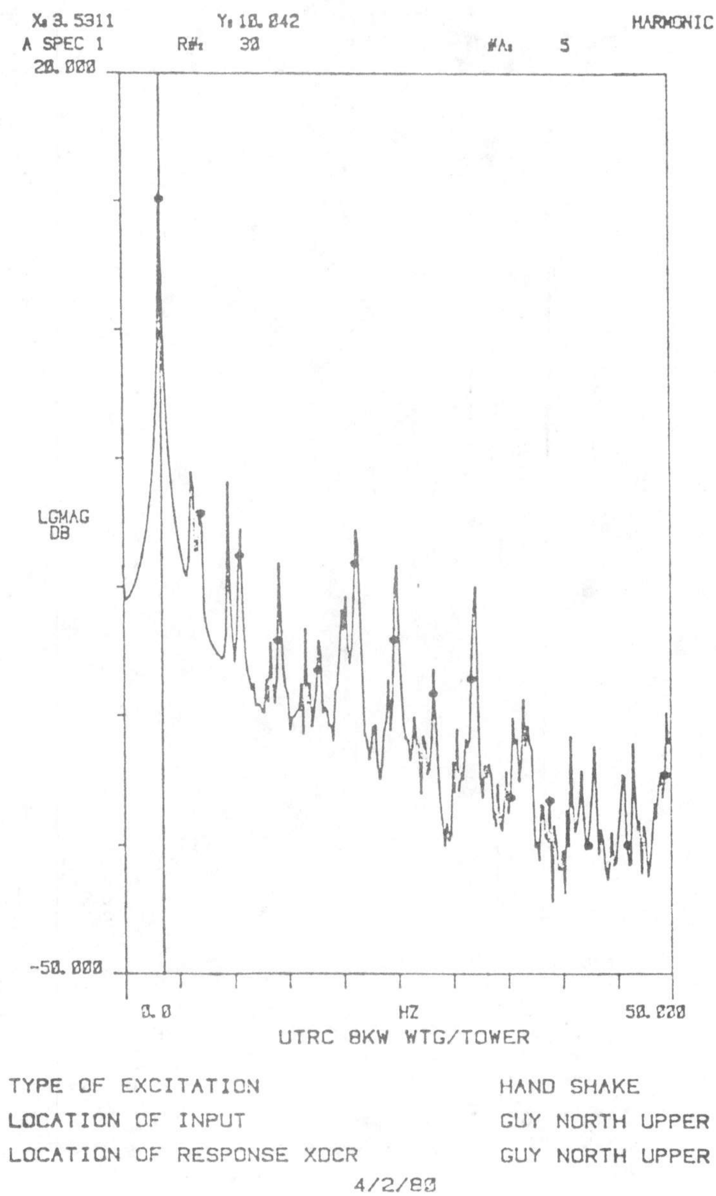

Figure 24

Guy Frequency

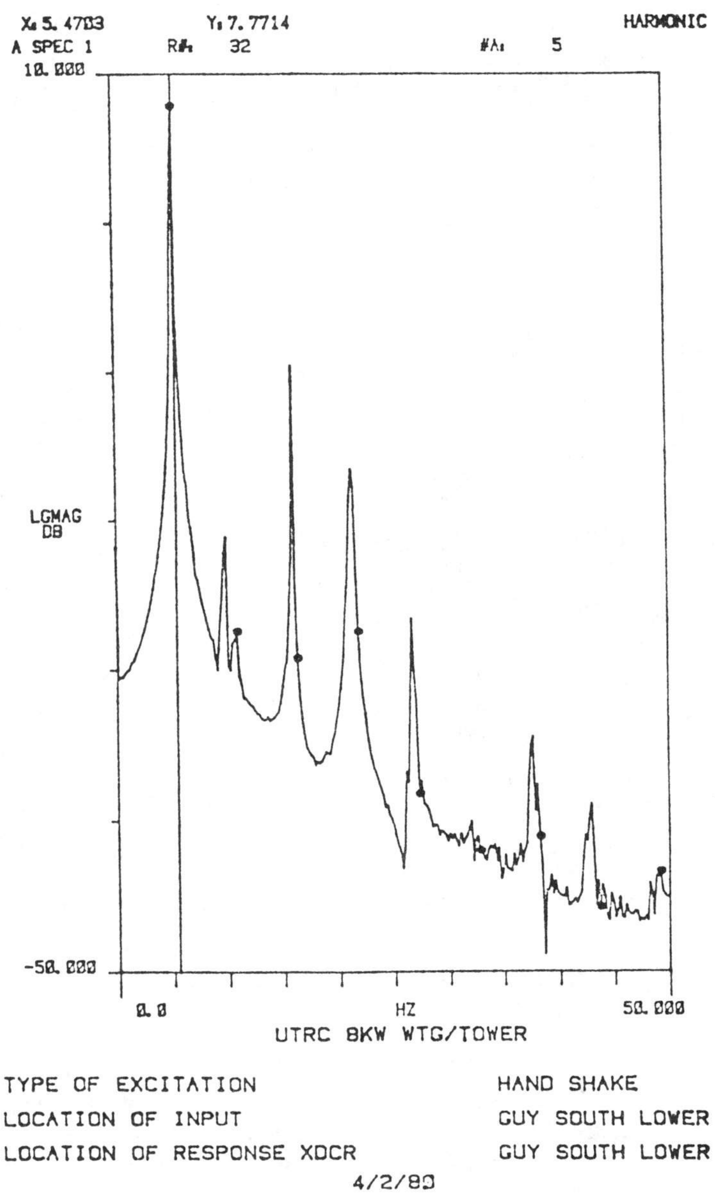

Figure 25

Guy Frequency

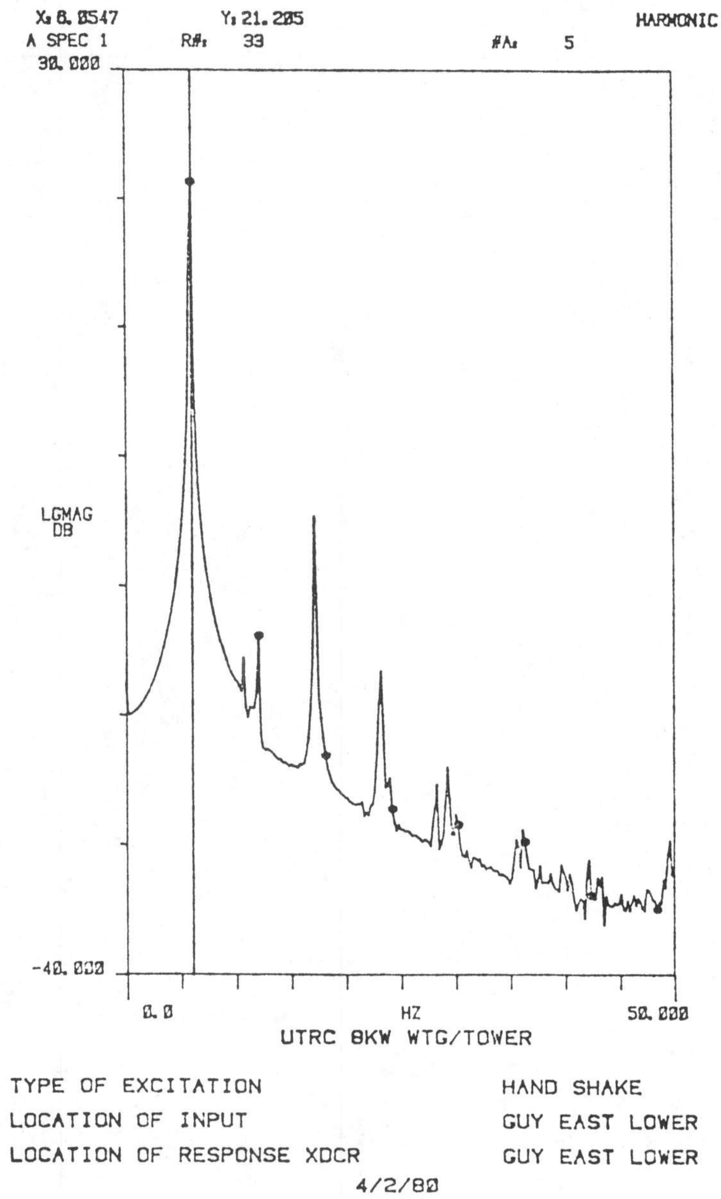

Figure 26

Guy Frequency

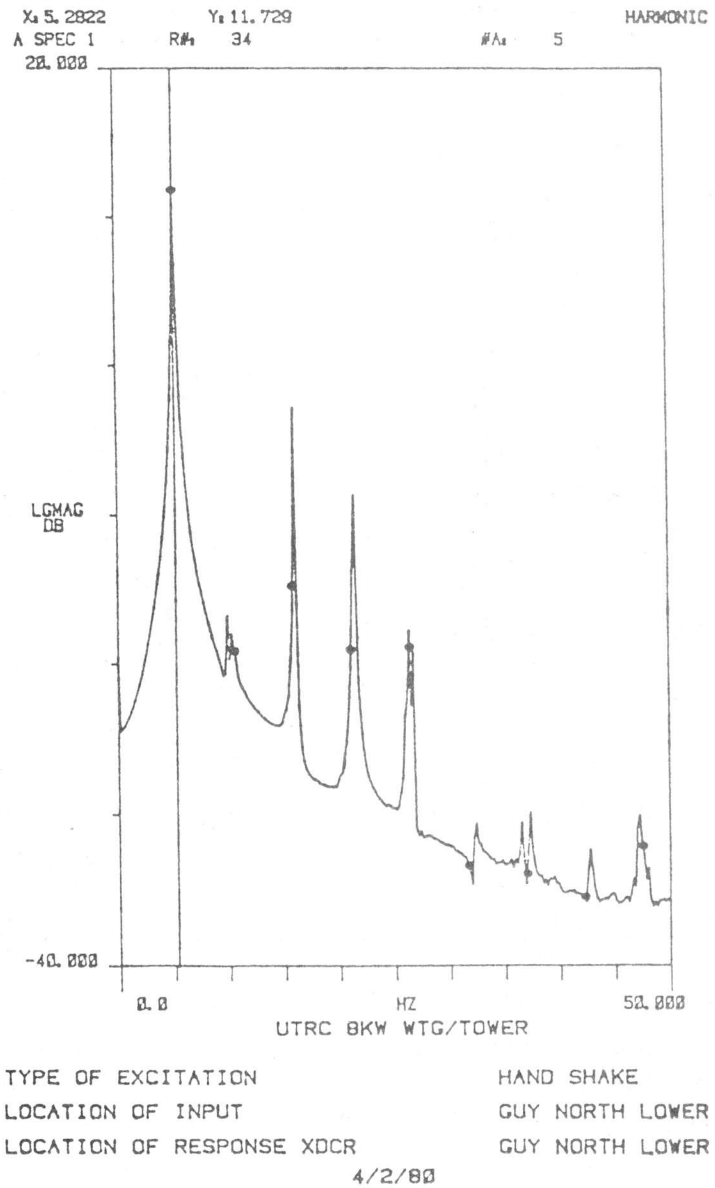

Figure 27

Guy Frequency

Auto Spectrum (Machine Operating) Tests

Accelerometers were mounted on the tower to gather data pertaining to the prototype's vibrational characteristics while in operation. The accelerometers were mounted on the tower as shown in Figure 28.

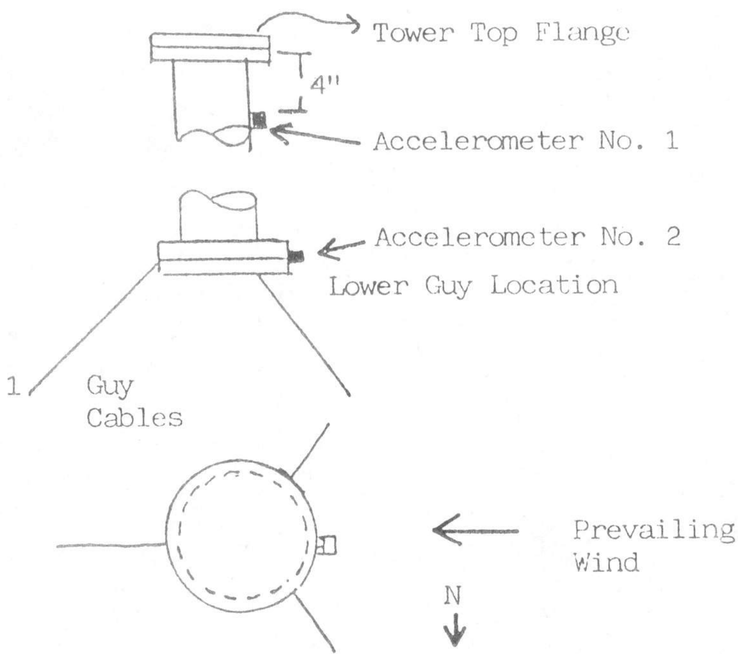

Figure 28
Accelerometer Locations

Figure 29 depicts the auto spectrum at Location 1. Data reflected in Figure 30 were taken at Location 2. The machine was generating 6 kW during the measurements, but RPM and wind speed data were not available due to instrumentation problems. As can be seen from both plots, the first and second bending modes were excited during machine operation. While excitation of the first bending mode is not, at the present time, considered serious, the second bending mode can be visually observed at the point where the tower sections are bolted together. Please note that the frequencies between the first and second tower bending modes are guy wire frequencies (Figures 22-27).

UTRC representatives were present during these tests and felt that while the second bending mode was a concern, the amplitudes were such that the machine could operate in its present configuration. Test site personnel concurred with this opinion. However, excitation of the second bending mode remains a concern that will require close observation and monitoring.

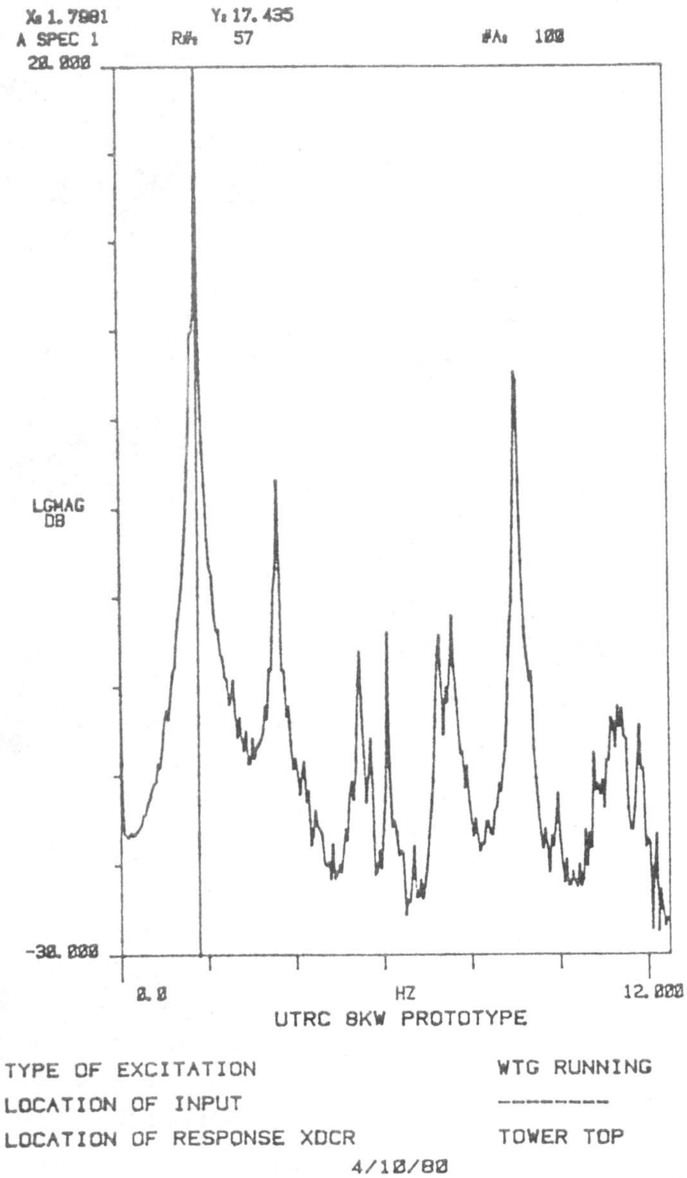

Figure 29

Auto Spectrum Location #1

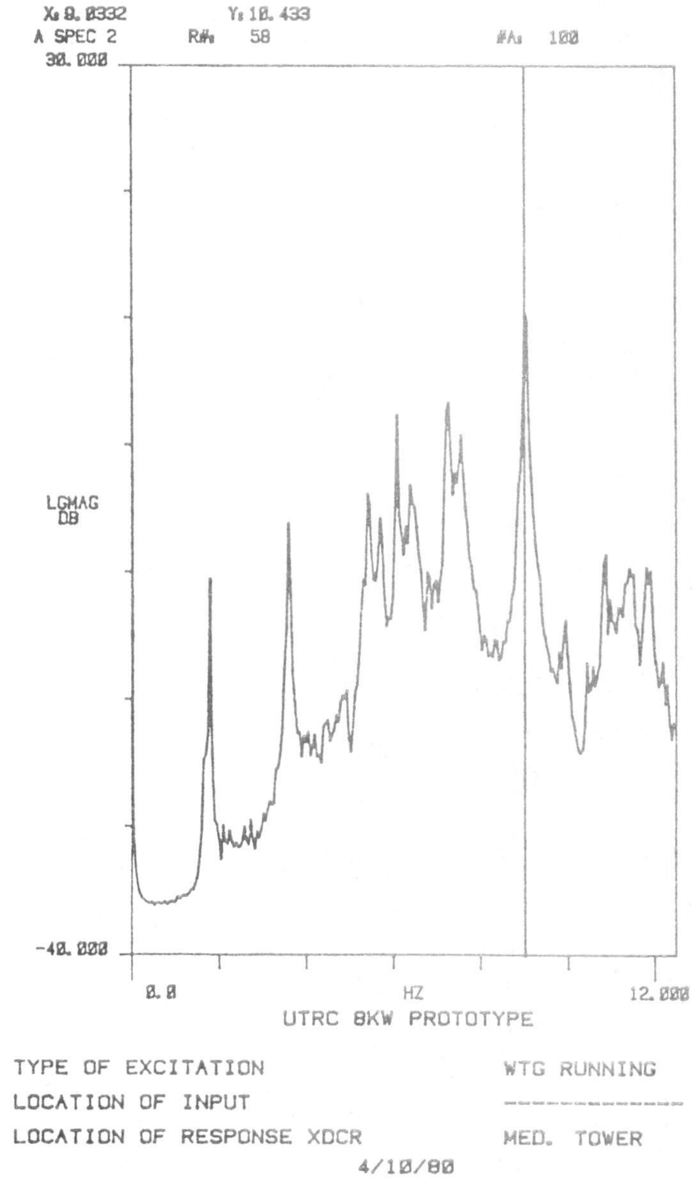

Figure 30

Auto Spectrum Location #2

LIST OF ABBREVIATIONS

Auto	–	Auto Spectrum
dB	–	Decibel
FFT	–	Fast Fourier Transform
ω	–	Frequency in Hertz
Hz	–	Hertz
LG	–	Log
Mag	–	Magnitude
S( )	–	Test Series (Number)
Trans	–	Transfer Function
FMB	–	First Mode Bending
SMB	–	Second Mode Bending
TMB	–	Third Mode Bending
FtMB	–	Fourth Mode Bending
FvMB	–	Fifth Mode Bending
FMT	–	First Mode Torsional
SMT	–	Second Mode Torsional
TMT	–	Third Mode Torsional

TN-80-10

MODIFICATIONS TO THE SPEED CONTROL BOX OF THE UNITED TECHNOLOGIES RESEARCH CENTER 8kW PROTOTYPE WIND TURBINE GENERATOR

S. L. West

August 1980

Additional available reports on the United Technologies Research Center (UTRC) 8 kW prototype wind turbine generator are listed below and are available from National Technical Information Service.

1. Development of an 8 kW Wind Turbine Generator for Residential Type Applications, Phase I - Design and Analysis, June 25, 1979, M. C. Cheney, et al., United Technologies Research Center, Volume I - Executive Summary, 10 pp., (RFP-3006-1); Volume II - Technical Report, 202 pp., (RFP-3006-2).

2. UTRC 8 kW Wind System, Phase II - Fabrication and Test, February 4, 1981, R. B. Taylor and M. C. Cheney, United Technologies Research Center, Executive Summary, 13 pp., (RFP-3232-1); Technical Report, 93 pp., (RFP-3232-2)

3. United Technologies Research Center 8 kW Prototype Wind System, Final Test Report, September 1981, K. K. Higashi, 26 pp., $6.00. (RFP-3294).

MODIFICATIONS TO THE SPEED CONTROL BOX OF THE UNITED TECHNOLOGIES RESEARCH CENTER 8 kW PROTOTYPE WIND TURBINE GENERATOR

Introduction:

The United Technologies Research Center (UTRC) 8kW wind turbine generator (WTG) is a two-bladed, horizontal-axis, downwind, government-funded prototype with a rotor diameter of 9.5 m (31 ft). The machine began its atmospheric testing program at the Rocky Flats Small Wind Systems Test Center (WSTC) during April, 1980.

While undergoing testing, a problem was identified in the UTRC generator speed control box which monitors generator rpm and interconnects the machine to utility lines. This problem created eratic cycling of the preset drop-out delay time for disconnecting the machine from the utility grid. After bench testing of an identical control box for the UTRC 1/3 scale model resulted in the same type of failure, the problem was further defined to be the delay circuit of the control box. Examination of this circuit showed that the preset delay time for drop-out was inconsistent and created oscillation of a large contactor which sends excitation voltages to the induction generator. Thorough examination of the complete control box circuit indicated only the delay circuit was malfunctioning. Consequently, this Technical Note describes the modifications made to the delay circuit by WSTC personnel and not a lengthy discussion of the complete control circuit. The modifications to the delay circuit involved the addition of several small parts and the utilization of a previously non-used function of the timer circuit itself.

Discussion of Results:

The "heart" of the delay circuit is a 555 timer chip with an external resistor and capacitor whose time constant determines the length of the timing cycle. The 555 timer chip also has a provision for a reset, but it was not being used in this application. Instead, the reset was connected to +5Vdc - a normal configuration if the reset is not being used. After testing and observing the action of the delay circuit, it became apparent that the utilization of the reset function would enhance the circuit performance and correct the problem of inconsistent delay time.

Also, the addition of two resistors, one capacitor and one transistor was necessary to make the reset function operational. Then, a properly timed pulse was located elsewhere in the electronic external circuits and applied to the reset via the additional parts.

Figure 1 depicts the timing circuit as well as the part of the external circuits where the reset pulse was extracted. The reset pulse comes from pin 8 of IC9, a "D" type edge triggered "flip-flop". This output goes to a low state immediately after the high setpoint is exceeded. This is the correct time to reset the timer so it will be able to time out should the rpm decrease below the low setpoint setting. Transistor Q1 (which was added) holds the reset high until the reset pulse arrives from IC9. This pulse momentarily turns off transistor Q1, thereby effectively grounding the reset through R2 (the 2.7k ohm resistor) and resetting the timer.

After extensive bench testing of the speed control box incorporating the modifications described above, it was installed on the UTRC during gusty wind conditions. It has, to the present time, performed well and maintained the delay period consistently. Adjustments have been made to set the delay at four seconds, the high setpoint to 1855 rpm and the low setpoint to 1795 rpm. It should also be noted that these modifications were made only to the replacement speed control box, and the original unit has not been modified.

Recommendations:

As of the present time, the modified speed control box is still installed on the UTRC 8kW prototype and apparently functioning properly. It is felt that continued testing of the modified speed control box under varying wind conditions would be advantageous to both WSTC personnel and the manufacturer.

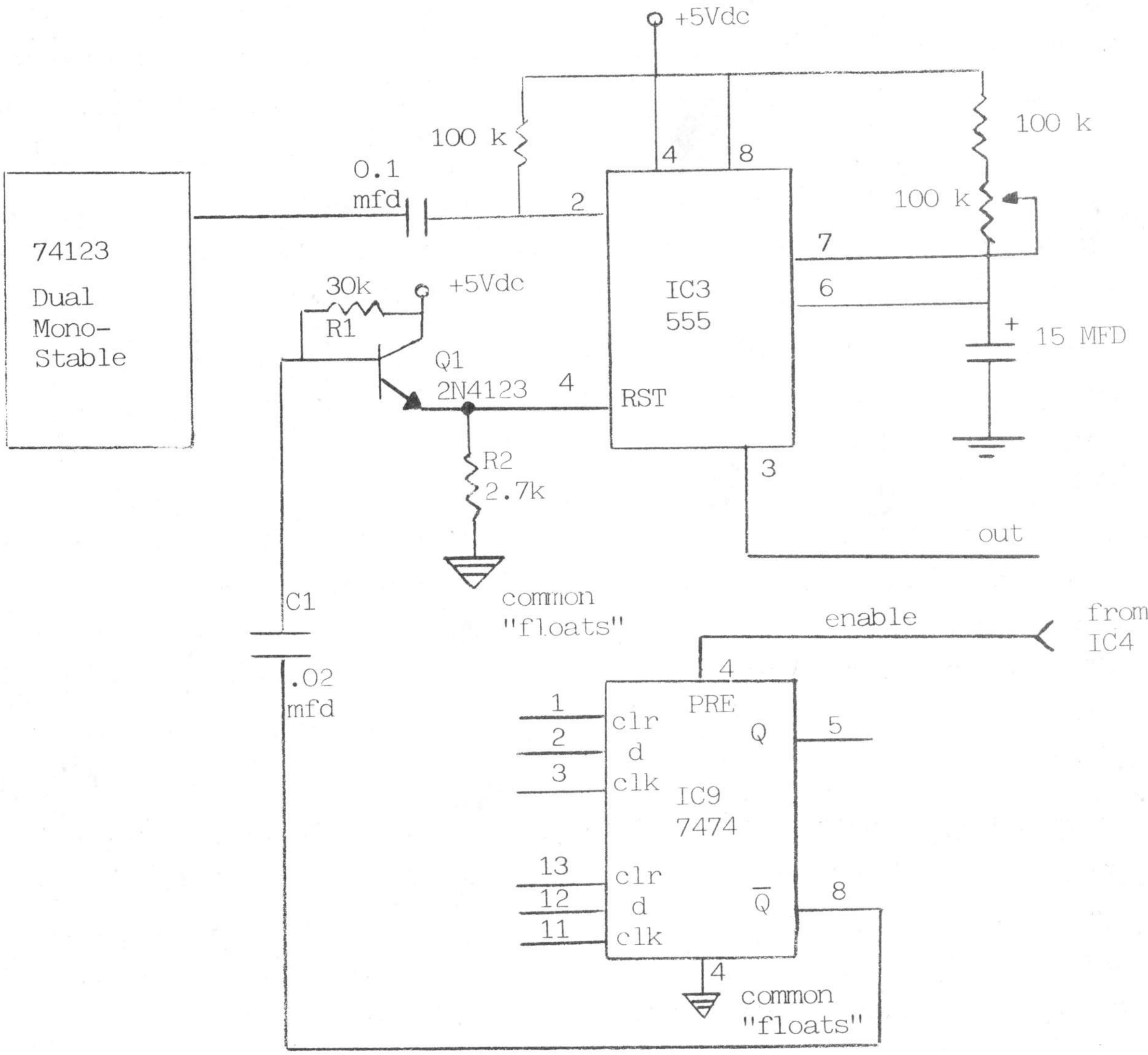

Figure 1

Timing Circuits

TN-80-11

ALTERNATOR OUTPUT FREQUENCY MONITORING

FOR

RPM DATA COLLECTION

S. L. West

August 1980

FIGURES

ALTERNATOR OUTPUT FREQUENCY MONITORING
FOR
RPM DATA COLLECTION

Introduction:

Wind turbine generators (WTG's) utilizing alternators are different from induction generators in that they are not synchronous with line voltage. Therefore, it is possible to monitor an alternator output frequency for the purpose of obtaining rpm data. The conversion of output frequency to rpm data depends upon the number of poles an alternator has and is calculated where F = frequency and NP = number of poles by performing:

$$\text{rpm} = \frac{2F}{NP} \times 60$$

Calculating rpm data by the use of a frequency monitoring device has several advantages over more conventional methods such as magnetic pickup transducers or optical sensors. One advantage is that magnetic transducers and optical sensors require geartooth or slotted disc hardware mounting, respectively; alternator frequency monitoring does not. Also, sensors and transducers require the installation of slip rings and cables for transfering data to the instrument inputs at ground level. These types of additions can be costly and their installation time consuming. In most cases, frequency monitoring requires no additional equipment except connection of a monitoring unit to the ac side of the output power line. This type of installation has been used at the WSTC on the Whirlwind A240 (MOD), Windworks 8kW prototype and the Aero Power SL1000 WTG's. These machines have control boxes at ground level.

However, some WTG's have alternators which rectify the ac output at the alternator itself. This situation requires a cable carrying the ac signal to be interconnected with the frequency monitoring unit on the ground. This configuration is being used to monitor rpm data of the Enertech High Reliability prototype during its testing program at RF.

This note discusses the design and implementation of different frequency monitoring units used at the WSTC.

DISCUSSION:

Various schemes for looking at the frequency of the output power lines indicated that special precautions would have to be taken to eliminate the problems (such as erroneous rpm count) noise could create when using the frequency monitoring technique. Also, isolation circuitry was required for "floating" power output systems, and input inpedance had to be considered due to the fact that some alternators are regulated (i.e., 30V) and some are non-regulated (i.e., 200Vac or over). The input circuitry designs of frequency monitoring units for various WTG outputs (regulated and non-regulated) are depicted in Figures 1a, 1b and 1c .

Figure 1a shows the input design of a monitoring system for a 30V regulated WTG (Enertech High Reliability). The 1.2k resistor (R1) limits the current going to the optical isolator light emitting diode to approximately 25 milli-amps during positive excursion of the sinewave. Diode D1 clamps the negative half cycle of the signal.

Figures 1b and 1c show two different methods to current limit non-regulated alternators using a F40X, 26.8V filament transformer. In Figure 1b, the primary of the F40X acts as a high impedance choke in series with the light emitting diode to limit current to the diode. In this case, the secondary of the transformer is left disconnected. Figure 1c illustrates another method of current limiting by using the primary and secondary of the F40X to step-down the voltage to a useable level. This method also accomplishes isolation, therefore eliminating the need for a 4N32 optical isolator. The 1200 ohm resistor (R1) limits the current to the 5V Zener Diode. Output waveforms are then held to the 5V level with all of these input circuits in order to interface with the TTL circuits.

At this point, noise that was present in the WTG output lines is also retained and must be eliminated for accurate data collection. Figure 2 is a schematic showing an active low pass digital filter with output latch circuitry. In order to cut-off high frequency noise, this filter

Figure 1a

Inputing and Isolating 30Vac Regulated Alternators

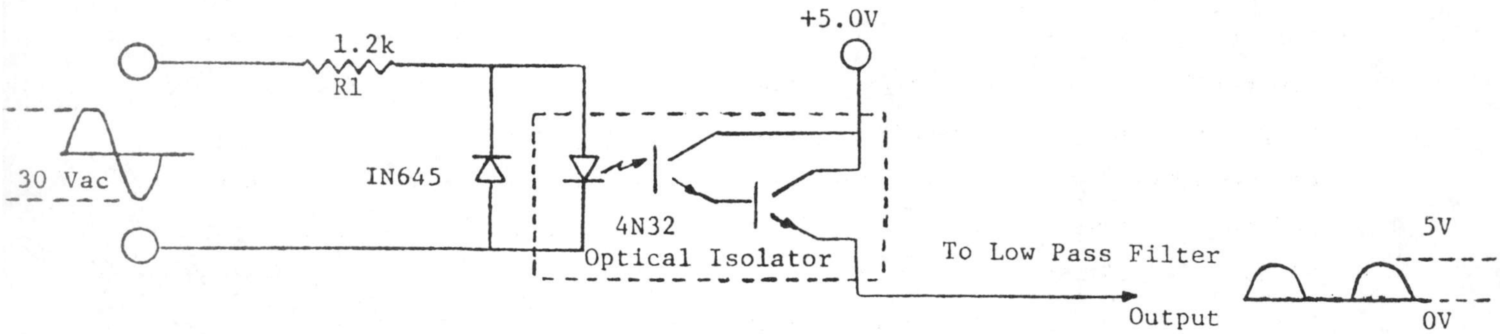

Figure 1b

Inputing and Isolating Non-Regulated Alternators
(≈ 250 Vac)

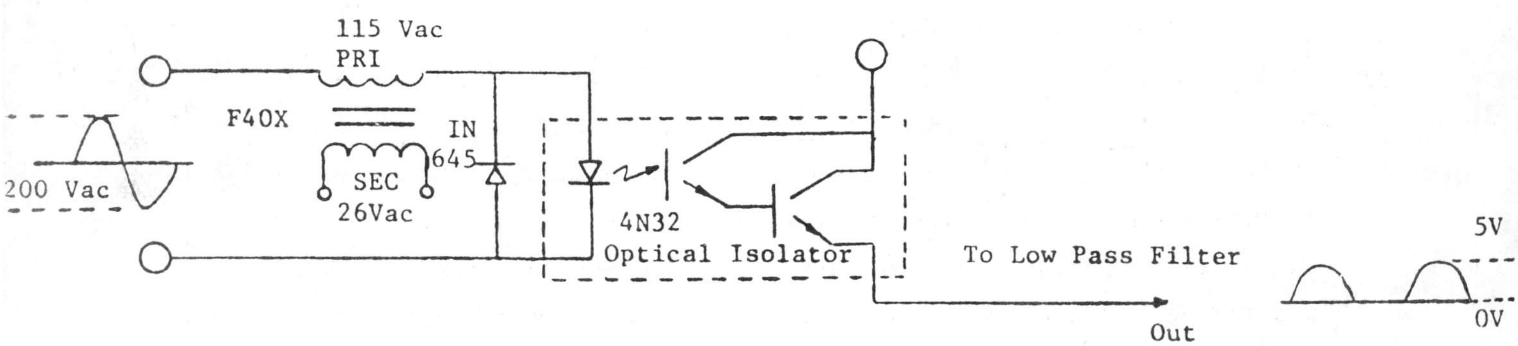

Figure 1c

Using Filament Transformer for Isolation on Non-Regulated Alternators

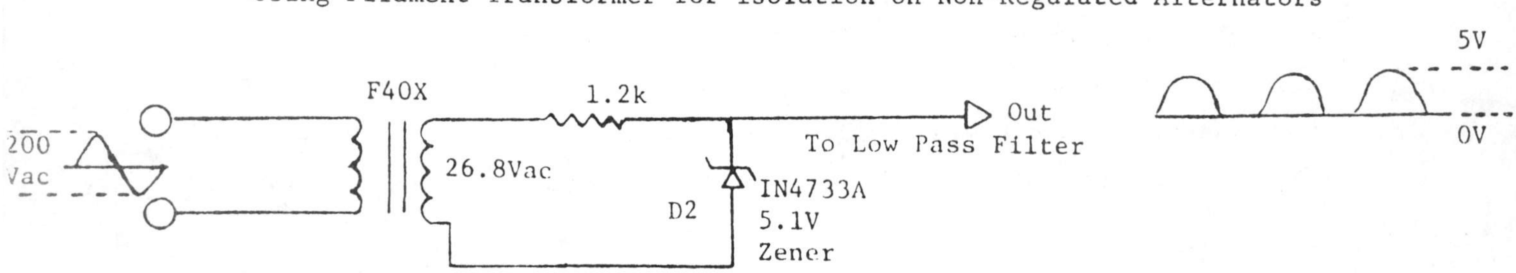

Figure 2

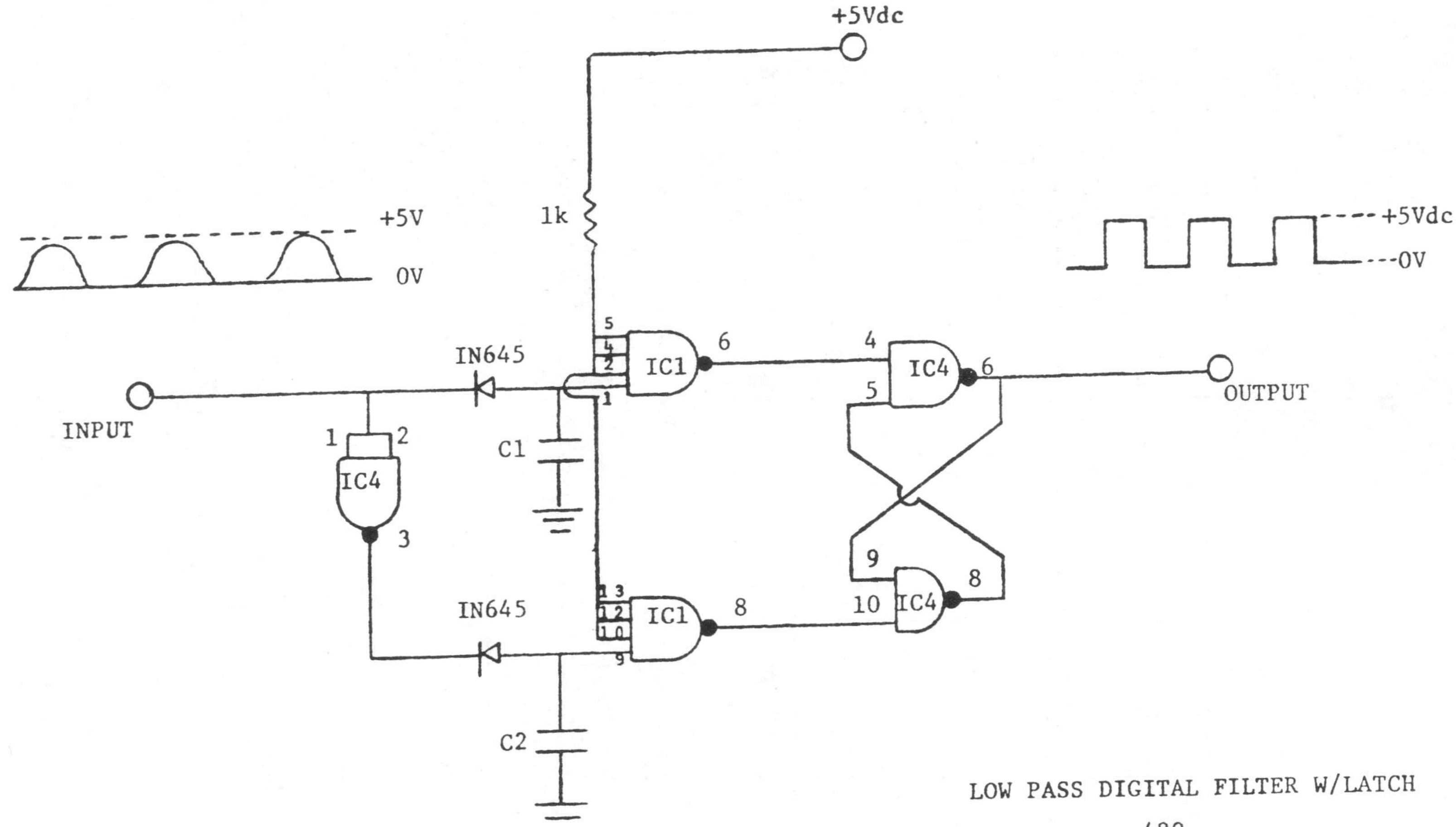

LOW PASS DIGITAL FILTER W/LATCH

$$C1=C2 \quad = \quad \frac{480}{Fc + 200}$$

Fc = Cut-off Frequency

IC1 = 7413

IC4 = 7400

has a sharp cut-off frequency which is adjusted by the selection of capacitors C1 and C2. Where Fc equals the cut-off frequency,

$$C1 = C2 = \frac{480}{Fc + 200}$$

The cut-off frequency of the low pass filter is selected to be approximately twice the maximum frequency counted in order to assure that all pertinent rpm data get through the filter. This filter uses two Ic chips: a 7413 Schmitt trigger and a 7400 quad nand gate (used for inversion to one input of the trigger and as an output latch circuit). The output of the latch is a 5V squarewave signal with fast rise and fall times and is ready to be interfaced with a micro, counter, printer, etc.

The designs of the first model power output frequency monitors have been discussed in the preceding paragraphs. However, after a period of operation in the field, it was found that data generated from some machines were acceptable, while data from "noisier" machines were poor due to noise pulses present in the output. It was determined that since the low pass filter was set to pass frequencies of twice the expected maximum output of the WTG to assure data collection during overspeed, it was allowing some inherent low frequency noise pulses to get through the filter to the output. Consequently, this problem prompted a search for further improvements in the design.

Most alternator WTG's are 3 phase machines, but the frequency counter discussed above used only one of the three phases. Figure 3a shows a normalized 3Ø voltage waveform, with phase 1, 2 and 3 labeled in that order. After close examination, it became evident that by inverting one phase, all three phases are high together at one period in the positive half cycle. Figure 3b (between dashed lines) depicts this concept by using phase 2 for the inversion. By the inversion of Ø2 and the following of gating circuitry, a "window" effect for better noise can be obtained. Figure 3c shows the squarewave signal at the output of the low pass filter latch circuits. By "and" gating, an output pulse of one-third (60^{o}) occurs at the output of the total 180 degree swing of the positive half cycles. It should also be noted that the inversion can be

Figure 3a - Normal 3Ø Voltage Waveform

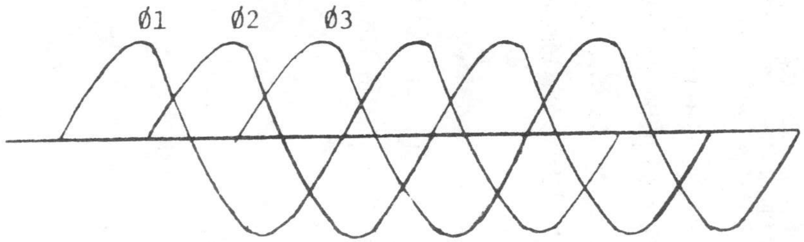

Figure 3b

3Ø Voltage Waveform with Phase 2 Inverted

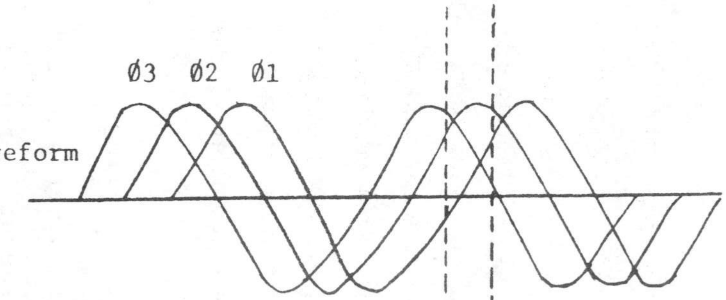

Figure 3c

Output of Latch Circuits (Different Amplitudes for Presentation Purposes Only)

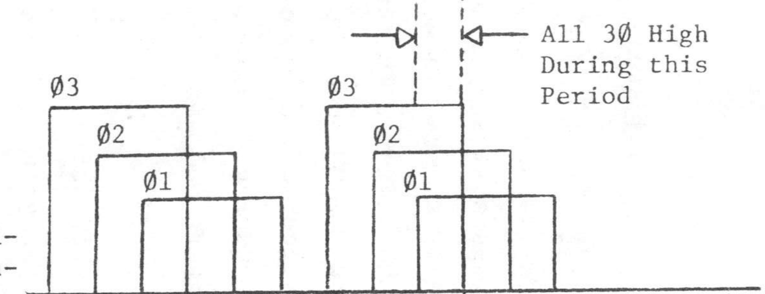

Figure 3d

Output of Gating Circuits

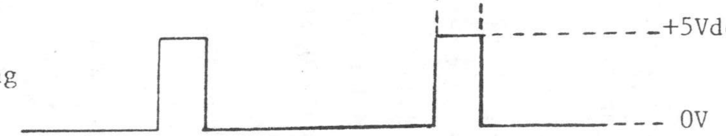

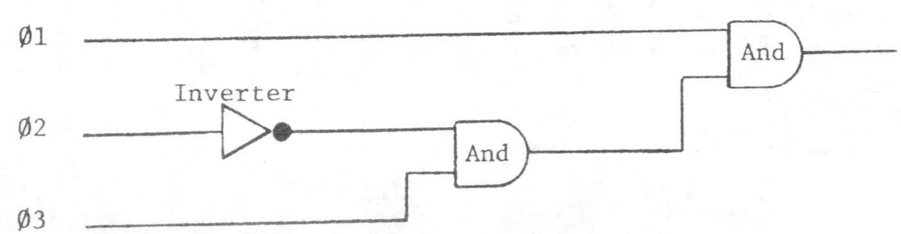

placed arbitrarily on any of the three phases and the same "window" effect would be observed, although shifted in respect to the phase itself. In actual operation, the inversion takes place after the latch circuit outputs digitize the ac sinewave signals, instead of prior to digitizing as is shown in Figures 3a and 3b. Figures 3a and 3b are intended to depict the correlation between a normal 3Ø sinewave and a sinewave with one phase inverted. Figures 4a, 4b, 4c and 4d show the normal 3Ø sinewave, the outputs of the low pass digital filter latches, the inversion of phase 2 and the outputs of the gate circuits, respectively. Figure 5 is a schematic of the completed circuit (inverter on phase 2, pins 12, 13 and 11 of IC5).

RECOMMENDATIONS:

Alternator output frequency monitoring systems have been in operation at RF for several months. As of this date, rpm data have been collected from three different WTG's (regulated and non-regulated) with good results. It is believed, therefore, that an alternator output frequency monitoring system can be used to collect rpm data accurately and efficiently in certain applications. It is important to remember, however, that two criteria must be met when considering a frequency monitoring unit: (1) the input design, which is determined by the voltage output of the alternator, must be ascertained; and (2) the frequency cut-off of the digital low pass filter, which is controlled by the number of poles and highest expected rpm of the alternator, must be determined. The remainder of the circuitry is standard for all 3Ø alternator WTG's.

Figure 4a

Normal 3Ø Waveform

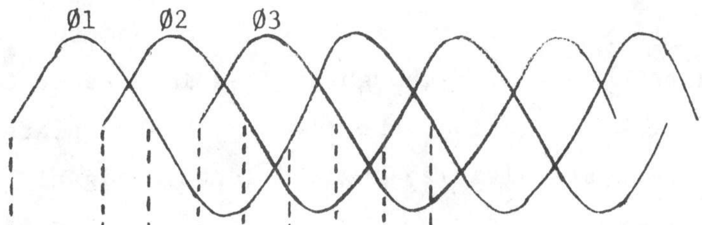

Figure 4b

Outputs of Low Pass Digital Filter Latches (Different Amplitudes Shown for Presentation Purposes Only)

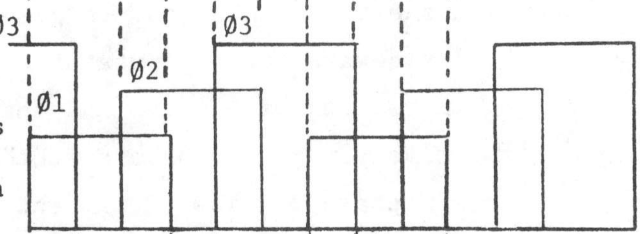

Figure 4c

Digital Signal After Ø2 Inverted

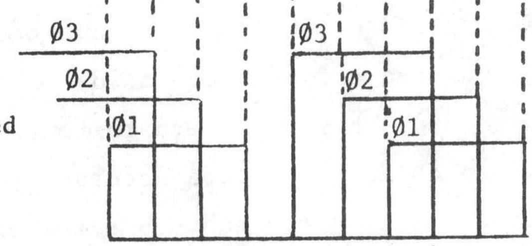

Figure 4d

Output of Final Gate

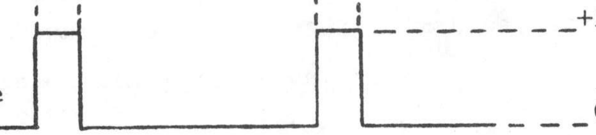

Gating Circuit

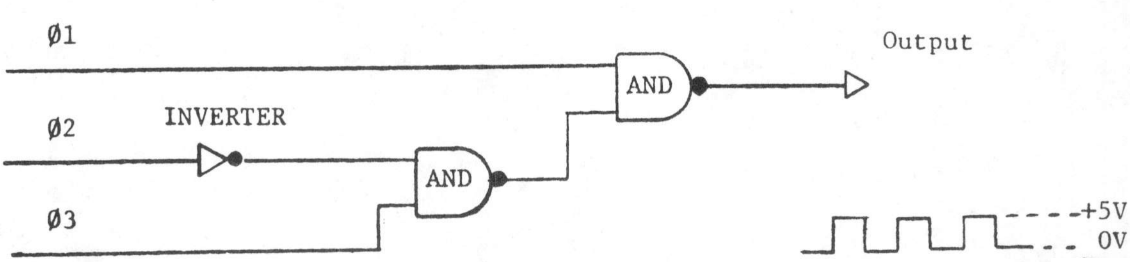

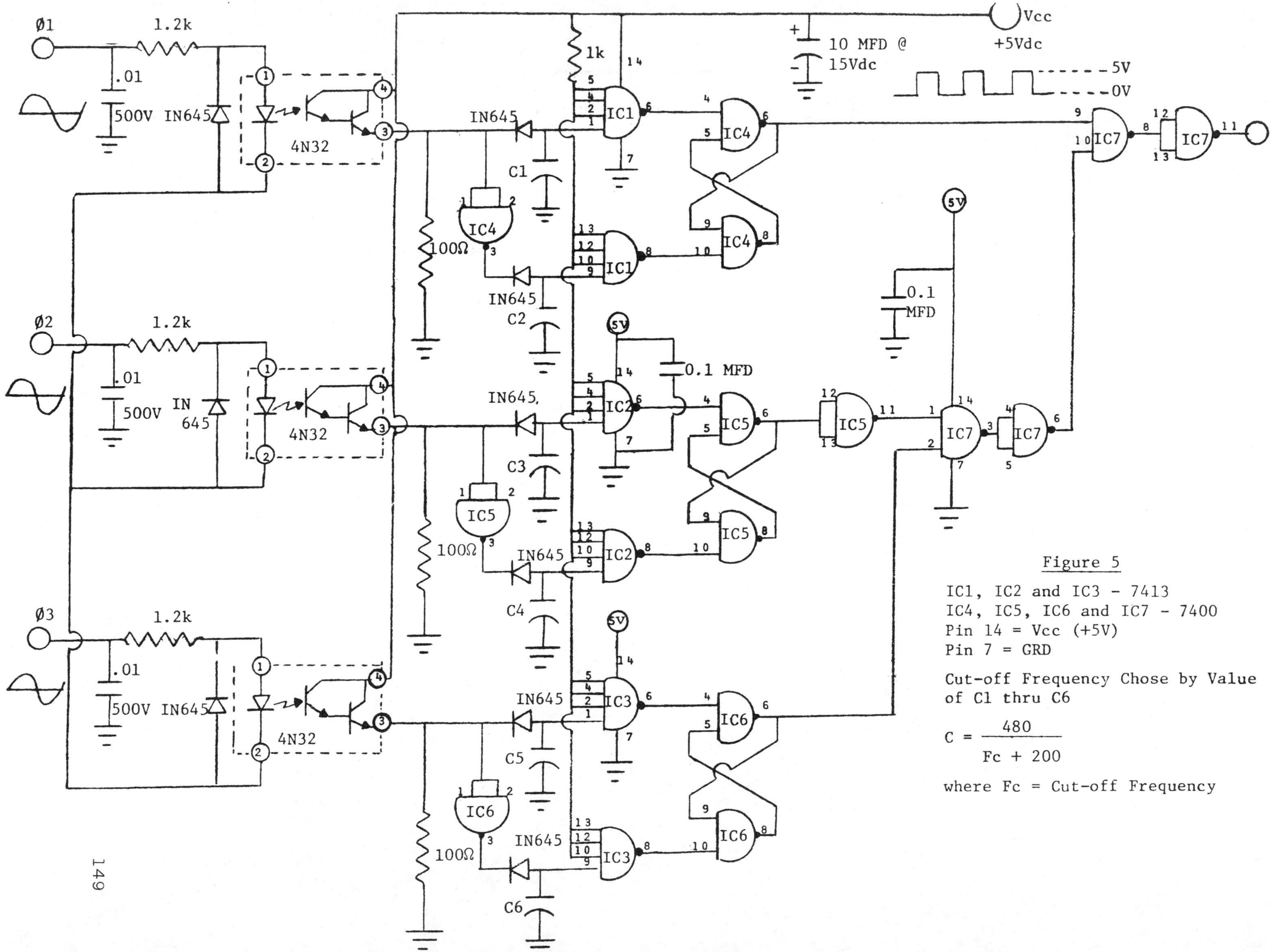

Figure 5

IC1, IC2 and IC3 - 7413
IC4, IC5, IC6 and IC7 - 7400
Pin 14 = Vcc (+5V)
Pin 7 = GRD

Cut-off Frequency Chose by Value of C1 thru C6

$$C = \frac{480}{Fc + 200}$$

where Fc = Cut-off Frequency

DYNAMOMETER TEST RESULTS

OF THE

PINSON C2E WIND TURBINE GENERATOR

G. D. Price

September 1980

Additional available reports on the Pinson C2E wind turbine generator are listed below and are available from National Technical Information Service.

Pinson C2E Wind Turbine Generator Failure Analysis and Corrective Design Modification, March 1980, M. J. Carr, V. K. Grotsky, and J. H. Sexton, 22 pp., $6.00, (RFP-3148).

FIGURES

DYNAMOMETER TEST RESULTS
OF THE
PINSON C2E WIND TURBINE GENERATOR

Introduction:

The Dynamometer Testing Facility at the Rocky Flats Small Wind Systems Test Center (WSTC) has the capability to define small wind energy conversion systems (SWECS) generator/gearbox performance for a broad variety of loads under controlled input. The data readout system produces measurements for input torque, rotor rotational speed, gearbox temperature and output power (watts). The dynamometer can also be adapted to provide additional electrical testing capabilities to include the driving of a generator matching variables of speed, voltage and frequency. The Dynamometer Testing Facility is capable of testing SWECS with outputs of up to 40 kW (Figures 1 and 2).

Test Specimen:

The Pinson C2E Wind Turbine Generator (WTG) is a commercially available machine manufactured by the Pinson Energy Corporation, Marston Mills, Massachusetts. The WTG is a vertical-axis, vertically straight-bladed machine with cyclically-pitched blades.

Dynamometer tests were performed on the alternator of the Pinson C2E wind system in an attempt to determine the cause of low power output during atmospheric testing at the WSTC. Manufactured by Winco/Dyna Technology, the alternator is an "off-the-shelf," internally excited unit that is wired for single-phase, 115/230V, 60 cycle, ac output. Power generated is designed to be dissipated into four 1 kW resistive heaters by a two-step control box. At startup, the alternator sees two 1 kW loads. As the machine speeds up, the control box switches in the remaining two 1 kW loads, making the total load 4 kW.

The drive train consists of a two-stage timing belt with 3.92:1 and 2.19:1 ratios for a total of 8.57:1. Maximum rotor shaft speed is 200 rpm, which equals an alternator speed of 1714 rpm. It should be noted, however, that dynamometer testing of the alternator was conducted without the drive train, and efficiency data presented in this Note are reflective of the alternator <u>only</u>.

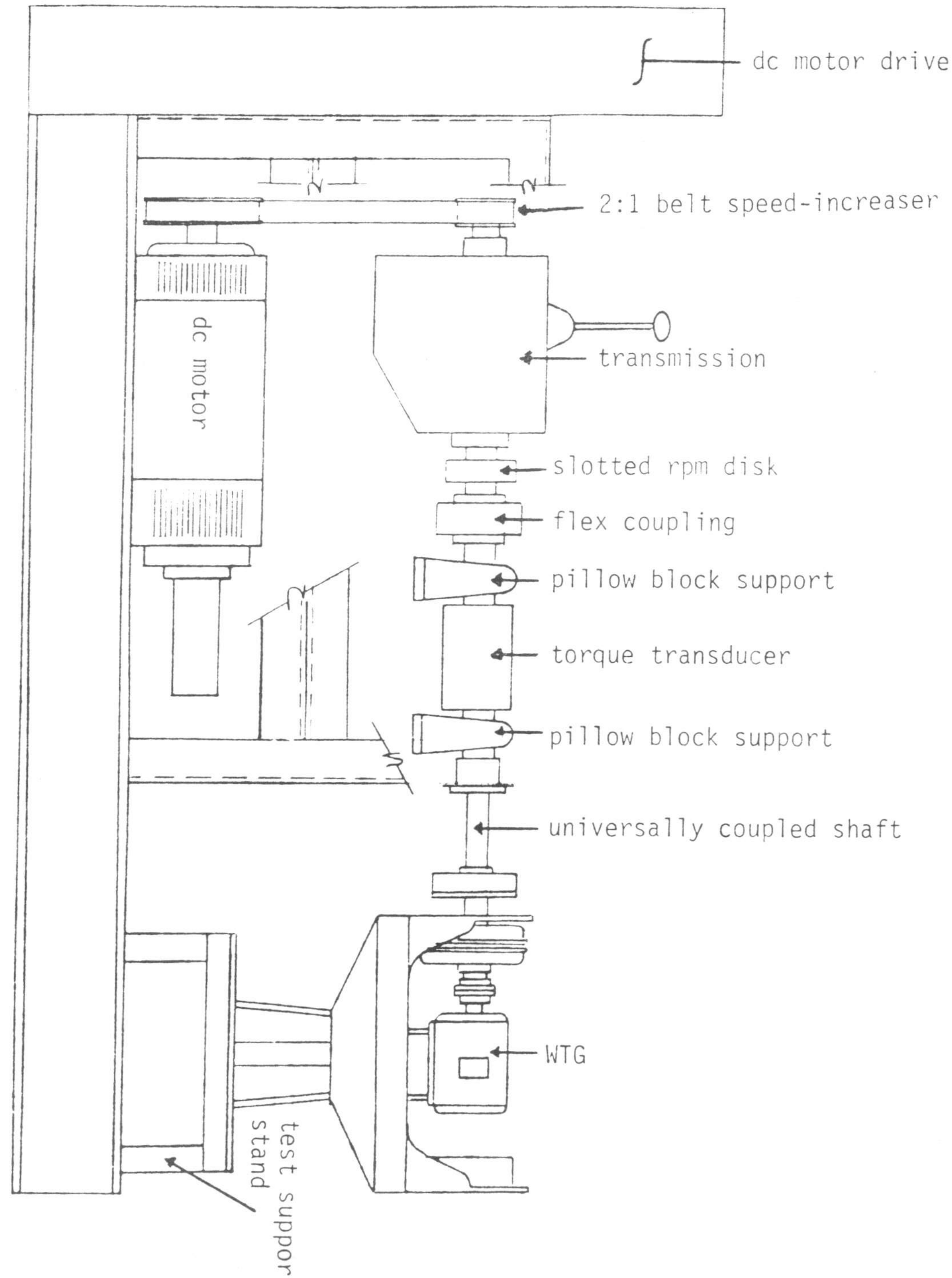

Figure 1
10 kW DYNAMOMETER

Figure 2

40 kW DYNAMOMETER

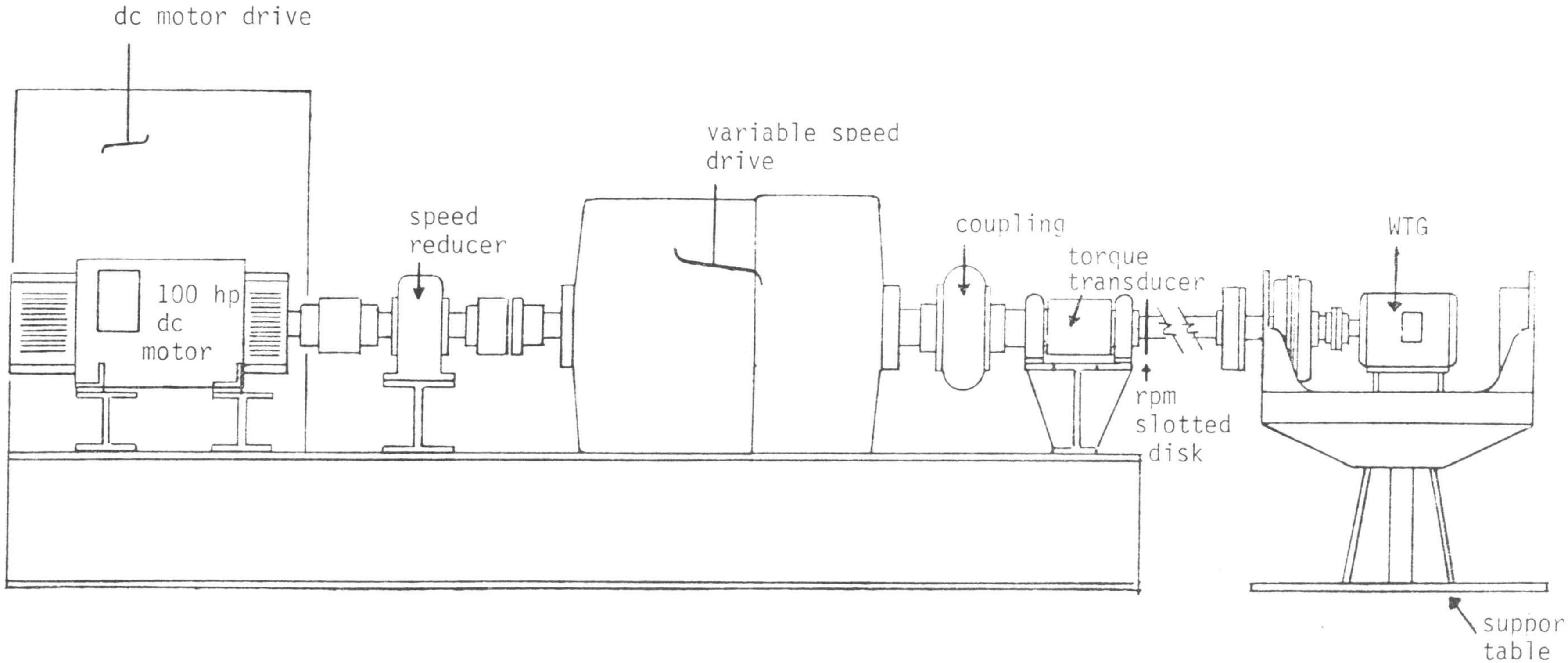

Test Instrumentation:

All instrumentation used for dynamometer testing of the Pinson C2E WTG was owned by DOE/Rockwell International. The following is a list of instrumentation used during the tests:

Instrumentation

Parameter Measured	Instrument and Manufacturer
Power Output (Amperes, Volts, Watts)	Magtrol Power Analyzer - Model 4610 Magtrol, Inc.
RPM	Digital Tachometer Rocky Flats
Torque	Shaft Torque Sensor - 1100 Series Lebow Associates, Inc.
Torque	Transducer Digital Indicator - Model 7535 Lebow Associates, Inc.

Discussion of Results:

The control box of the C2E was wired for atmospheric testing according to a sketch drawn by the manufacturer. However, when dynamometer testing started, it was found that power produced by the alternator was being dissipated into only two of the four resistive heaters. A subsequent inspection of the control box revealed the heater loads to be improperly wired to the control terminals by reversed wiring of the resistor load wires on terminals 6 and 8 (terminals are shown in Figure 3). Consequently, when C1 closed at 110 volts, the resistors on terminal 7 were not switched in. This limited the machine to a maximum output of 2 kW. Figure 3 is a schematic of the corrected wiring configuration that was used for the remainder of the tests.

During dynamometer testing of the Pinson C2E, the alternator 115 volt center tapped winding lead was not used. Instead, the full 230 volt winding was used to simulate atmospheric tests. Field current was not monitored or controlled since the alternator is internally self-excited. The alternator was driven by the prime mover at speeds from 0 to 1847 rpm. Speed, torque input, volts, amps and watt output were recorded at various

TEST SCHEMATIC

PINSON C2E

(WIRED CORRECTLY)

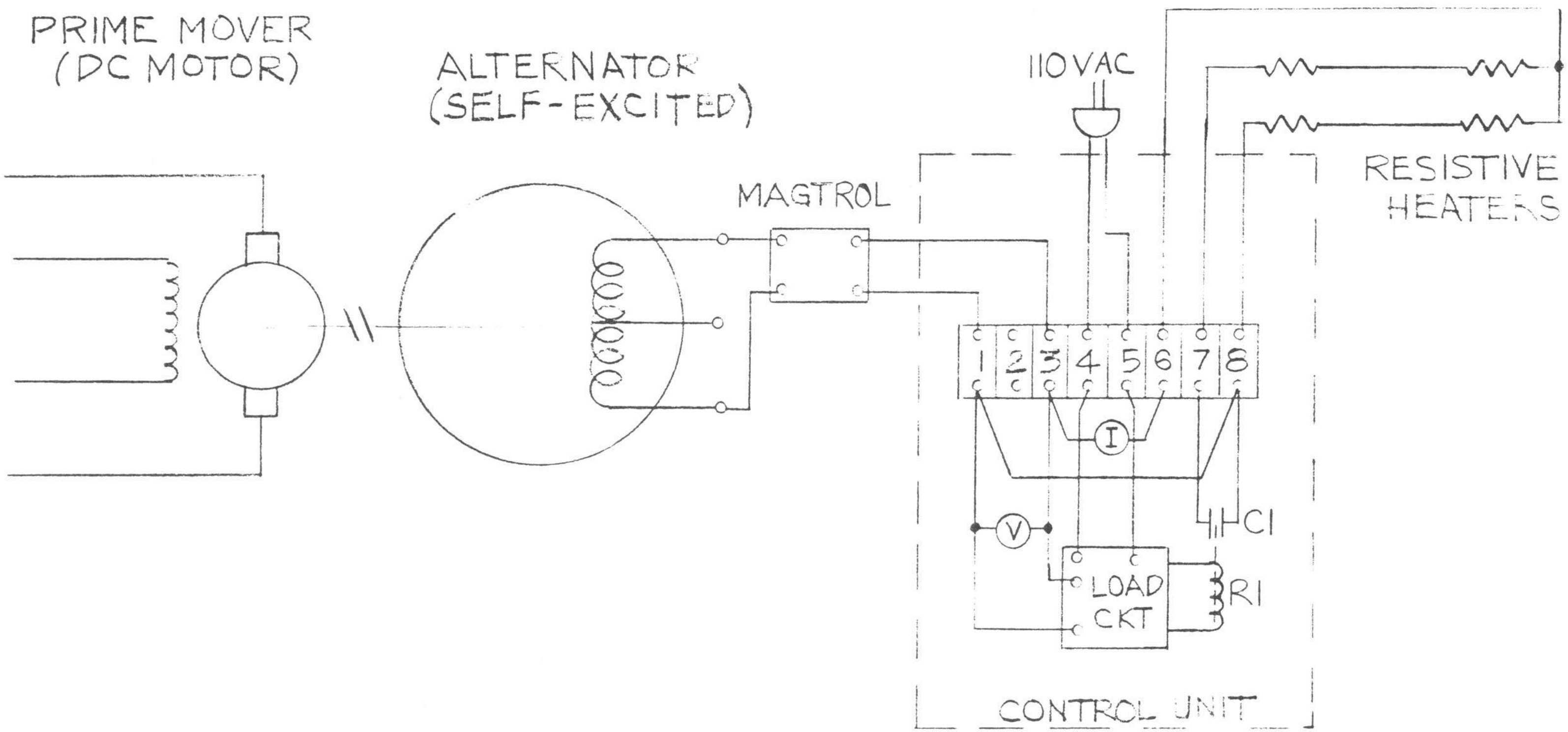

Figure 3

speeds. At 1805 rpm (the approximate rated generator speed), torque input was 260 inch-lbs, or 7.45 hp (hp = T x rpm/63.024), or 5555 watts (W_{in} = hp x 746); and output watts measured 4605 at a voltage of 248 (18.73 amps). The power factor was close to unity since the load was resistive. Efficiency was calculated at 82.9% ($E_{ff} = W_{out}/W_{in}$). Power output and efficiency curves are shown in Figures 4 and 5, respectively. Figure 4 shows the control relay operation that switches in the remaining two 1 kW loads. The dashed line represents the output before the wiring was corrected to allow all four resistive heaters to operate.

Figure 6 is tabulated test data from the C2E dynamometer tests. Comparison is made between the control box ammeter and voltmeter readings and the Magtrol volt and amp measurements. Full scale readings are 240 volts and 15 amps. The symbol "→" indicates an overscale reading. It should be noted that a 5% error was common because of difficulty in reading the small scale meters.

Recommendations:

Dynamometer testing of the Pinson C2E indicated the machine should undergo additional atmospheric testing with the correct wiring configuration. It is strongly felt that the machine is capable of producing its rated output. It is also suggested that as part of additional testing, the C2E be interfaced with a utility system. However, in the present configuration the self-excited alternator is limited to resistive heating applications because it produces variable frequency and voltage. In order to integrate the machine into a utility system, one of three modifications would have to be made: (1) the output would have to be rectified to dc and conditioned by a synchronous inverter; (2) the alternator would have to be replaced by an induction generator; or (3) the alternator would have to be replaced by a dc generator with an inverter.

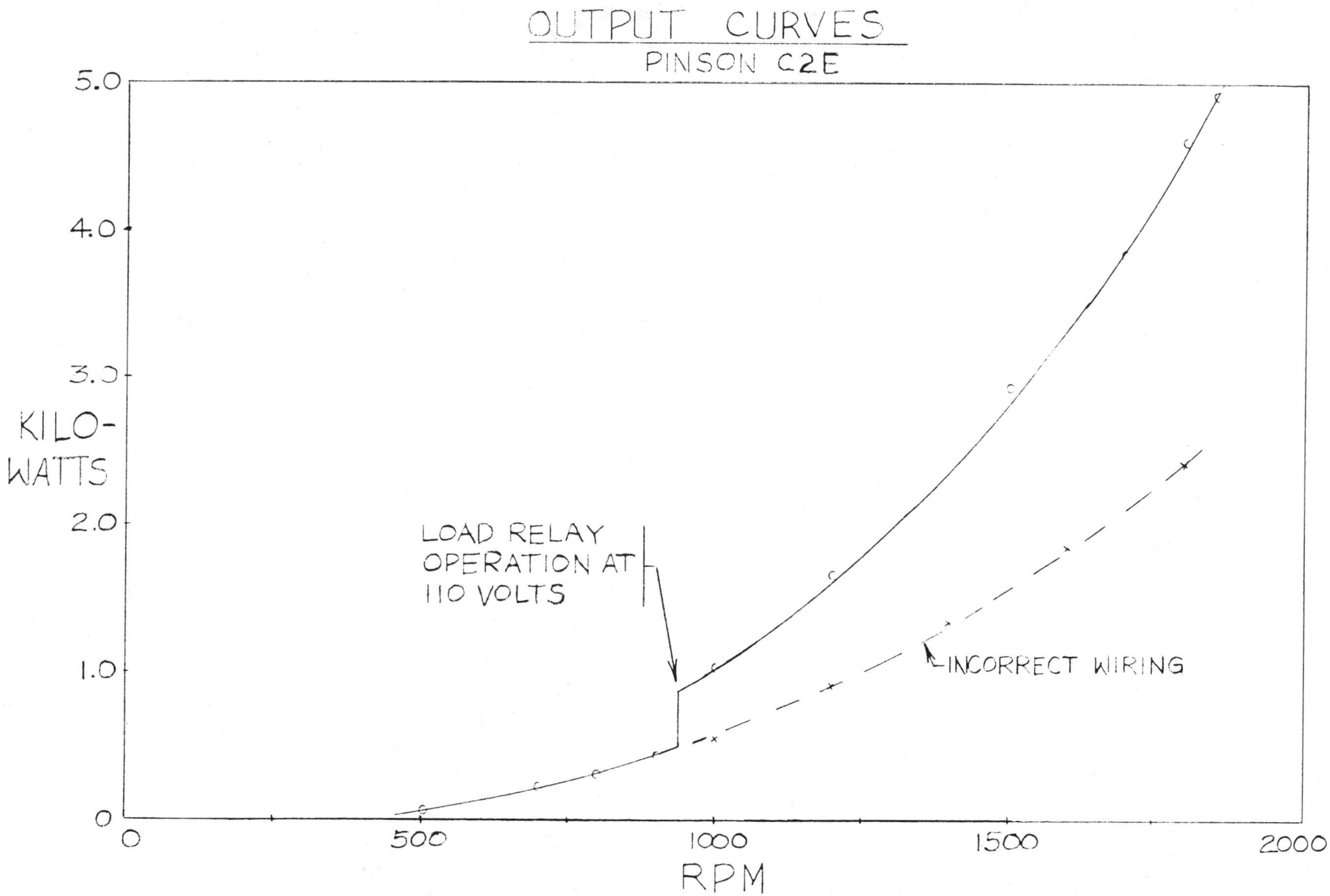
OUTPUT CURVES
PINSON C2E
5.0
4.0
3.0
2.0
1.0
0
KILO-
WATTS
LOAD RELAY
OPERATION AT
110 VOLTS
INCORRECT WIRING
0
500
1000
1500
2000
RPM

Figure 4

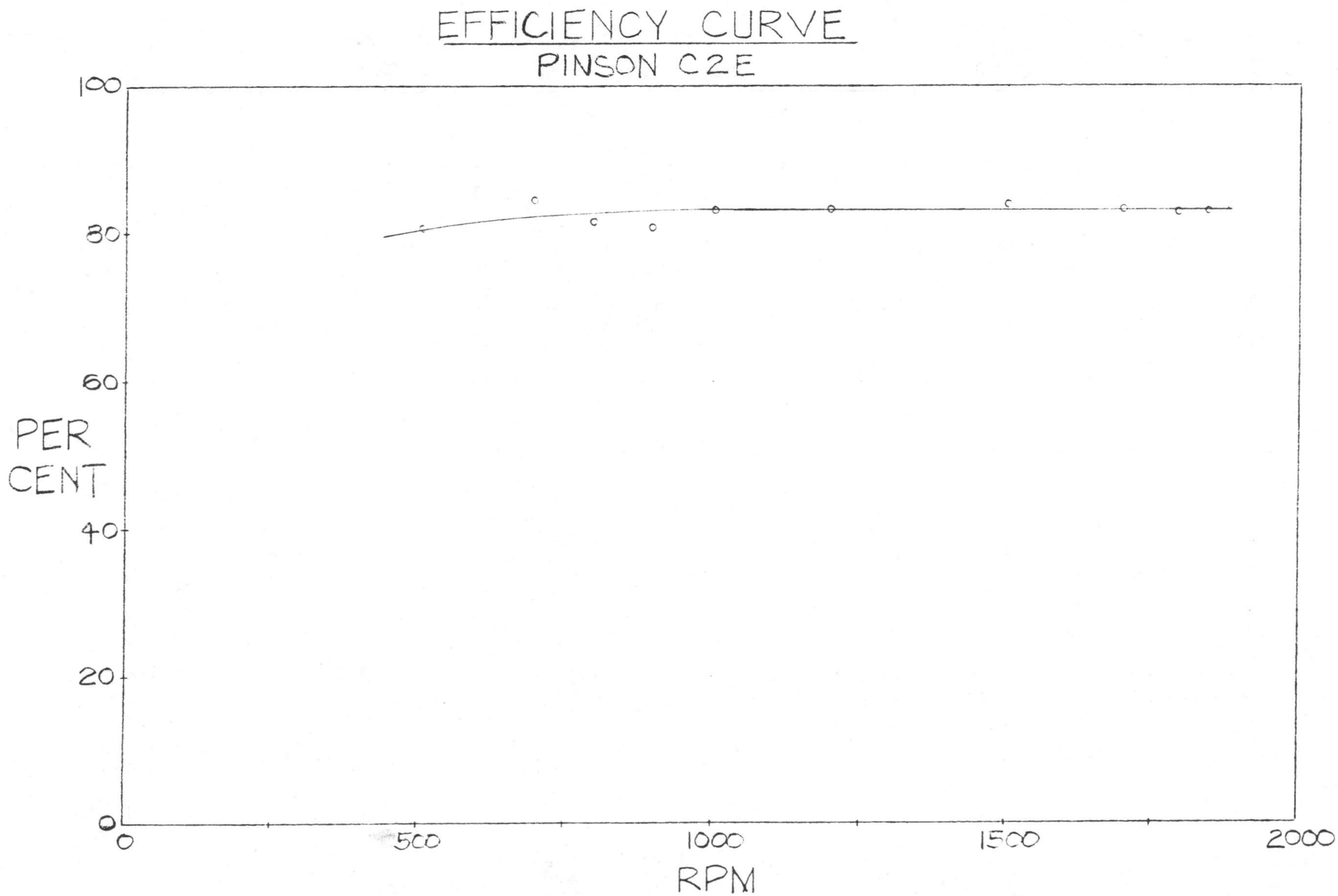
EFFICIENCY CURVE
PINSON C2E
PER CENT
100
80
60
40
20
0
0
500
1000
1500
2000
RPM

Figure 5

DYNAMOMETER TEST RESULTS

PINSON C2E

SPEED (RPM)	TORQUE (IN-LBS)	AMPS	VOLTS	WATTS	VOLTS	AMPS
		(MAGTROL)			(CONTROL BOX)	
404	0	.34	8.7	3	5	0
501	0	.26	6.3	1	75	2
504	15	1.65	42.9	72	55	2
604	20	2.26	56.3	129	30	2.5
701	30	2.90	72.2	211	75	2.0
801	40	3.50	88.2	310	90	4.0
907	50	4.12	105.6	435	110	4.5
1000	105	9.06	115.3	1038	120	9.0
1201	140	11.36	147.6	1666	155	11.0
1502	195	14.96	197	2925	200	15.0
1690	230	17.05	226	3835	230	↗
1805	260	18.73	248	4605	↗	↗
1847	270	19.34	256	4915	↗	↗

Figure 6

TN-80-13

CONTROLLED VELOCITY TESTING
OF THE
ASI/PINSON HIGH RELIABILITY WIND TURBINE GENERATOR

E. E. Bange

September 1980

Additional available reports on controlled velocity testing of small wind systems are listed below and are available from National Technical Information Service.

1. Controlled Velocity Testing of Small Wind Conversion Systems, November 1980, J. C. Balcerak, 45 pp., (RFP-3189).

2. Second Interim Report, Rocky Flats Small Wind Systems Test Center Activities, July 1979. Volume II, Controlled Velocity, Vibration and Dynamometer Testing of Small Wind Energy Conversion Systems, 42 pp., $6.00, (RF-3004-2)

TABLES

FIGURES

CONTROLLED VELOCITY TESTING OF THE ASI/PINSON HIGH RELIABILITY WIND TURBINE GENERATOR

TN-80-13

Introduction:

Controlled Velocity Testing (CVT) is a testing technique designed to test a SWECS under a controlled wind regime for rapid determination of performance characteristics and parametric changes. The CVT program is carried out at the Department of Transportation (DOT) rail site at Pueblo, Colorado. The test site is a section of straight precision (Grade 7) track approximately 2.5 miles long. In order to undergo CVT, a SWECS is mounted on a stub tower and secured to the first of two flat cars and pushed by a high speed railroad engine. The SWECS is mounted on the forward section of the lead flat car, while an instrumentation van and a portable generator are mounted on the aft section of the second flat car (Figure 1). The second flat car also serves as a buffer to reduce turbulence between the locomotive and the SWECS.

Test Specimen:

Manufactured by Aerospace Systems, Inc. (ASI) of Burlington, Massachusetts, the ASI/Pinson High Reliability Wind Turbine Generator (WTG) is a vertical-axis, three-bladed, cyclicly variable pitch machine designed to produce 1 KW of electrical output at 9 m/s (20 mph). This government funded prototype incorporates a 2.4 m in height x 4.6 m in width (8 ft x 15 ft) diameter rotor with three constant chord, 8-ft long aluminum rotor blades. The blade pitch is controlled by control rods which are actuated by a tilt-cam assembly. A "V"-vane tail assembly connected to the tilt-cam assembly orients the cam (with respect to wind direction) and actuates the desired cyclical pitch, thereby providing the basic rpm control. The machine is designed to cut-in at 2.2 m/s (5 mph) and produce maximum output at 160 rpm.

Test Set-up and Instrumentation:

When undergoing CVT, the ASI/Pinson was mounted on a Rohn SSV-6 tower section that was stiffened to give an overall tower and WTG natural frequency of 8.9 Hz. Instrumentation provided by the manufacturer for CVT included strain gages on one blade, one strut, one "L"-link and the gearbox torque reaction bar, as well as a Trump-Ross Encoder for rpm, a yaw position potentiometer and a linear position potentiometer for measuring travel of the actuator lever arm(trip mechanism movement). Transducers for output current, voltage, power, wind velocity and direction were supplied by Rocky Flats. A ground speed instrumentation sensor was supplied by DOT. However, wiring errors, damaged wiring and lack of timely information on the range of measurement

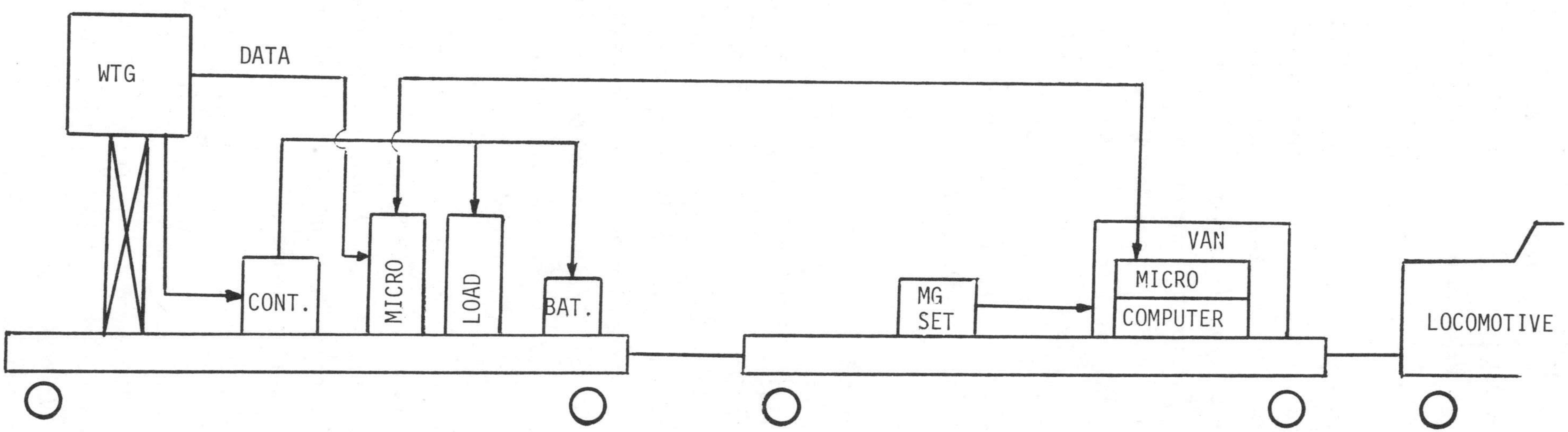

Figure 1
CVT Test Set-Up

from (ASI/Pinson) defeated the effort to calibrate the strain gages. The pulley attached to the actuator rod (used to drive the yaw position potentiometer) could not be kept tight, and the belt between this pulley and the potentiometer would not stay on. Also, the pulley attached to the main shaft, for the purpose of driving the rpm sensor, came loose and was cemented back into place. Based primarily on a rather tight test schedule, it was decided that data from these sensors (except rpm data) were not mandatory for the CVT tests.

Outputs of the active calibrated sensors were fed through signal conditioners to a microprocessor located in one of the instrumentation racks (flatcar #1). A second microprocessor was located in the instrumentation van (flatcar #2) and interfaced with a Hewlett-Packard 9845A desk top computer. Another instrumentation rack contained two programmable solid state loads (PS^2L) rated at 1 kW each. These were connected in parallel with a battery and were set to regulate at voltage levels above or below, or at the voltage level of, the battery.

Using the instrumentation and data acquisitions systems described above, plots of all data points collected for power/windspeed and rpm/windspeed were obtained from the HP 9845A within seconds of a run completion. A "Method of Bins" program, which averages all data points collected (one each second) at each unit of windspeed during a run, can be used to generate selected plots of power/windspeed, rpm/windspeed, Cp/windspeed, tip speed ratio/windspeed etc. within a few minutes of run completion.

Discussion of Results:

During CVT of the ASI/Pinson, test runs were made at three different sets of ground speed: 0 to 30 mph in 5 mph increments; slow, steady runs the full length of the track at 10, 15 and 20 mph to provide large amounts of data relative to cut-in velocity; and accelerations from 25-30 mph to 60 mph. Table I is a matrix of tests completed during CVT of the ASI/Pinson, including the corresponding wind speeds.

When CVT of the ASI/Pinson began, immediate attempts were made to adjust the cut-out point to the recommended 160 rpm. Several runs were made after adjusting the trip mechanism between each run. However, results were not consistent (i.e., they did not always reflect the direction of the adjustment). During one run, an overspeed condition caused the rotor to reach 235 rpm, and several rivets that tie the blade skin to the extruded leading edge "popped"

TABLE I

TESTS COMPLETED MATRIX

TASKS		Wind Speed (mph)		
		0 to 30	10, 15, 20	30 to 60
Tail Alignment	- Wind velocity at which tail aligns with wind direction	✓	✓ (10,15 only)	X
Rotor Start	- Wind velocity at which rotor starts to turn	✓	✓ (10,15 only)	X
Cut-In	- Wind velocity at which cut-in occurs	✓	✓ (10,15 only)	X
Cut-Out	- Wind velocity at which WTG shuts down	X	X	✓
Power Curve	- Plot output power vs. wind speed	✓	✓	✓
Load Variation	- Power curve with varying load voltages	✓	✓	✓
Improve Startup	- Minor changes made in configuration to lower cut-in velocity	✓	✓	X

TABLE II

PROBLEM AREAS

Problems Encountered	Solutions
One airfoil of the tail assembly damaged during shipment to DOT.	Local sheet metal shop made satisfactory repairs. It is believed there was no effect on machine performance.
Two welds on tail boom found to be cracked.	Welded locally.
Tachometer pulley loose on output shaft of gear box.	No apparent way to fix mechanically. Cemented the bushing, pulley shaft and face to gearbox shaft with Duco Cement - it worked.
Yaw pulley loose on actuator rod. Up-down movement caused drive belt to jump off pulleys.	Unable to fix this one. Tested without it. No tracking error data available.
Two of the three bolts in the swivel body and nut in swivel-end of actuator lever found loose.	Retightened.
Rotor oversped during two runs.	Reason traced to tail assembly airfoils rotating on single attach point resulting in much less lift. Sheet metal straps added to prevent rotation.
Rivets popped and skin peeled on two blades.	Blades repaired locally.
Locknut on top of swivel came loose. Resulted in shortened travel of actuator rod and did not allow mechanism to reach full run position.	Locknut retightened.
Power curves consistently indicated output in excess of 2 kW.	Instrumentation and calibration checked. No clear answer as yet. Natural Power, Inc. is investigating. A dynamometer test is planned at WSTC to investigate this area.

TABLE II (Cont.)

PROBLEM AREAS

Problems Encountered	Solutions
Drawings or manual do not contain information on hookup of linear pot to measure activator rod travel.	Unable to obtain information for ASI/Pinson, fabbed a jury rig.
Damaged strain gauges, wiring errors and lack of firm information on calibration range.	Unable to resolve in time for CVT. No data collected.

out of blades 2 and 3. Figure 2 reflects power data generated during this time frame. Data collection continued beyond the maximum rpm and power points through shutdown and almost to complete stop. It is felt that high centrifugal and aerodynamic loads caused the rivet failures, and an investigation is planned to establish the pull strengths of the rivets. After new rivets were installed, another test was made to verify the cut-out point. This test run resulted in the same overspeed condition and the test was stopped.

Examination revealed that the airfoils on the "V"-vane tail assembly had rotated about their single attachment point to the tail boom. The trailing edges had moved approximately 4 inches apart, in comparison to a starting point of less than 1/4" apart. This movement decreased the angle of attack and amount of lift required to actuate the trip mechanism for shutdown. Figure 3 presents rpm data generated just prior to discovery of the airfoil rotation with critical points noted. Figure 3 plainly shows the trip mechanism starting to shut down at a windspeed of approximately 18 m/s (40 mph). Then, the airfoils apparently rotated and allowed the rotor to run up to 235 rpm in approximately 10 seconds. The test run was stopped at this point.

Repair was initiated consisting of two 2" sheet metal straps extending between the two airfoils and across the boom. One strap was located just ahead of the attachment point, the other at the trailing edge. The airfoils were rotated such that the trailing edges were nearly touching.

After making several additional test runs with the modification, it was evident that the cut-out rpm was now far too low, although the cut-out wind speed was normal (Figure 4). A number of trip mechanism adjustments produced no improvement. A close examination of the trip mechanism revealed that the locknut holding the threaded rod (bolt) in the actuator rod swivel had worked loose. This shortened the stroke of the actuator rod and the remainder of the trip mechanism. The locknut was tightened and a few more runs were made to locate the cut-out point. In this configuration, the machine would go into a deep stall and nearly stop rotating. Power and rpm data reflected in Figures 5 and 6, respectively, were generated after tightening the loose swivel locknut. These data reflect a significantly high cut-in wind speed (10 m/s) and low cut-out wind speed (15 m/s).

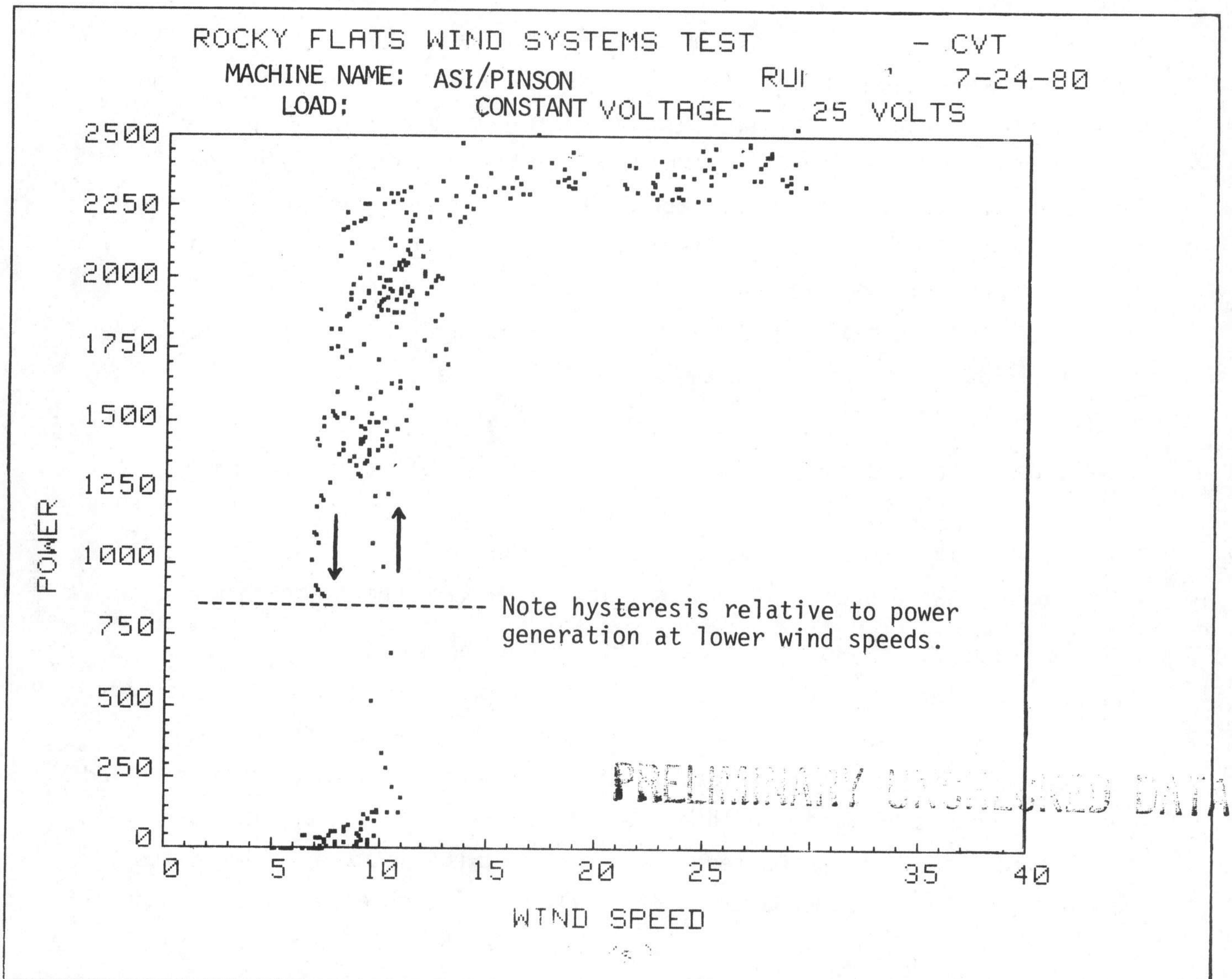

TOTAL DATA PO

FIGURE 2
OVERSPEED CONDITION

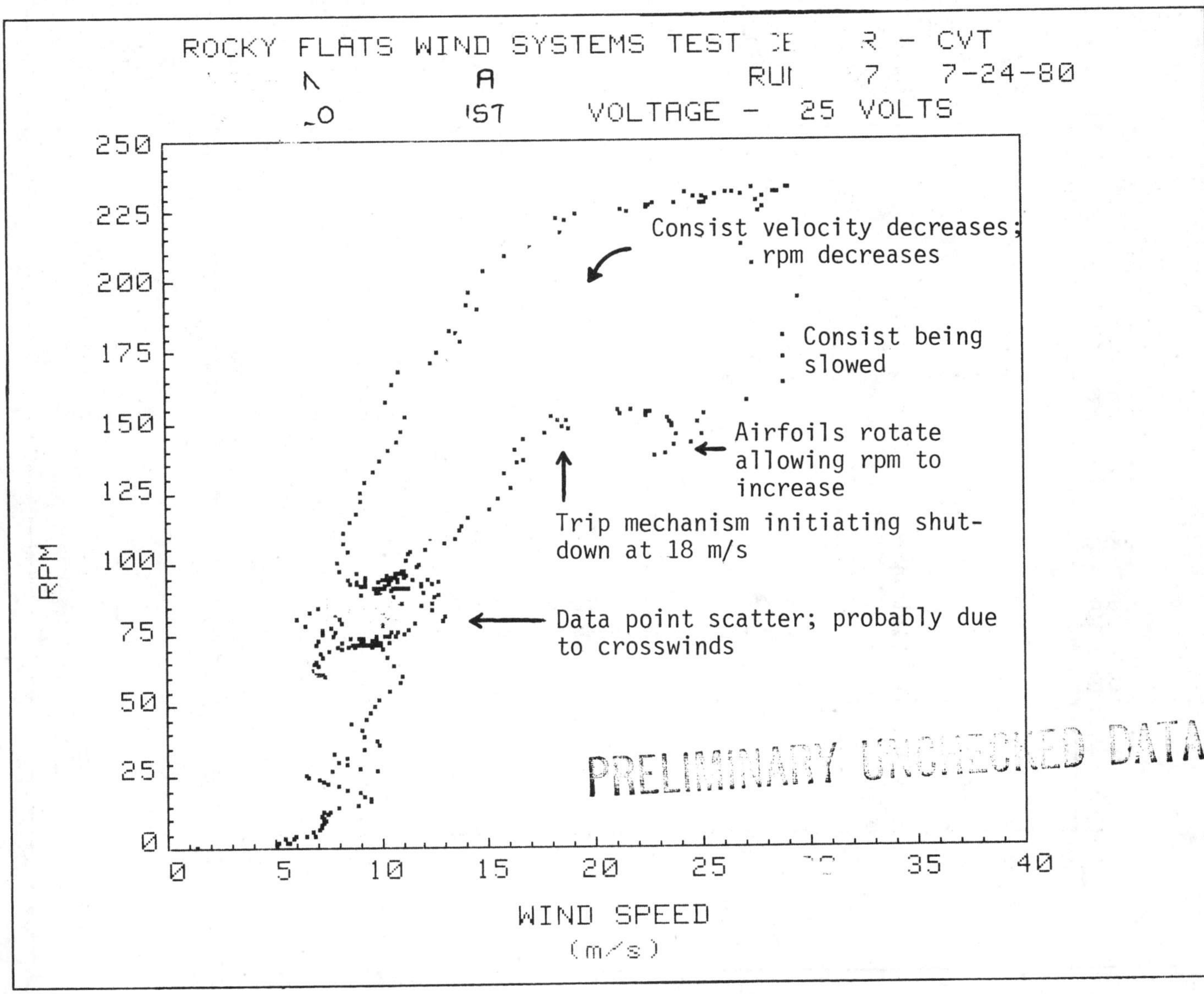

TOTAL DATA PO

FIGURE 3

OVERSPEED CONDITION

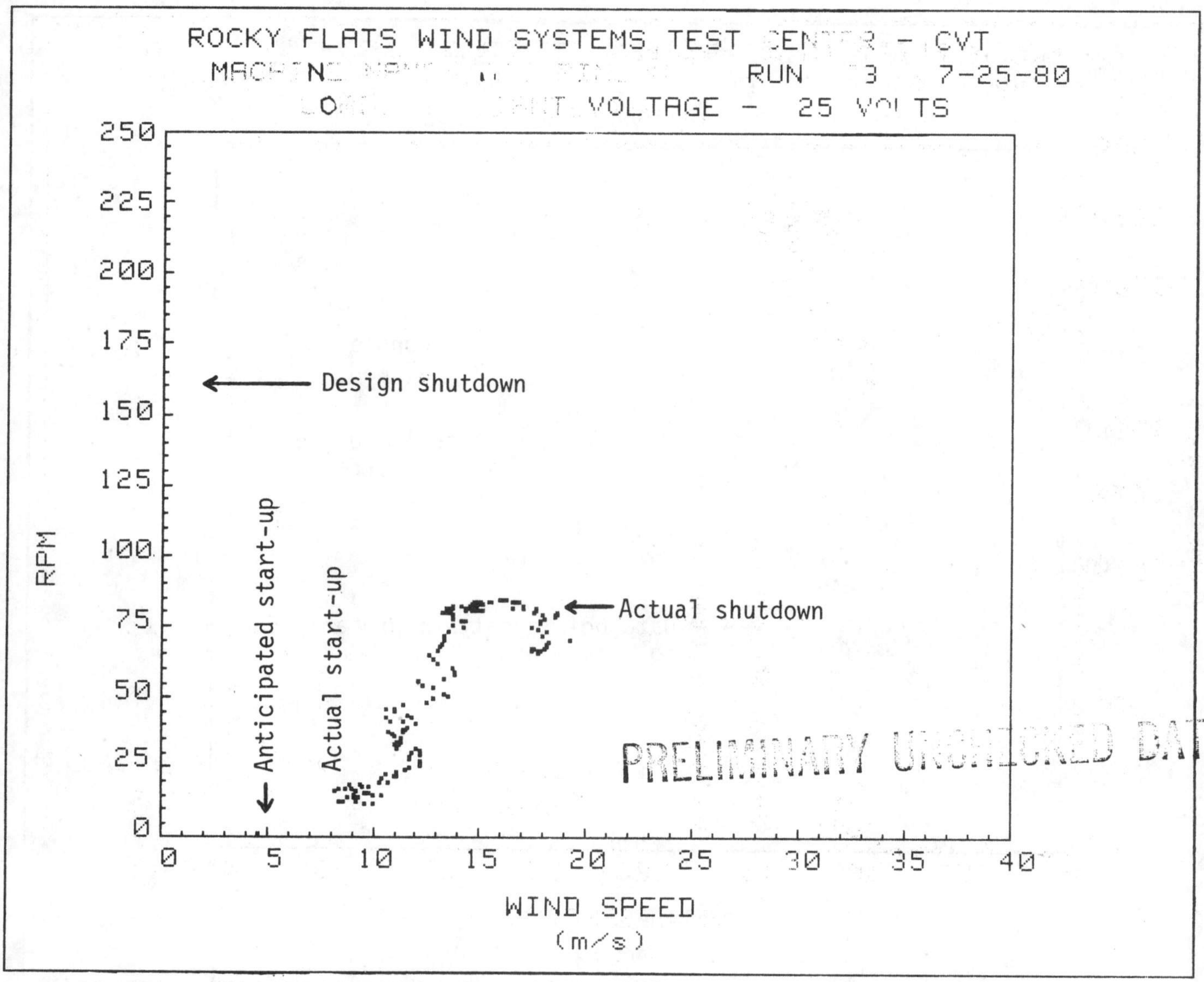

TOTAL DATA POINTS

FIGURE 4

EARLY SHUTDOWN

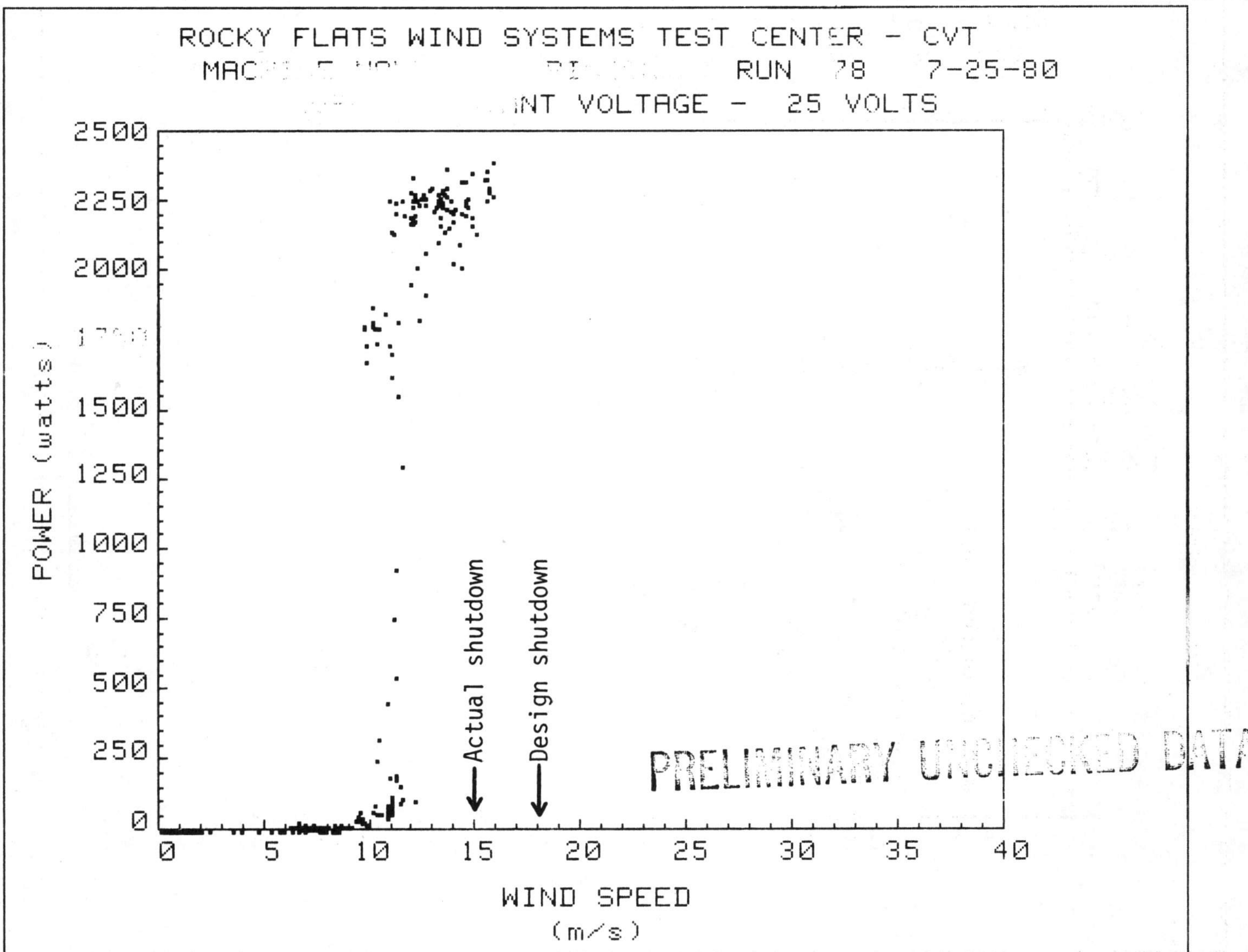

TOTAL DATA PO

Figure 5

TRIP MECHANISM STROKE NORMALIZED

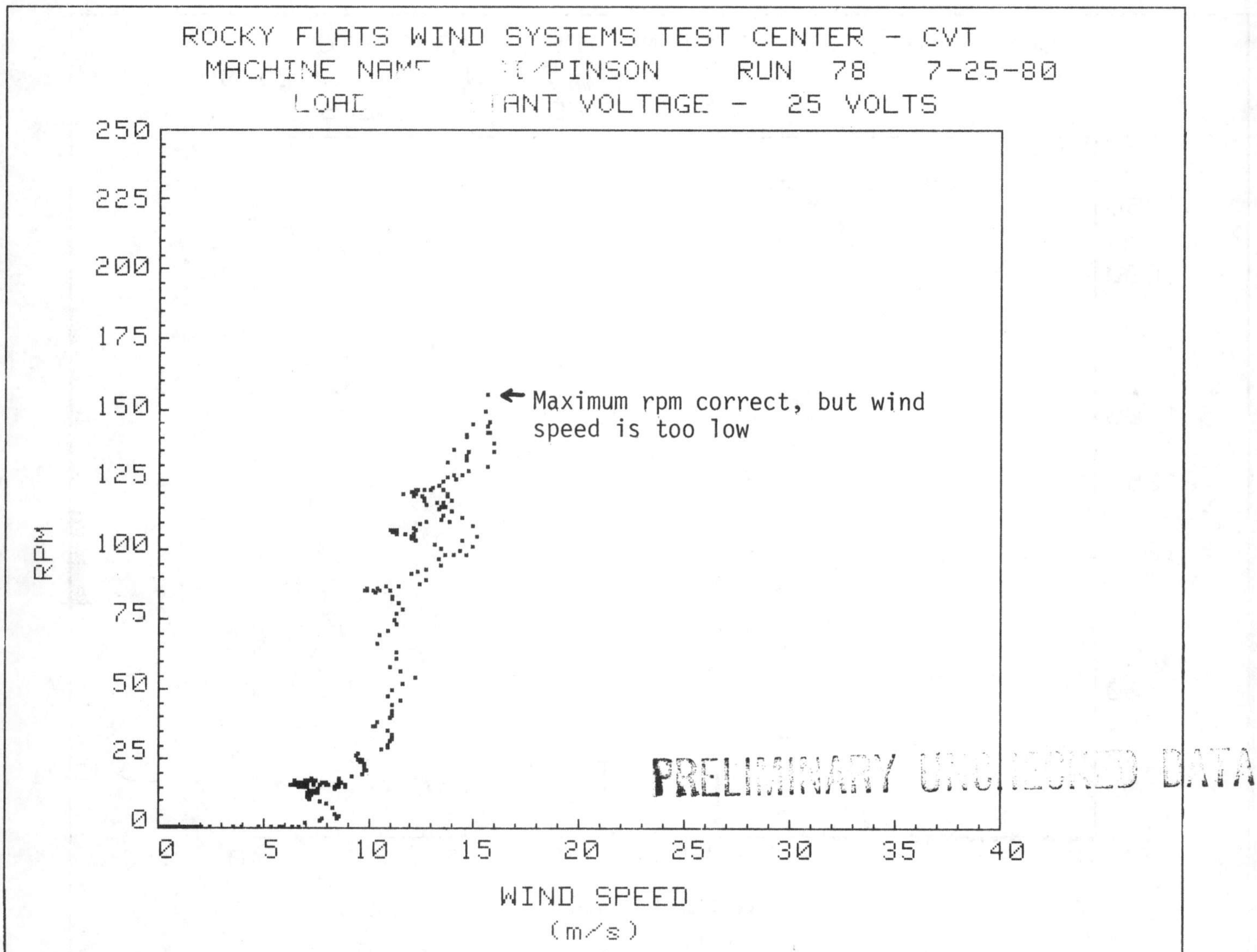

TOTAL DATA POINT

FIGURE 6

TRIP MECHANISM STROKE NORMALIZED

The tail was again modified to allow a 2" separation between the airfoil trailing edges (roughly the mid-point of the previous configurations). Several more runs and one additional adjustment of the trip mechanism indicated the WTG was then operating normally and further testing could be performed. Figures 7 and 8 contain data generated during testing in this configuration with the trip mechanism adjusted for shutdown at an rpm of just under 160. Note that the WTG restarted after shutdown. This configuration was kept for the remainder of the tests, and cut-in and cut-out were re-checked and re-verified. Figures 9 through 12 are plots of data generated on the same run as Figures 7 and 8 after using the "Method of Bins." These data (Figures 9 through 12) indicate that shutdown occurs at the proper rpm, but just above a wind velocity of 13.4 m/s (30 mph). Design shutdown wind velocity is approximately 17.9 m/s (40 mph). Also note that maximum Cp and power do not occur at the same wind speed. This could indicate an improper match between the rotor and load. Table II is a summary of all problem areas encountered during CVT of the ASI/Pinson.

Although a major objective of CVT on the ASI/Pinson was to obtain power curves, it is also important to remember that considerable effort was expended to improve performance and perform adjustments in an attempt to achieve the optimum configuration of the WTG. Testing at three different positions of the airfoils of the tail assembly, while not pre-planned, provided valuable data relative to shutdown rpm and wind velocity. The collective pitch adjustment was changed late in the testing period to increase the angle of attack in an effort to improve start-up. Unfortunately, the effects of this change were clouded by changes in performance induced by the trip mechanism stroke being shortened when the locknut came loose. As part of the CVT Test Plan, load voltage settings were also varied from 22 to 25 volts. Results of these varied settings showed that power output increased from approximately 2050 watts at 22 volts to approximately 2350 watts at 25 volts. In addition, a number of configuration changes for improving start-up were suggested by the ASI representative visiting the facility. The changes were tried but did not materially improve start-up. It should also be noted that a Pinson representative paid a visit to the WSTC prior to shipment of the machine to DOT. The WTG was judged to be properly "tuned" per manufacturer's specifications and ready for test.

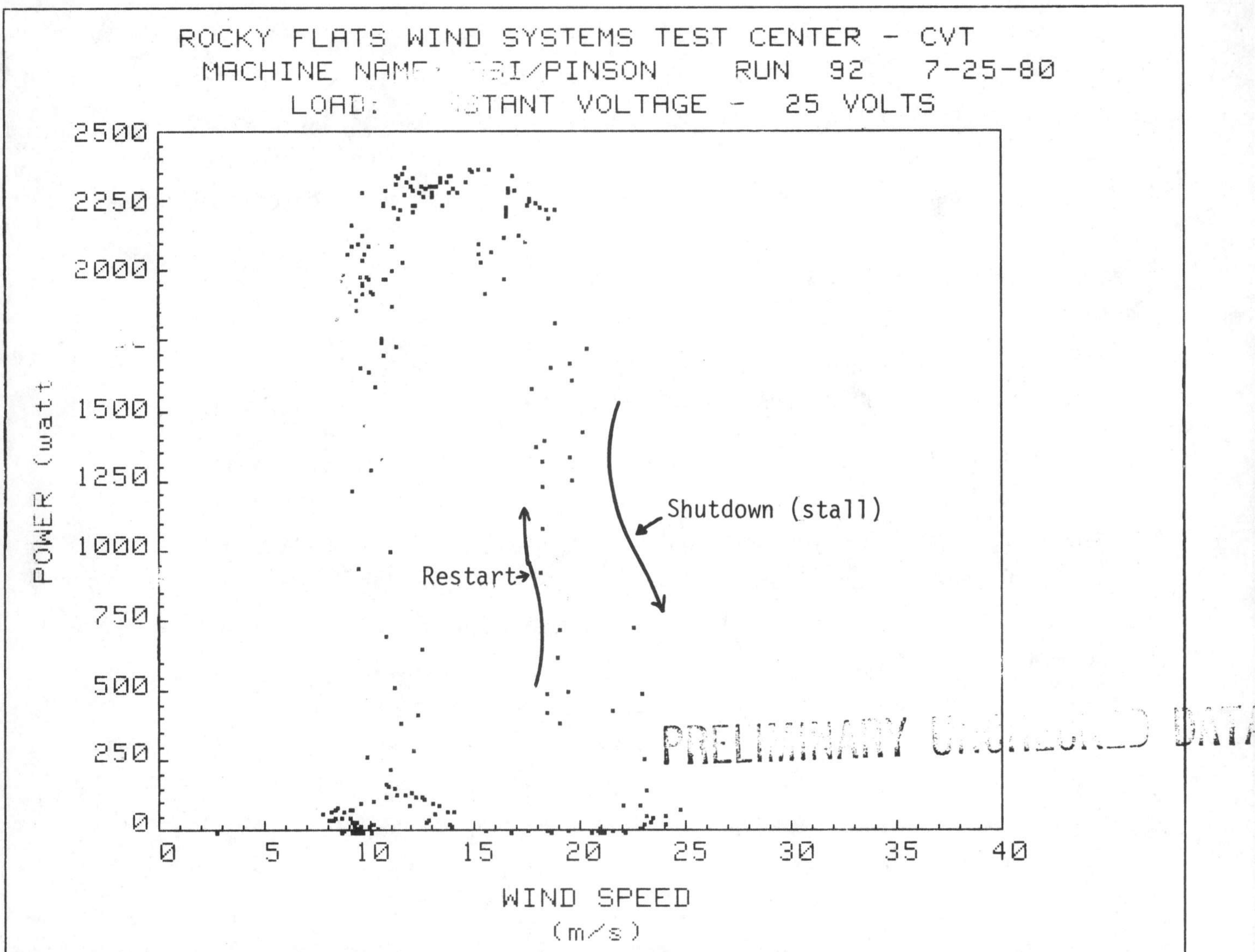

TOTAL DATA POINT

FIGURE 7

WTG NORMAL - RPM REGULATED ABOVE SHUTDOWN

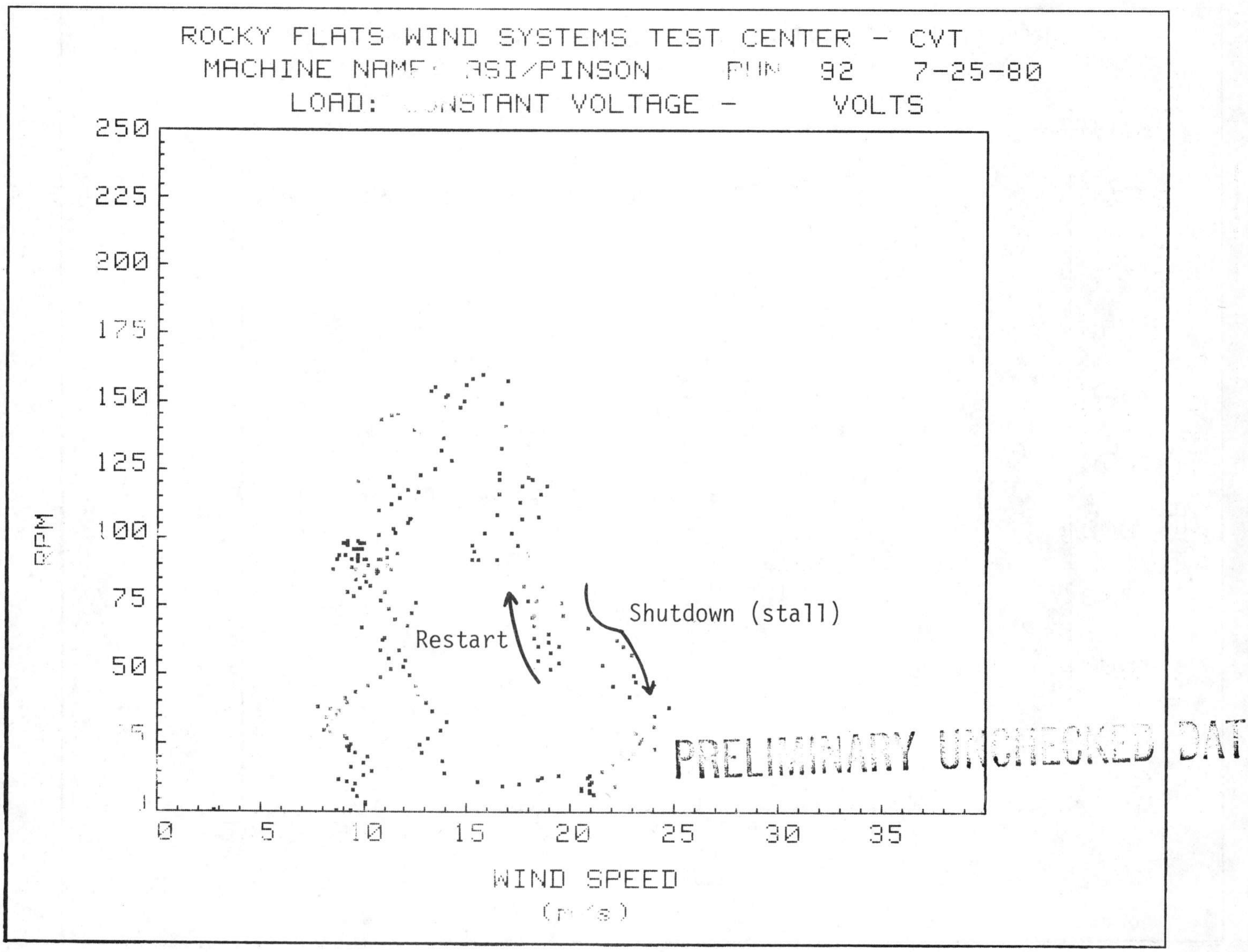

TOTAL DATA POINT

FIGURE 8

WTG NORMAL - RPM REGULATED ABOVE SHUTDOWN

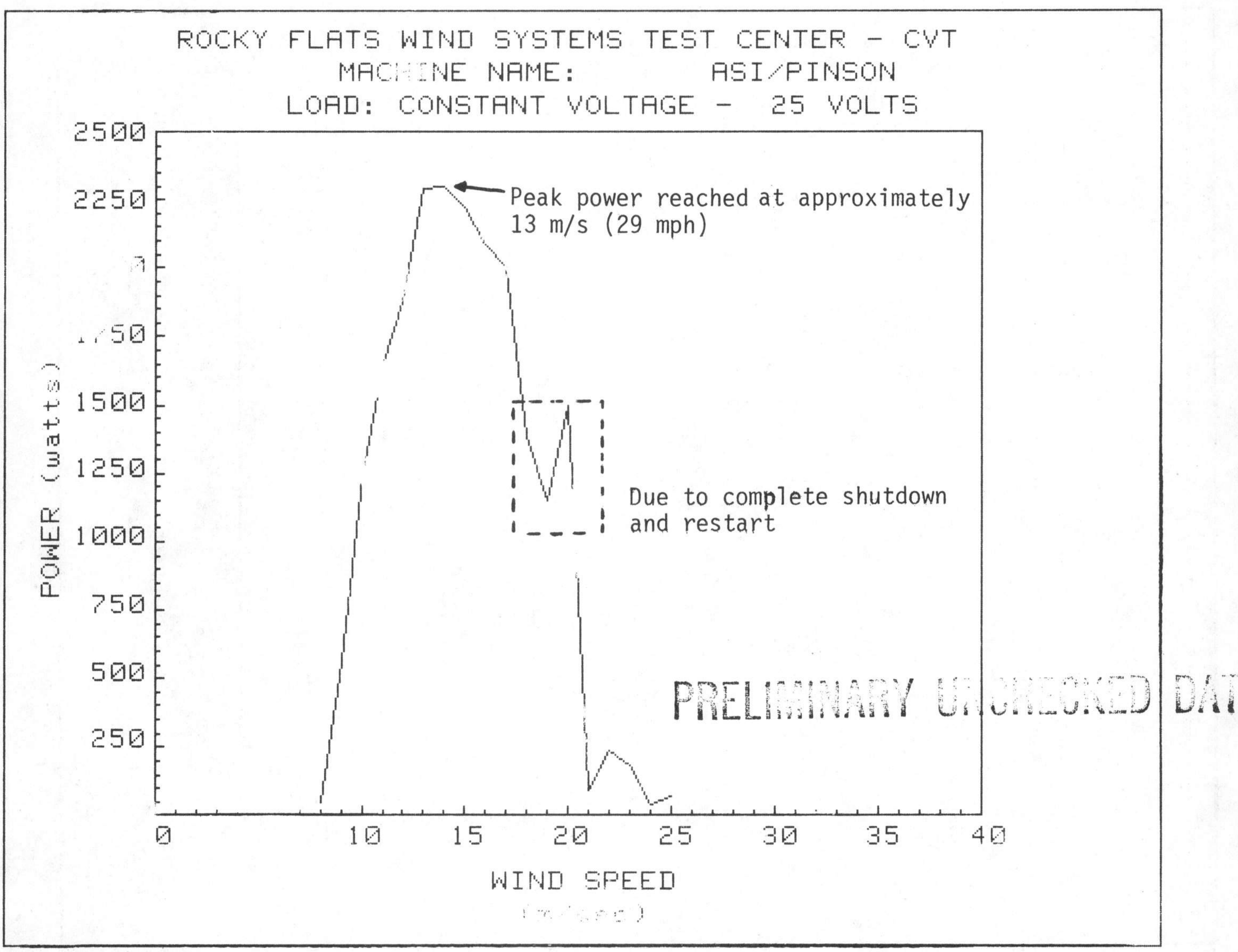

TOTAL DAT

FIGURE 9

RUN 92 AFTER USING "METHOD OF BINS"

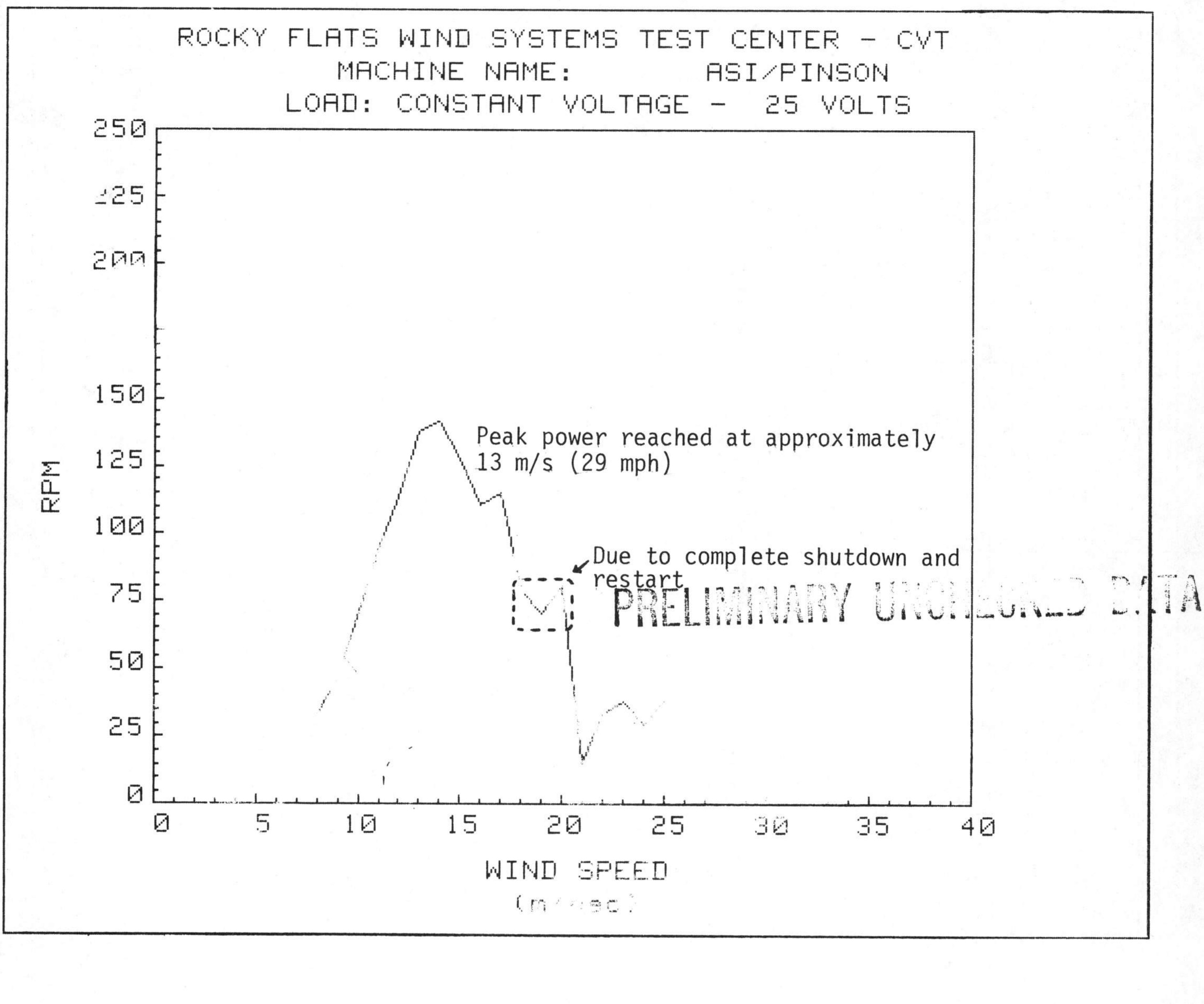

TOTAL DATA

FIGURE 10
RUN 92 AFTER USING "METHOD OF BINS"

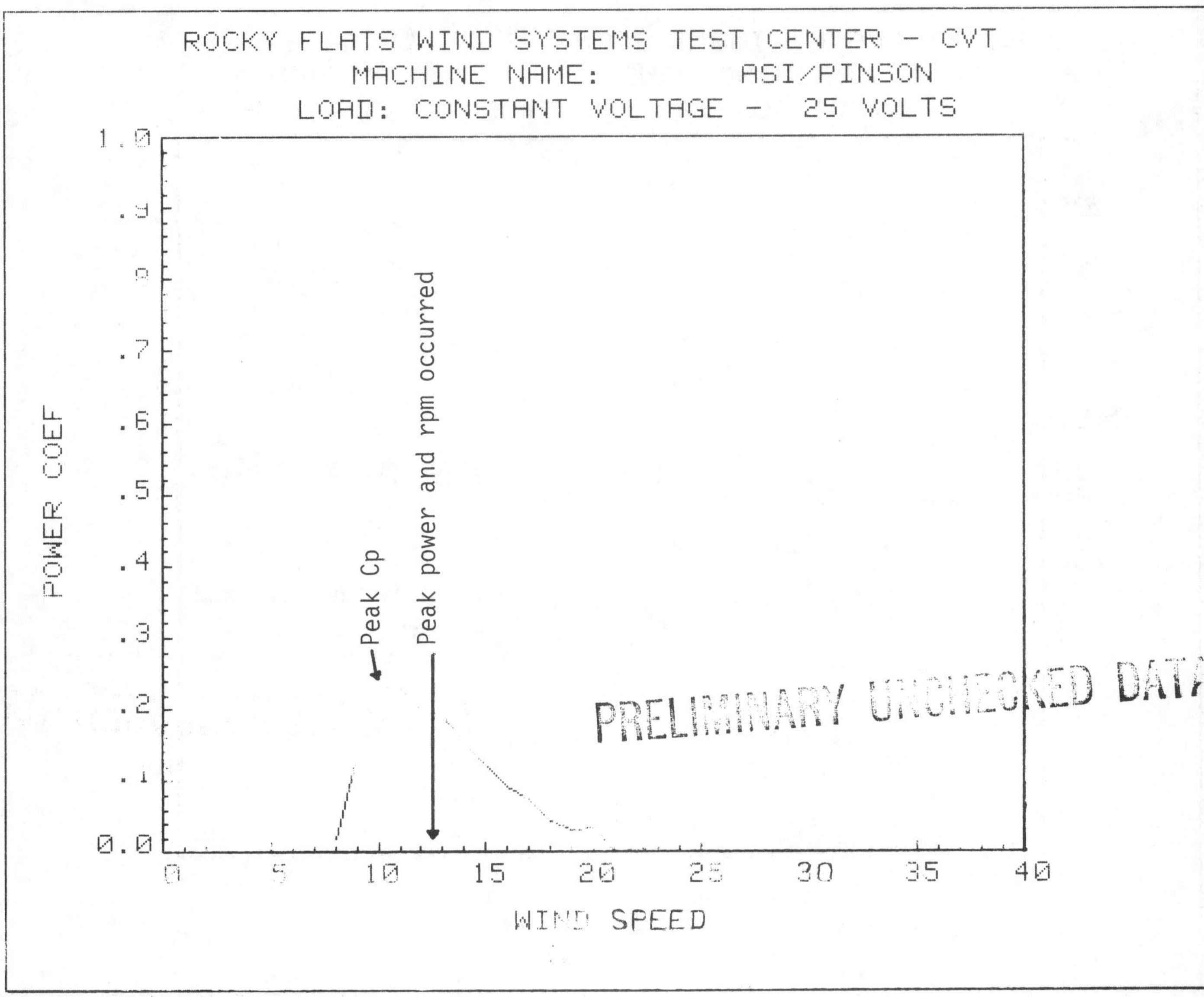

TOTAL

186

Figure 11
Run 92 after using "Method of Bins"

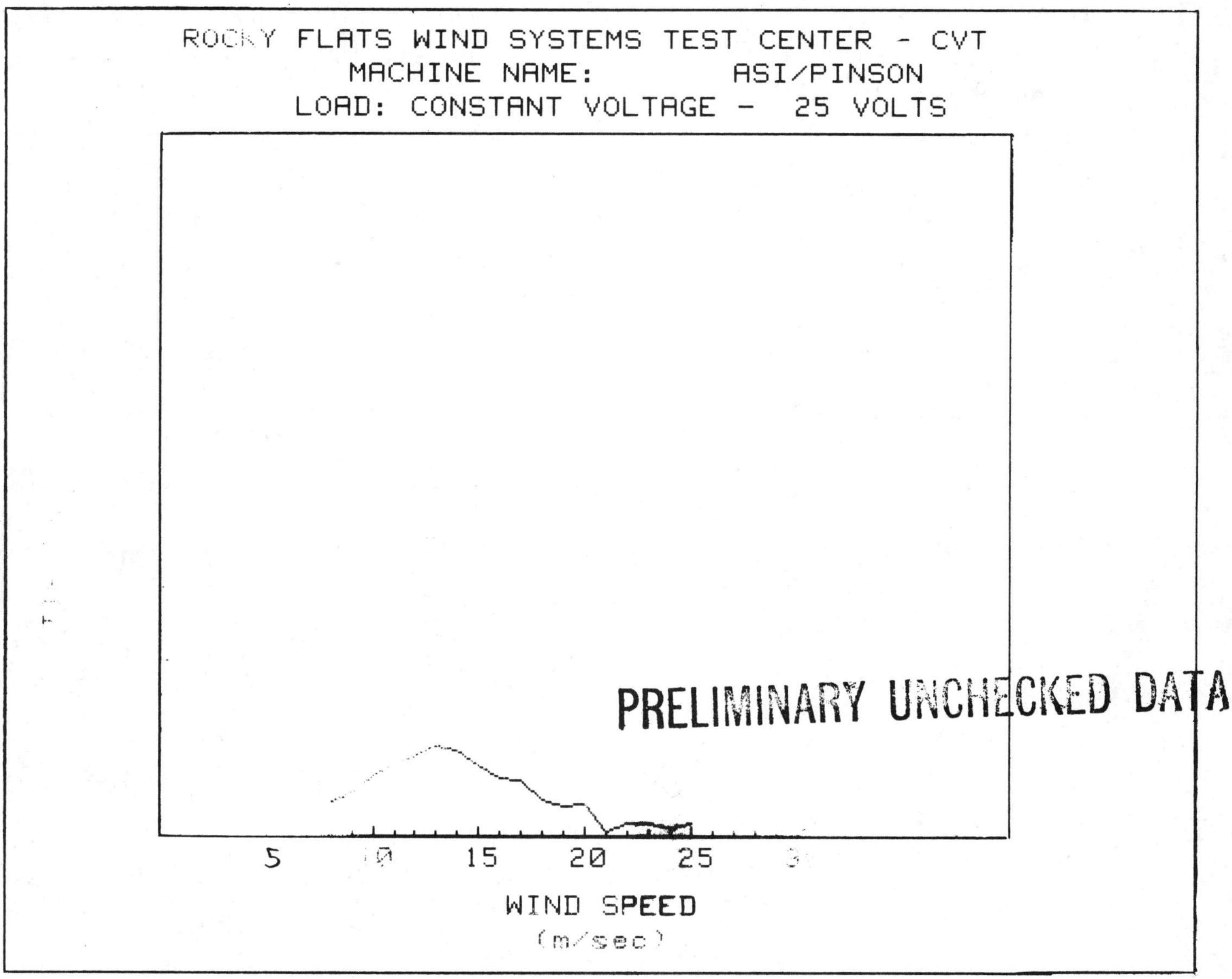

TOTAL

FIGURE 12
RUN 92 AFTER USING "METHOD OF BINS"

CONCLUSIONS/RECOMMENDATIONS:

Although a "tight" test schedule prohibited extensive parameter testing after the ASI/Pinson began operating normally, it is felt that CVT produced a great deal of useful data in a very short time period. A number of problems were discovered and corrective actions were either taken or defined which should have future value to both Rocky Flats and the manufacturer. Despite the fact that the optimum WTG control configuration was not defined, definite improvements were made. The test methodology clearly could be employed to define such optimum configurations in a time and cost effective manner. Conclusions and recommendations derived from CVT are summarized in the following paragraphs.

Of the design specifications that could be evaluated by CVT, quantitative data indicated the machine failed to meet specifications in three areas:

- Although the maximum output of the ASI/Pinson was measured to be in excess of 2 kW at 13 m/s (29 mph), the output at the machine's rated wind speed (9 m/s - 20 mph) was only 600 watts. The high maximum power output will be investigated through dynamometer testing at RF.
- Design specifications of the machine call for a cut-in wind speed of 2.2 m/s (5 mph). However, the cut-in wind speed measured by CVT was in excess of 7 m/s (16 mph).
- The cut-out wind speed of the WTG was determined to be less than the design specification of 17.9 m/s (40 mph).

Qualitative data generated from CVT showed that the ASI/Pinson would not perform up to design specifications under atmospheric test conditions due to the following problems:

- The angle of attack of the tail assembly airfoils was not originally, and may not yet be, set to the otpimum point. It is believed that this problem contributed significantly to the low cut-out wind speed (see above).
- The method of attaching the airfoils to the tail boom is inadequate. Once the optimum angle of attack is determined (see the preceding problem), a positive method of attaching the tail assembly airfoils to the tail boom must be developed in order to retain the optimum point.
- The attachment of the swivel-to-actuator rod (used to pitch the blades) is not adequate or reliable.

In relation to the instrumentation provided for CVT by the manufacturer, the following problems were discovered:

- The method of attaching the tachometer pulley to the drive shaft is not adequate.
- The method of attaching the yaw pulley to the actuator rod is not reliable and must be improved.
- No means of attaching the linear potentiometer (for measuring actuator rod travel) was provided.

☆U.S. GOVERNMENT PRINTING OFFICE:1982—578-729 / 236